

**THE CONTROL OF SELECTIVITY IN FREE RADICAL REACTIONS:
A MECHANISTIC AND SYNTHETIC APPROACH**

A thesis submitted in partial fulfilment of the requirements for the degree of
Doctor of Philosophy of the University of London.

by

VALERIE DIART

Department of Chemistry,
University College London,
20 Gordon Street,
London WC1H 0AJ.

May 1995

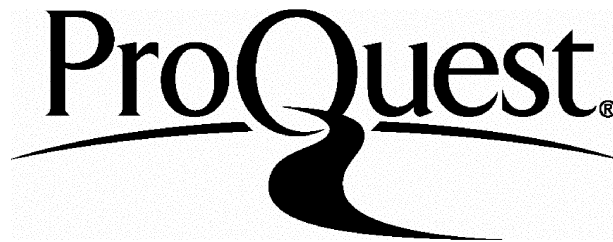
ProQuest Number: 10018472

All rights reserved

INFORMATION TO ALL USERS

The quality of this reproduction is dependent upon the quality of the copy submitted.

In the unlikely event that the author did not send a complete manuscript and there are missing pages, these will be noted. Also, if material had to be removed, a note will indicate the deletion.



ProQuest 10018472

Published by ProQuest LLC(2016). Copyright of the Dissertation is held by the Author.

All rights reserved.

This work is protected against unauthorized copying under Title 17, United States Code.
Microform Edition © ProQuest LLC.

ProQuest LLC
789 East Eisenhower Parkway
P.O. Box 1346
Ann Arbor, MI 48106-1346

ABSTRACT

This thesis is divided into three sections.

SECTION A:

ESR spectroscopic studies of the addition of α -(alkoxycarbonyl)alkyl radicals to terminal alkenes, furan and isocyanides were carried out in cyclopropane solution at low temperatures. The radical addenda were generated by UV photolysis of di-*t*-butyl peroxide in the presence of the corresponding ester and trimethylamine-butylborane as a polarity reversal catalyst. For all acceptors, addition of each of the electrophilic α -(alkoxycarbonyl)alkyl radicals is faster than the corresponding addition of simple (nucleophilic) alkyl radicals, a result which is attributed to the importance of polar effects in the transition states. The radical $\text{H}_2\text{C}=\text{CH}(\text{CH}_2)_3\dot{\text{C}}(\text{CO}_2\text{Et})_2$ undergoes 5-*exo*-cyclisation more rapidly than the unsubstituted hex-5-enyl radical; this is attributed to the electrophilic nature of the radical centre in the former species.

SECTION B:

A variety of optically active amine-borane complexes have been used as polarity reversal catalysts for the kinetic resolution of racemic carbonyl-

containing compounds at $-74\text{ }^{\circ}\text{C}$ in oxirane solvent. The key step involves enantioselective abstraction of hydrogen from a C-H bond α to the carbonyl function by optically active amine-boryl radicals. The more reactive substrate enantiomer can generally be predicted by consideration of the steric interactions between the substituents attached to the reacting centres in the transition states. However, hydrogen-bonding, dipole-dipole interactions, together with stereoelectronic effects, may also play a part in determining enantioselectivity particularly when there is not marked steric asymmetry around the reacting centres.

The molecular structures of optically active quinuclidine-isopinocampheylborane and of the polycyclic amine-borane formed by cyclisation of *N*-(1*R*)-nopylpyrrolidine-borane have been determined by X-ray crystallography. The steric demands of a variety of amine-boryl radicals in H-atom transfer reactions have been assessed by determining the relative rates of abstraction from the α -C-H bonds in $\text{H}_2\text{C}(\text{CO}_2\text{Et})_2$ and $\text{Me}(\text{H})\text{C}(\text{CO}_2\text{Et})_2$.

SECTION C:

The polycyclic amine-borane formed by cyclisation of *N*-(1*R*)-nopylpiperidine-borane was used, in the presence of $\text{BF}_3\cdot\text{OEt}_2$, for the asymmetric hydroboration of 1-methylcyclohexene and for the asymmetric reduction of acetophenone, in a variety of solvents at $25\text{ }^{\circ}\text{C}$ and $-78\text{ }^{\circ}\text{C}$.

Hydroboration of 1-methylcyclohexene proceeds in good yield at 25 °C and *trans*-2-methylcyclohexanol with an e.e. of up to 52% was obtained after oxidation of the organoborane. Reduction of acetophenone was found to proceed rapidly, even at -78 °C, to give the alcohol with an e.e. of 15%.

ACKNOWLEDGEMENTS

I would like to thank my supervisor Dr. B.P. Roberts, for all his help during the course of this project.

Thanks are also due to all the members of my group especially Dang, James and Tony for their help and discussions in the lab. Also to Alan Stones, Steve Corker, Gill Maxwell and Chris Cooksey for all their help throughout.

I would also like to thank all my friends in particular Gill, Paula, Yut-Mei, Navjot, Peter and *etc.* Finally some very special thanks go to Mukesh Shinhmar.

N' oublions surtout pas de mentioner mes parents et mes grand-parents ainsi que Benoit, Julie, Matthieu et Gaëtan.

CONTENTS

	Page
ABSTRACT	2-4
ACKNOWLEDGEMENTS	5
SECTION A: ESR STUDIES OF THE ADDITION OF 1,1-BIS(ALKOXYCARBONYL)ALKYL RADICALS AND TRIS(ETHOXYCARBONYL)METHYL RADICALS TO ALKENES AND TO ALKYL ISOCYANIDES	
Chapter 1: INTRODUCTION	12-34
1.1. Polar Effects in Hydrogen-Atom Abstraction Reactions	12
1.2. Polarity Reversal Catalysis	15
1.3. Amine-Boryl Radicals	19
1.4. Radical Addition to Alkenes	23
1.5. Free Radical Addition to Alkyl Isocyanides	26
1.6. Cyclisation of Alkenyl Radicals	28
1.7. References to Chapter 1	30

Chapter 2: RESULTS AND DISCUSSION 35-81

2.1. (Alkoxy carbonyl)alkyl Radicals $R^1\dot{C}(CO_2R^2)_2$	35
2.2. Addition of $H\dot{C}(CO_2R)_2$, $Me\dot{C}(CO_2Et)_2$ and $\dot{C}(CO_2Et)_3$ to Alkenes	45
2.3. Addition of $H\dot{C}(CO_2Et)_2$, $Me\dot{C}(CO_2Et)_2$ and $\dot{C}(CO_2Et)_3$ to Furan	52
2.4. Absolute Rate Constants for Addition of $HC(CO_2Et)_2$ and $\dot{C}(CO_2Et)_3$ to Ethene	55
2.5. Relative Rates of Addition to Alkenes	57
2.6. Cyclisation of the 1,1-Bis(ethoxycarbonyl)hex-5-enyl Radical	59
2.7. Radical Addition to Alkyl Isocyanides	65
2.8. Relative Rates of Addition to Alkyl Isocyanide	70
2.9. Imidoyl Radicals Derived from $Bu^1N=^{13}C$	76
2.10. References to Chapter 2	79

Chapter 3: EXPERIMENTAL 82-89

3.1. ESR Spectroscopy and Computer Simulations	82
3.2. NMR Spectroscopy	84
3.3. Materials	84
3.4. References to Chapter 3	88

SECTION B: ENANTIOSELECTIVE HYDROGEN-ATOM ABSTRACTION BY OPTICALLY ACTIVE AMINE-BORYL RADICALS

Chapter 4: INTRODUCTION	91-103
4.1. Methods for Resolution	91
4.2. Kinetic Resolution	93
4.3. Enantioselective Hydrogen-Atom Abstraction	97
4.4. References to Chapter 4	102
Chapter 5: RESULTS AND DISCUSSION	104-154
5.1. Synthesis of Catalysts	104
5.2. Kinetic Resolution of Substrates Using IpcT	115
5.3. The Steric Strain Model for Kinetic Resolutions	123
5.4. Kinetic Resolutions Using 5.1.3-5.1.13	130
5.5. Relationships Between Structure, Reactivity and Enantioselectivity for Hydrogen-Atom Abstraction by Chiral Amine-Boryl Radicals	140
5.6. Conclusion	151
5.7. References to Chapter 5	152
Chapter 6: EXPERIMENTAL	155-180
6.1. NMR Spectroscopy	155

6.2. ESR Spectroscopy	155
6.3. Gas Liquid Chromatography (GLC)	156
6.4. High-Performance Liquid Chromatography (HPLC)	156
6.5. Column Chromatography and Thin Layer Chromatography (TLC)	157
6.6. Optical Rotations	157
6.7. Materials	157
6.8. Kinetic Resolutions	175
6.9. X-Ray Crystallography	176
6.10. References to Chapter 6	178

**SECTION C: HYDROBORATION OF 1-METHYLCYCLOHEXENE AND
REDUCTION OF ACETOPHENONE USING THE POLYCYCLIC AMINE-
BORANE FORMED BY CYCLISATION OF *N*-NOPYLPYPERIDINE-BORANE**

Chapter 7: INTRODUCTION 182-193

7.1. Hydroboration of Alkenes	182
7.2. Reduction of Ketones	185
7.3. References to Chapter 7	191

Chapter 8: RESULTS AND DISCUSSION 194-208

8.1. Hydroboration of 1-Methylcyclohexene	194
---	-----

8.2. Asymmetric Reduction of Acetophenone	201
8.3. Conclusion	206
8.4. References to Chapter 8	208

Chapter 9: EXPERIMENTAL 209-213

9.1. NMR Spectroscopy	209
9.2. Column Chromatography and Thin Layer Chromatography	209
9.3. Optical Rotations	209
9.4. Materials	209
9.5. References to Chapter 9	213

Chapter 10: ESR SPECTROSCOPY 214-223

10.1. Principles of ESR Spectroscopy	214
10.2. Characteristics of ESR Spectra	216
10.3. Second-Order Effects	220
10.4. Methods of Radical Generation	221
10.5. References to Chapter 10	223

LIST OF ABBREVIATIONS 224

**SECTION A: ESR STUDIES OF THE ADDITION OF 1,1-
BIS(ALKOXYCARBONYL)ALKYL RADICALS AND
TRIS(ETHOXYCARBONYL)METHYL RADICALS TO ALKENES AND TO
ALKYL ISOCYANIDES**

Chapter 1: INTRODUCTION

1.1. Polar Effects in Hydrogen-Atom Abstraction Reactions

Polar effects (*i.e.* the effects of charge separation in the transition state) are known to play an important role in determining the chemo- and regio-selectivities of hydrogen-atom transfer reactions [eqn. (1.1.1)].¹⁻⁴



For example, the rates of H-atom abstraction from ring-substituted toluenes by the relatively non-polar methyl radical are unaffected by the presence of electron withdrawing groups (EWGs) or electron donating groups (EDGs) on the ring,⁵ whereas EWGs at the *para*-position of toluene decrease the rate of H-atom abstraction by the electrophilic bromine atom, (EWGs destabilise a positive charge). On the other hand, the presence of EDGs at the *para*-position of toluene increase the rate of abstraction (EDGs stabilise positive charge which builds up at the benzylic carbon atom in the transition state).

The influence of polar effects in H-atom abstraction is further illustrated in the abstraction of hydrogen from propionic acid by either the methyl radical or the chlorine atom [eqn. (1.1.2) and (1.1.3)]⁶ and the relative rates of abstraction from the α and β carbons are shown in Table 1.1.1.

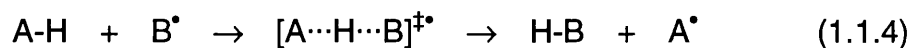
Table 1.1.1: Relative reactivities for hydrogen-atom abstraction from propionic acid ($C_\beta H_3 C_\alpha H_2 CO_2 H$) by the methyl radical and the chlorine atom at *ca.* 90 °C.

Relative Reactivity Per H-atom		
	$C_\beta H_3$	$C_\alpha H_2$
CH_3^\bullet	1	7.8
Cl^\bullet	1	0.03

When the relatively non-polar CH_3^\bullet does the abstracting, abstraction takes place mainly from C_α , but when Cl^\bullet abstracts a hydrogen this now takes place predominantly from C_β .

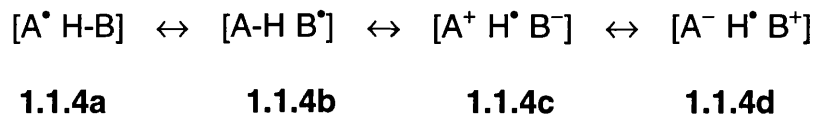


Polar effects can be explained by consideration of the transition state (TS) for a hydrogen-atom transfer reaction [eqn. (1.1.4)]. The TS for such a

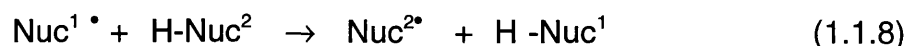


reaction is more or less linear⁷ and can be represented as a hybrid of canonical structures **1.1.4a-1.1.4d**.⁸ The stability of the TS will increase with increasing contribution from the charge separated structures **1.1.4c** and **1.1.4d**. As a

result, the activation energies for a set of similarly exothermic H-atom



transfer reactions will decrease as the properties of the attacking and departing radicals become more mutually conducive to the participation of charge transfer in the transition state.⁸ A radical is termed electrophilic when the contribution of structure **1.1.4d** to the TS is more important and nucleophilic when structure **1.1.4c** is more important. It is clear that the terms "nucleophilic" and "electrophilic" are only relative. Whether a radical A^\bullet behaves as a net electrophile or as a net nucleophile in reaction (1.1.4) will depend on the nature of B^\bullet (*i.e.* the electronegativity difference between A^\bullet and B^\bullet). Thus if EI^\bullet and Nuc^\bullet are an electrophilic and a nucleophilic radical, respectively, then the H-atom abstractions (1.1.5) and (1.1.6) will be favoured because of favourable charge transfer in the TS, whereas the reactions (1.1.7) and (1.1.8) will not.

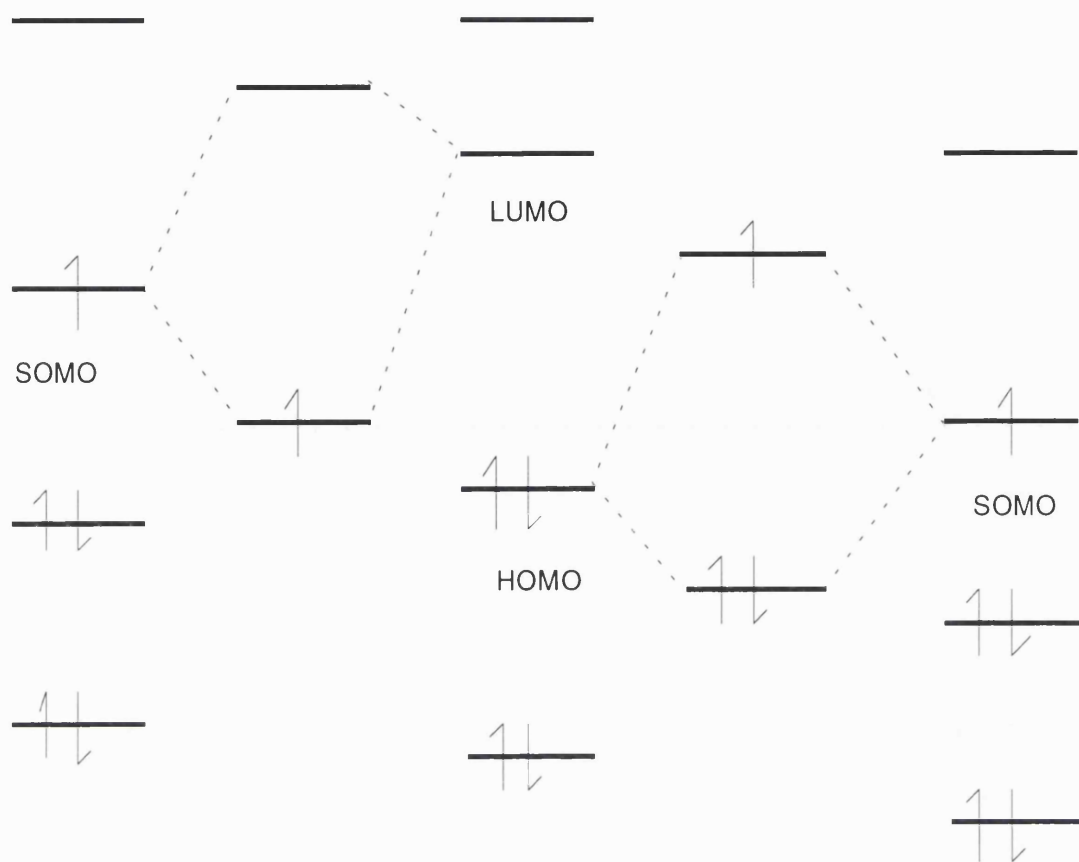


The same conclusions can be arrived at by consideration of the frontier

molecular orbital interactions for the reaction (1.1.4) (Figure 1.1.1). The principle interactions between an attacking radical (A^\bullet) and a substrate (H-B) will be between the radical's singly occupied molecular orbital (SOMO) and the highest occupied molecular orbital (HOMO, σ) and the lowest unoccupied molecular orbital (LUMO, σ^*) of the hydrogen donor. Both interactions result in a net stabilising effect, the extent of stabilisation depends on the reciprocal of the energy difference between the SOMO and the HOMO or LUMO of H-B. Radicals with a high energy SOMO, *i.e.* a relatively low ionisation energy (nucleophilic radicals) react readily with substrates having a low energy LUMO (when B is electron withdrawing): the reaction is fast because the SOMO-LUMO interaction is particularly stabilising. In contrast, radicals with a low energy SOMO (electrophilic radicals) will react more rapidly with substrates having a high energy HOMO (when B is electron donating), because the SOMO-HOMO interaction will now be strongly stabilising. Thus, as from the previous valence bond analysis, we conclude that the hydrogen-atom abstractions (1.1.5) and (1.1.6) will be favoured by polar effects, and the reactions (1.1.7) and (1.1.8) will not.

1.2. Polarity Reversal Catalysis^{8,9}

The previous analysis points to the concept of polarity reversal catalysis. Polarity reversal catalysis (PRC) is a process by which the single slow steps (1.1.7) and (1.1.8) are replaced by a series of fast consecutive steps (1.2.1)-



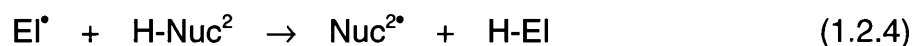
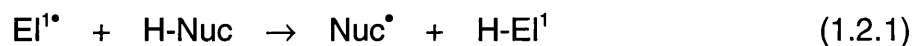
a) a nucleophilic radical

B-H

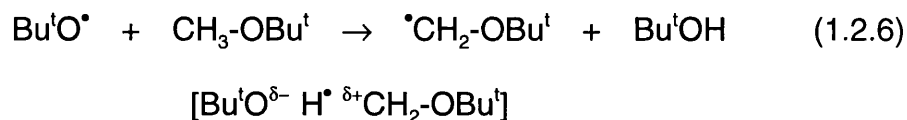
b) an electrophilic radical

Figure 1.1.1: Important frontier orbital interactions for radicals with a) high-energy SOMOs and b) low-energy SOMOs and a hydrogen donor B-H.

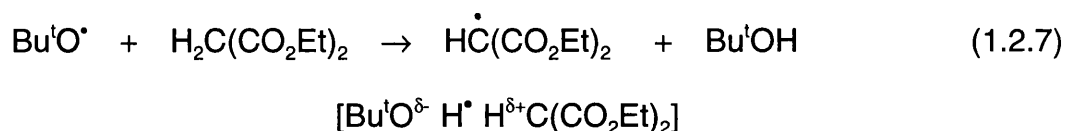
(1.2.2) and (1.2.3)-(1.2.4), respectively. Both steps in each catalytic cycle now benefit from favourable polar effects.



The molecules H-Nuc and H-EI are referred to as "donor" and "acceptor" polarity reversal catalyst, respectively.^{8,9} For most of the work presented in this thesis we have used amine-alkylborane complexes ($\text{X}_3\text{N} \rightarrow \text{BH}_2\text{R}$) to act as donor polarity reversal catalysts, in order to facilitate H-atom abstraction from electron deficient C-H bonds by the readily available t-butoxyl radical ($\text{Bu}^t\text{O}^{\bullet}$) [eqn.(1.2.5)]. This radical, like other alkoxy radicals, is highly electrophilic,²⁻⁴ its ionisation energy and electron affinity are 12 and 1.89 eV.

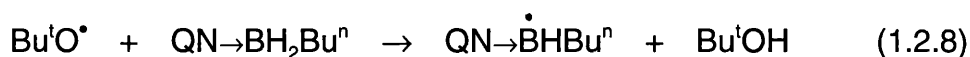


1.2.1



1.2.2

respectively, and as such its chemical reactivity is strongly influenced by polar factors. The t-butoxyl radical readily abstracts the electron rich hydrogen from a C-H bond adjacent to an electron donating group^{8,9} such as O in alcohols and ethers [eqn. (1.2.6)], while abstraction of an electron deficient hydrogen *e.g.* from a C-H adjacent to an electron withdrawing group, such as in esters, nitriles, ketones *etc.* [eqn. (1.2.7)] is usually slow because of unfavourable polar effects, the charge transfer structure of the type shown in 1.2.2 being disfavoured. In the presence of an amine-alkylborane (*e.g.* $\text{QN} \rightarrow \text{BH}_2\text{Bu}^n$; QN = quinuclidine), the single slow step (1.2.7) is replaced by two fast steps (1.2.8) and (1.2.9), both of which now benefit from favourable polar effects. The charge transfer structure 1.2.3 is now making an appreciable contribution to the TS.



1.2.3

When a sample containing di-*t*-butyl peroxide (DTBP), diethyl malonate and quinuclidine-methylborane in oxirane solvent is UV irradiated in the cavity of the ESR spectrometer, only the malonyl radical $\dot{\text{H}}\text{C}(\text{CO}_2\text{Et})_2$ [$a(\text{H}_\alpha) = 20.35$, $a(4\text{H}_\beta) = 1.40$ G, $g = 2.0040$ (Figure 1.2.1a)] can be detected. In the absence of quinuclidine-methylborane abstraction from diethyl malonate does not take place and, instead the *t*-butoxyl radical abstracts a hydrogen from the oxirane solvent to form the oxiranyl radical [$a(\text{H}_\alpha) = 24.55$, $a(2\text{H}_\beta) = 5.40$ G, $g = 2.0030$ (Figure 1.2.1b)].

1.3. Amine-Boryl Radicals

The N→B linkage in amine-boryl radicals and amine-boranes is isoelectronic with the C-C moiety of organic systems. Ammonia-borane ($\text{H}_3\text{N}\rightarrow\text{BH}_3$) is isoelectronic with ethane and the two possible radicals derived by H-atom abstraction from ammonia-borane ($\text{H}_3\text{N}\rightarrow\dot{\text{B}}\text{H}_2$ and $\text{H}_2\dot{\text{N}}\rightarrow\text{BH}_3$) are isoelectronic with the ethyl radical ($\text{CH}_3\dot{\text{C}}\text{H}_2$). ESR studies of the temperature dependence of the ^{11}B and α -proton coupling constants for amine-boryl radicals show that the geometry of these radicals is pyramidal at the boron centre.^{10,11} The ^{11}B ($I = 3/2$, natural abundance 80.2%) splittings are large (ca. 60 G) and correspond to 8.9 % unpaired electron of the B-2s atomic orbital.¹² The value of $a(^{11}\text{B})$ decreases slightly with increasing temperature, which implies that the time average configuration becomes more nearly planar at higher temperature, as expected for a pyramidal equilibrium geometry.

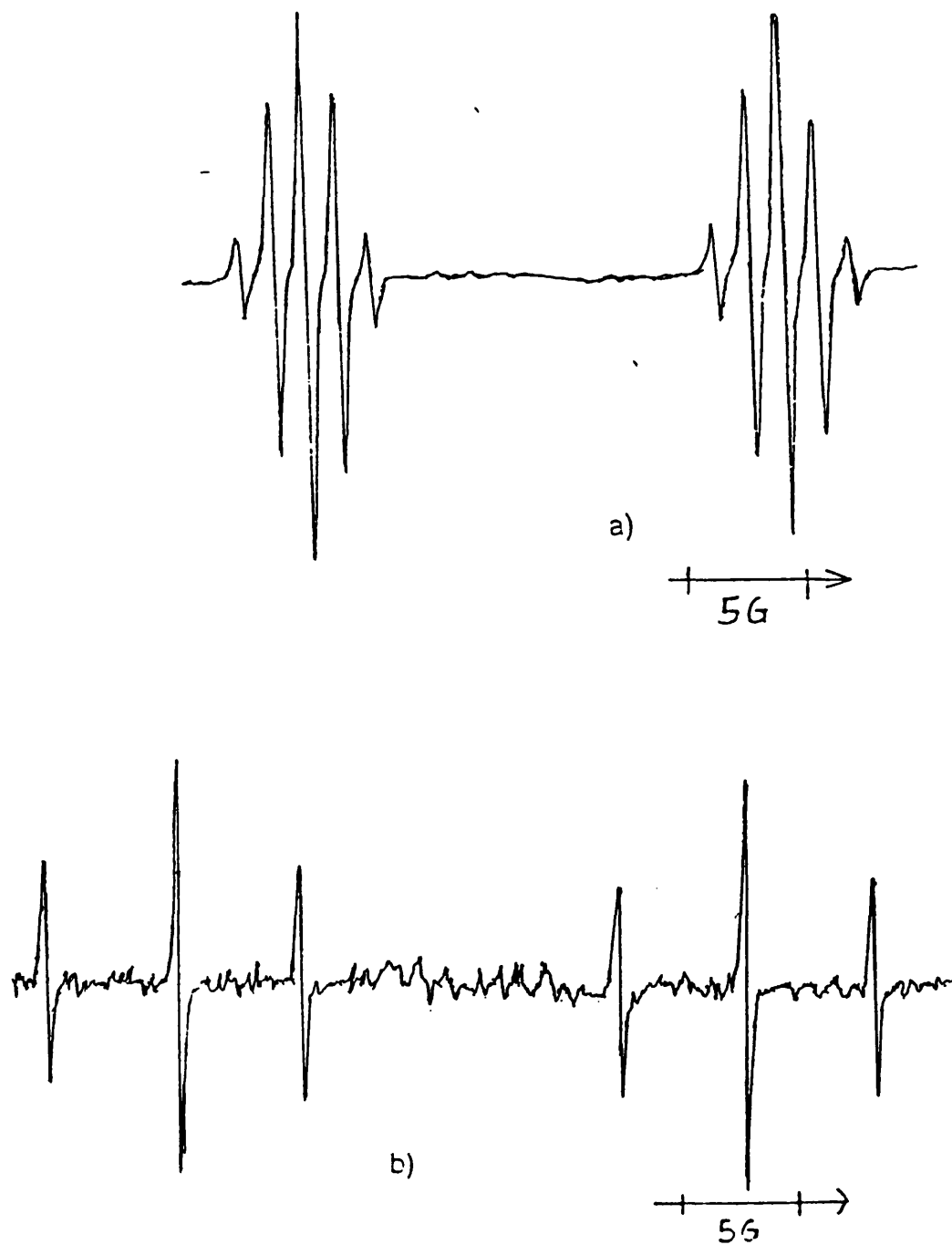
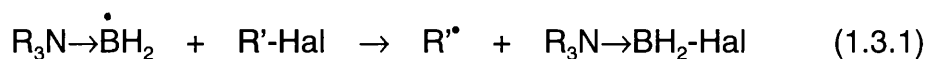


Figure 1.2.1: ESR spectra recorded during UV photolysis of a) DTBP in the presence of diethyl malonate and QN-BH₂Bu, and b) in the absence of the amine-borane.

As well as readily abstracting a hydrogen atom from electron deficient C-H bonds, amine-boryl radicals react rapidly with both alkyl chlorides and alkyl bromides to give alkyl radicals [eqn. (1.3.1)]. In general, bromine abstraction from an alkyl bromide by a ligated boryl radical is faster than chlorine



abstraction from alkyl chloride.¹³ In these reactions, the behaviour of $\text{R}_3\text{N}\rightarrow\dot{\text{B}}\text{H}_2$ resembles more that of trialkylsilyl radicals,¹⁴⁻¹⁶ rather than that of the isoelectronic alkyl radicals and reflects the "diagonal" relationship between boron and silicon in the Periodic Table. The higher reactivity of amine-boryl radicals ($\text{R}_3\text{N}\rightarrow\dot{\text{B}}\text{H}_2$) towards alkyl halide than their isoelectronic alkyl radical counterparts ($\text{R}_3\text{C}\cdot\text{CH}_2$) is due to the influence of both thermodynamic and polar factors. The transition state for dehalogenation of an alkyl halide by an amine-boryl radical involves a considerable degree of charge transfer from $\text{R}_3\text{N}\rightarrow\dot{\text{B}}\text{H}_2$ to the alkyl halide which favours abstraction by the nucleophilic boron-centred radical, (**1.3.1a-1.3.1b**). The B-halogen bond is probably stronger than the C-halogen bond, because of the electropositive nature of boron.

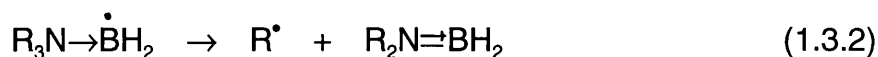


1.3.1a

1.3.1b

Unlike alkylsilyl radicals, amine-boryl radicals may undergo ready

unimolecular β -scission [eqn. (1.3.2)] and, they do so much more readily than alkyl radicals.¹⁰ This is an important point which must be considered when designing new polarity reversal catalysts.



1.3.2

For example, the t-butyl dimethylamine-boryl radical **1.3.3** undergoes rapid β -scission to form the t-butyl radical and **1.3.4** [eqn. (1.3.3)]¹⁰ unlike the isoelectronic $Bu^tMe_2C\cdot\dot{C}H_2$, which shows no sign of decomposition under similar conditions. β -Scission also takes place rapidly for $Pr^i_2EtN\rightarrow\dot{B}H_2$ to form the isopropyl radical (Pr^i^\bullet), although it is *ca.* 3.7 times slower than that of $Bu^tMe_2N\rightarrow\dot{B}H_2$ at 221 K.¹⁷



1.3.3

1.3.4

The high rate of β -scission of amine-boryl radicals compared with isoelectronic alkyl radicals is attributed to thermodynamic factors, with the difference in strength of the $N\rightarrow B$ and $N\rightleftharpoons B$ being much greater than the corresponding difference in strengths of the $C-C$ and $C=C$ bonds.¹⁷

1.4. Radical Addition to Alkenes

Addition of carbon-centred radicals to a coordinatively unsaturated carbon in a suitable acceptor molecule, especially an alkene, is an important synthetic tool for the formation of C-C bonds.¹⁸⁻²⁰ A number of factors are thought to play an important role in determining the rate of radical addition to alkenes.²¹ The overall thermochemistry of addition is important as well as polar, steric and stereoelectronic effects which all influence the energy of the transition state. Such homolytic addition to alkenes [eqn. (1.4.1)] is markedly influenced by polar factors^{10,22-25} and simple alkyl radicals add only relatively slowly unless EWGs are attached to the C=C moiety. For example, addition



of cyclohexyl radicals to $\text{CH}_2=\text{CHZ}$ is 6000 times faster when Z is CN than when it is n-butyl.²⁶ Electrophilic carbon radicals, with one or more EWGs attached to C_α , add more readily to simple alkenes¹⁹⁻²⁰ and there is much current interest in synthetic methods based on inter- and intra-molecular additions of radicals of the type $\dot{\text{R}}\text{C}(\text{EWG})_2$ (EWG = CO_2R or CN in particular).^{18-19,27-33}

The origin of polar effects in radical addition to alkenes can be understood in terms of frontier molecular orbital theory or valence bond

theory.³⁴ The interactions between the methyl radical and ethene, (Figure 1.4.1a), serve as a point of reference and, will be mainly between the radical's SOMO and the alkene's π HOMO, and its π^* LUMO. Both interactions are roughly equal and, as a result the overall stabilisation is relatively small. If the alkene has an electron withdrawing substituent (Figure 1.4.1b), then its LUMO will be lower in energy and the SOMO-LUMO interaction will be more important than the SOMO-HOMO interaction; the SOMO is then lowered in energy, resulting in stabilisation of the transition state. If the radical has a π -donating group at C_α (Figure 1.4.1c), then its SOMO will be raised in energy and will interact more strongly with the alkene's LUMO than its HOMO, again resulting in stabilisation. Therefore, a nucleophilic radical (high energy SOMO) will react more readily with an alkene having a low energy LUMO (EWGs attached to the alkene moiety) and, conversely, an electrophilic radical (low energy SOMO) will react faster with an alkene having a high energy HOMO (EDGs attached to the alkene moiety). For example, the t-butyl radical, with 3π -donating methyl groups, reacts 24 times faster with diethyl vinylphosphonate than does the methyl radical at 233 K. Replacing CH_3 by electron withdrawing substituents such as CN, further decreases the rate of addition.²³

Another interesting point about radical addition to alkenes is the regioselectivity of the addition. The normal regioselectivity for the addition of

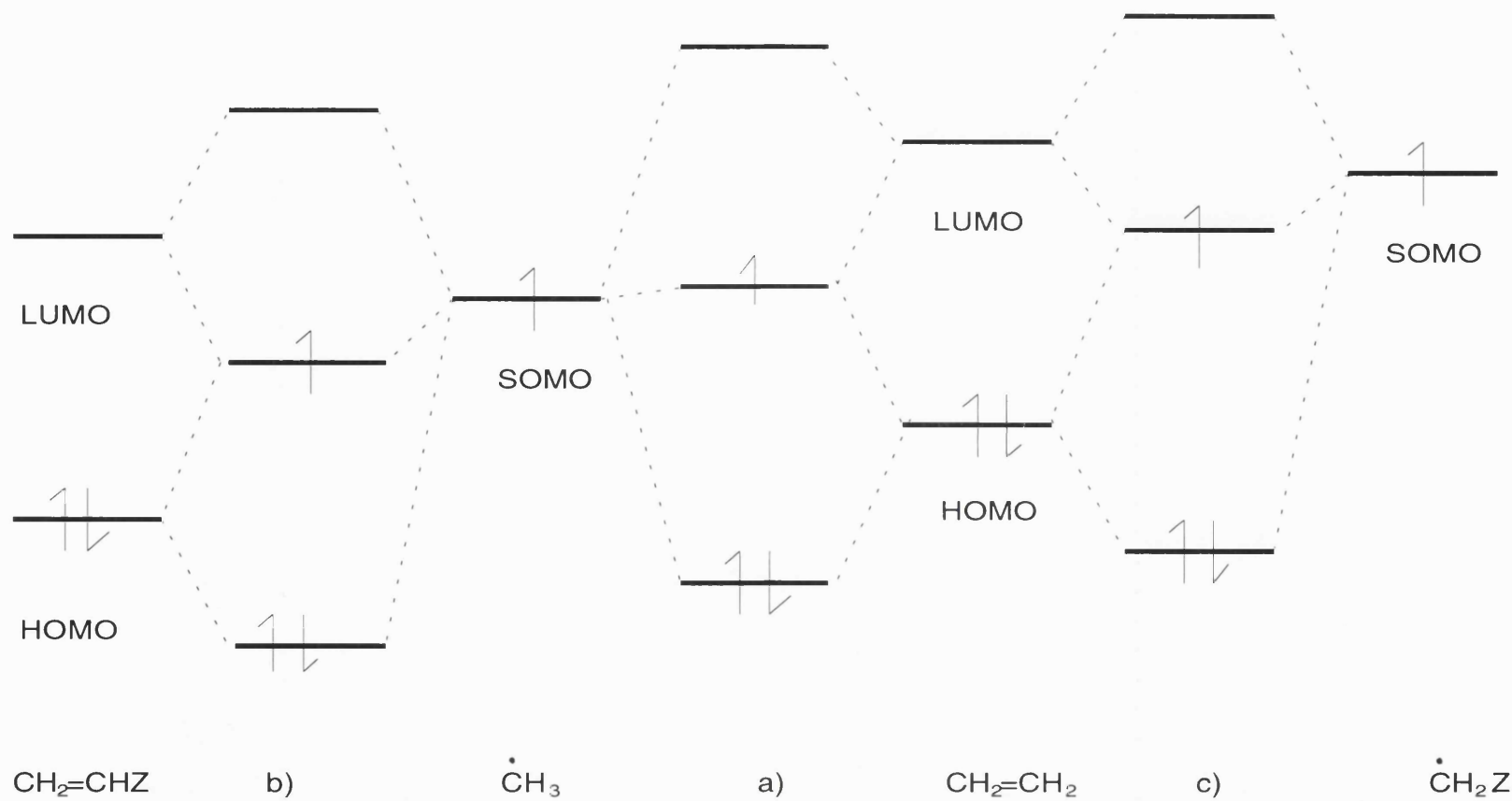
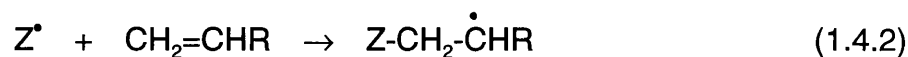


Figure 1.4.1: Important frontier orbital interactions for a radical and an alkene, a) between the methyl radical and ethene (reference point), b) $Z = \text{EWG}$, low-energy LUMO, c) nucleophilic radical, high energy SOMO.

a radical to an alkene is addition to the least substituted end of the double bond [eqn. (1.4.2)].³⁵ Studies of the relative rates of addition to alkenes show that



although electron-withdrawing and -donating effects are important in determining the relative rates of addition, the regioselectivity is primarily determined by steric effects which make the terminal position more accessible to the attacking radical, as well as electronic factors that make a secondary radical more stable than its primary counterpart.

1.5. Free Radical Addition to Alkyl Isocyanides

There is renewed interest in the addition of carbon-centred radicals to alkyl isocyanides which can provide a novel method for one carbon-bond homologation.³⁶⁻³⁸ There are comparatively very few methods using free radicals to extend the chain by just one carbon atom. Such examples may be found with carbon monoxide, isoelectronic counterpart of an alkyl isocyanide, which may be used to trap carbon-centred radicals, to form acyl radicals. These acyl radicals can undergo addition to an alkene, eventually to form a ketone.³⁹⁻⁴¹ Radical addition to formaldehyde can also provide a route for one-carbon chain extension, eventual products being alcohols or aldehydes.⁴²

A variety of reactive free radicals are known to add to the terminal carbon atom of an isocyanide to form an imidoyl radical [1.5.1, eqn. (1.5.1)].⁴³⁻⁴⁹

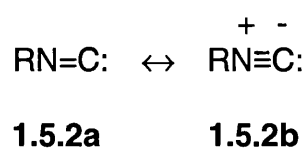
While many types of radical X[•] (e.g. RO[•], R₃Si[•], RS[•], R₃Sn[•]) add rapidly to give



1.5.1

imidoyl radicals, simple alkyl radicals such as CH₃[•] add only very slowly.⁴⁸⁻⁵¹

Alkyl isocyanides are neutral, two electron donor ligands which are isoelectronic with carbon monoxide and dinitrogen. In valence bond theory, alkyl isocyanides may be described as a hybrid of canonical structures 1.5.2a and 1.5.2b. Consideration of structure 1.5.2b indicates that the terminal carbon of an isocyanide is relatively electron rich and this suggests that polar effects should favour the addition of more electrophilic carbon-centred radicals to form imidoyl radicals.



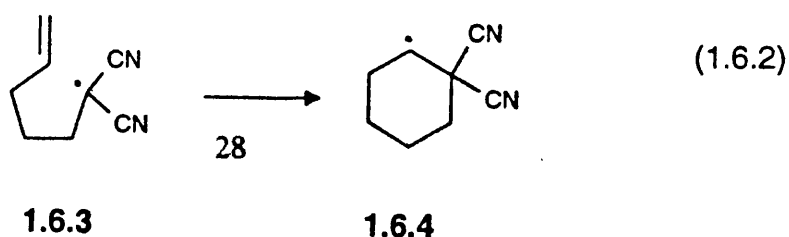
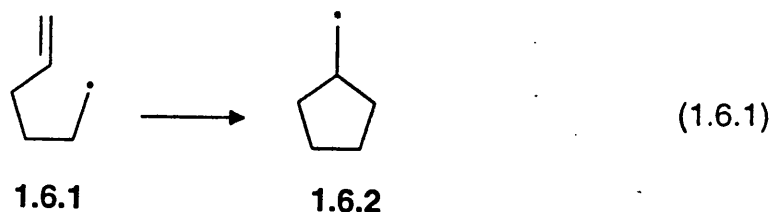
Imidoyl radicals 1.5.1 are isoelectronic with vinyl and acyl radicals, they exhibit relatively low *g*-factors (e.g. 2.0016 for Bu¹N=[•]CBu¹), less than the free spin value (2.0023) and relatively small splitting from any β-hydrogen atom in

the X group. These ESR parameters are consistent with the formulation of 1.5.1 as " σ -type" radicals,^{48-49,52} in which the unpaired electron is in an orbital which occupies the NCX plane.⁵³

1.6. Cyclisation of Alkenyl Radicals

Cyclisation reactions of the hex-5-enyl radical 1.6.1 and its derivatives have attracted considerable interest from both a theoretical and practical point of view.^{27-29,32,54-58} Radical cyclisations have emerged as a mild and powerful method for the formation of rings,^{27-29,32,54-55} because of the regioselectivity with which alkenyl radicals cyclise.

The hex-5-enyl radicals 1.6.1 cyclise irreversibly to yield mainly the cyclopentylmethyl radical⁵⁶⁻⁵⁸ [1.6.2, eqn. (1.6.1)], with a rate constant of $k_c = 1 \times 10^5 \text{ s}^{-1}$ at 25 °C; the isomeric cyclohexyl radical is formed only to the extent of about 2%. However, the secondary cyclohexyl radical produced by 1,6-*endo*-cyclisation is thermodynamically more stable and the kinetic preference for the cyclopentylmethyl radical is attributed to stereoelectronic factors.



The ideal SOMO-LUMO overlap (attack angle *ca.* 109 °) is better accommodated in the transition state for 5-*exo*-cyclisation than in the 6-*endo*-cyclisation. In addition because the transition state is early, the torsional strain in the 5-*exo*-cyclisation resembles a 6-membered ring whilst the transition state for 6-*endo*-cyclisation resembles a 7-membered ring.^{27,59}

In contrast cyclisation of stabilised radicals of the type **1.6.3** is readily reversible and under conditions of thermodynamic control, gives rise to products containing a 6-membered ring [eqn. (1.6.2)]. The stabilising groups at the carbon radical centre decrease the rate of cyclisation and increase the rate of ring opening of the cyclised radical.²⁸

1.7. References to Chapter 1

- 1 C. Walling, *Free Radicals in solution*, Wiley, New York, 1957
- 2 G. A. Russell, in *Free Radicals*, ed. J.K. Kochi, Wiley-Interscience, vol.1.
- 3 F. Minisci and A. Citterio, *Adv. Free Radical Chem.*, 1980, **6**, 65.
- 4 *Substituent Effects in Free Radical Chemistry*, eds. H. G. Viehe, Z. Janousek and R. Merenyi, Reidel, Dordrecht, 1986.
- 5 R.E. Pearson and J.C. Martin, *J. Am. Chem. Soc.*, 1963, **85**, 354.
- 6 G. A. Russell, ref. 2, p. 311.
- 7 G. A. Russell, ref. 2, p. 275.
- 8 S.J. Cole, J.N. Kirwan, B.P. Roberts and C.R. Willis, *J. Chem. Soc., Perkin Trans. 2*, 1991, 103.
- 9 P. Kaushal, P.L.H. Mok and B.P. Roberts, *J. Chem. Soc., Perkin Trans. 2*, 1990, 1663.
- 10 J.A. Baban and B.P. Roberts, *J. Chem. Soc., Perkin Trans. 2*, 1981, 161.
- 11 V. Paul and B.P. Roberts, *J. Chem. Soc., Perkin Trans. 2*, 1988, 1183.
- 12 M.C.R. Symons, *Chemical and Biochemical Aspects of Electron Spin Resonance Spectroscopy*, Van Nostrand Reinhold, London, 1978.
- 13 J.A. Baban and B.P. Roberts, *J. Chem. Soc., Chem. Commun.*, 1983, 1224.
- 14 R.A. Jackson, *Essays on Free Radical Chemistry, Chem. Soc. Special Publication 24*, The Chemical Society, 1970, ch. 12.

- 15 A. Hudson and R.A. Jackson, *J. Chem. Soc., Chem. Commun.*, 1969, 1323.
- 16 C. Chatgililoglu, K.U. Ingold and J.C. Scaiano, *J. Am. Chem. Soc.*, 1982, **104**, 5123.
- 17 J.A. Baban and B.P. Roberts, *J. Chem. Research (S)*, 1986, 30.
- 18 B. Giese, *Radicals in Organic Synthesis: Formation of Carbon-Carbon Bonds*, Pergamon Press, Oxford, 1986.
- 19 A. Ghosez, B. Giese and H. Zipse in *Methoden der Organischen Chemie (Houben-Weyl): C-Radikale*, eds. M. Regitz and B. Giese, Thieme, Stuttgart, 1989, ch.9.
- 20 D.P. Curran, *Synthesis*, 1988, 417, 489.
- 21 D.C. Nonhebel and J.C. Walton, *Free Radical Chemistry*, Cambridge University Press, Cambridge, 1974, ch.8.
- 22 J.M. Tedder and J.C. Walton, *Tetrahedron*, 1980, **36**, 701.
- 23 J.M. Tedder, *Angew. Chem., Internat. Edn. Engl.*, 1982, **21**, 401.
- 24 P.L. Abell, in *Free Radicals*, ed. J.K. Kochi, Wiley-Interscience, New York, 1973, vol. 2, ch. 13.
- 25 B. Giese and J. Meister, *Angew. Chem., Internat. Ed. Engl.*, 1977, **16**,178.
- 26 B. Giese, *Angew. Chem., Internat. Ed. Engl.*, 1983, **22**, 753.
- 27 D.P. Curran and C.-T. Chang, *J. Org. Chem.*, 1989, **54**, 3140.
- 28 D.P. Curran, E. Bosch, J. Kaplan and M. Newcomb, *J. Org. Chem.*, 1989, **54**, 1826.

- 29 D.P. Curran, M.-H. Chen, E. Spletzer, C.M. Seong and C.-T. Chang, *J. Am. Chem. Soc.*, 1989, **111**, 8872.
- 30 B. Giese, H. Horler and M. Leising, *Chem. Ber.*, 1986, **119**, 444.
- 31 J.H. Byers and G.C. Lane, *Tetrahedron Lett.*, 1990, **31**, 5697.
- 32 D.P. Curran and C.M. Seong, *J. Am. Chem. Soc.*, 1990, **112**, 9401.
- 33 K. Riemenschneider, H.M. Bartels, R. Dornow, E. Drechsel-Grau, W. Eichel, H. Luthe, Y. Matter, W. Michaelis and P. Boldt, *J. Org. Chem.*, 1987, **52**, 205.
- 34 K.S. Lowry and T.H. Richardson, *Advanced Organic Chemistry*, eds. K.S. Laury and T.H. Richardson, 3rd ed.
- 35 G.J. Gleicher, B. Mahiou and A.J. Aretakis, *J. Org. Chem.*, 1989, **54**, 308.
- 36 M.D. Bachi and D. Denenmark, *J. Am. Chem. Soc.*, 1989, **111**, 1886.
- 37 C. Chatgililoglu, B. Giese and B. Kopping, *Tetrahedron Lett.*, 1990, **31**, 6013.
- 38 D.P. Curran and H. Liu, *J. Am. Chem. Soc.*, 1991, **113**, 2127.
- 39 I. Ryu, K. Kusano, H. Yamasaki and N. Sonoda, *J. Org. Chem.*, 1991, **56**, 5003.
- 40 I. Ryu, K. Kusano, A. Ogawa, N. Kambe and N. Sonoda, *J. Am. Chem. Soc.*, 1990, **112**, 1295.
- 41 I. Ryu, K. Kusano, M. Hasegawa, N. Kambe and N. Sonoda, *J. Chem. Soc., Chem. Commun.*, 1991, 1018.
- 42 J.R. Sanderson, J.J. Lin, R.G. Duranleau, E.L. Yeakey and E.T. Marquis,

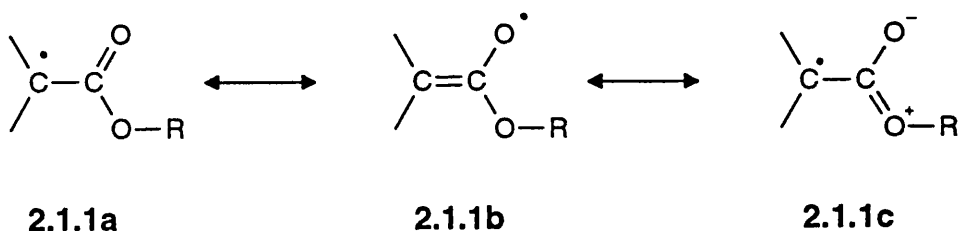
- J. Org. Chem.*, 1988, **53**, 2859.
- 43 T. Saegusa and Y. Ito, in *Isonitrile Chemistry*, ed. I. Ugi, Academic Press, New York, 1971, ch. 4.
- 44 R.E. Banks, R.N. Haszeldine and C.W. Stephens, *Tetrahedron Lett.*, 1972, 3699.
- 45 L.A. Singer and S.S. Kim, *Tetrahedron Lett.*, 1974, 861.
- 46 S.S. Kim, *Tetrahedron Lett.*, 1977, 2741.
- 47 M. Meier and C. Rüchardt, *Tetrahedron Lett.*, 1983, **24**, 4671.
- 48 P.M. Blum and B.P. Roberts, *J. Chem. Soc., Chem. Commun.*, 1976, 535.
- 49 P.M. Blum and B.P. Roberts, *J. Chem. Soc., Perkin Trans. 2*, 1978, 1313.
- 50 G. Stork and P.M. Sher, *J. Am. Chem. Soc.*, 1983, **105**, 6765.
- 51 G. Stork, P.M. Sher and H.-L. Chen, *J. Am. Chem. Soc.*, 1986, **108**, 6384.
- 52 W.C. Danen and C.T. West, *J. Am. Chem. Soc.*, **95**, 1973, 6872.
- 53 R.O.C. Norman and B.C. Gilbert, *J. Phys. Chem.*, 1967, **71**, 14.
- 54 E. Baciocchi, A.B. Paolobelli and R. Ruzziconi, *Tetrahedron*, 1992, **48**, 4617.
- 55 D.P. Curran, T.M. Morgan, C.E. Schwartz, B.B. Snider and M.A. Dombronski, *J. Am. Chem. Soc.*, 1991, **113**, 6607.
- 56 D. Lal, D. Griller, S. Husband and K.U. Ingold, *J. Am. Chem. Soc.*, 1974, **96**, 6355.

- 57 P. Schmidt, D. Griller and K.U. Ingold, *Internat. J. Chem. Kinetics*, 1979, **10**, 333
- 58 C. Chatgililoglu, K.U. Ingold and J.C. Scaiano, *J. Am. Chem. Soc.*, 1981, **103**, 7739.
- 59 A.L.J. Beckwith and S. Glover, *Aust. J. Chem.*, 1978, **40**, 157.

Chapter 2: RESULTS AND DISCUSSION

2.1. (Alkoxy carbonyl)alkyl Radicals $R^1\dot{C}(CO_2R^2)_2$

Many α -(alkoxy carbonyl)alkyl radicals have already been studied by ESR spectroscopy in solids and liquid solutions. The ESR parameters have generally been discussed in terms of the general planar bonding structure **2.1.1a-c** with some spin delocalisation and partial π -electron delocalisation.¹

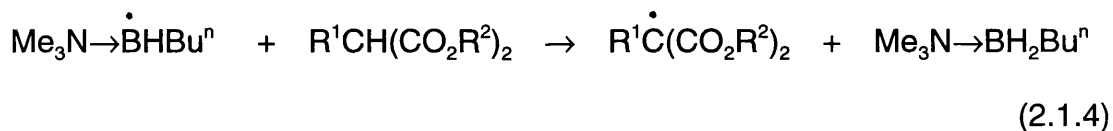
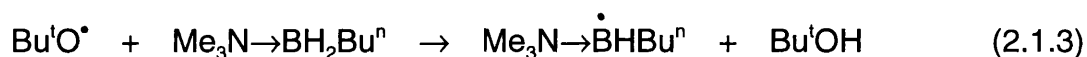


In order to generate the electrophilic (alkoxy carbonyl)alkyl radicals efficiently we made use of the principle of polarity reversal catalysis.²

The t-butoxyl radical (Bu^1O^*) may be produced readily by UV irradiation of t-butyl peroxide (DTBP) [eqn. (2.1.1)], but these radicals are electrophilic and abstract an α -hydrogen atom only very slowly from malonates $R^1CH(CO_2R^2)_2$ or from $HC(CO_2Et)_3$ because of unfavourable polar effects.²



However this abstraction is efficiently promoted in the presence of trimethylamine-butyborane,³ which acts as a polarity reversal catalyst,²⁻⁸ such that the single step (2.1.2) is replaced by the catalytic cycle of fast reactions (2.1.3) and (2.1.4).



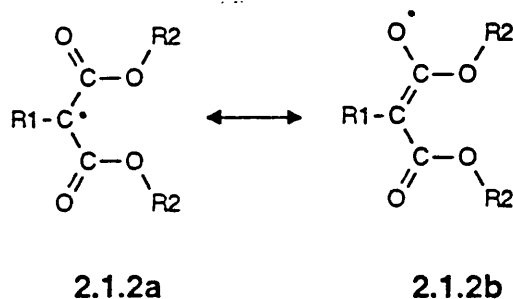
This method of radical production avoids the possible complications which often arise from chain reactions and from the reactive by-products accompanying the use of α -halogenomalonates.

UV irradiation at 180-230 K of a cyclopropane solution containing DTBP (ca. 15 % v/v), an ester $\text{R}^1\text{CH}(\text{CO}_2\text{R}^2)_2$ (0.5-1 mol dm⁻³) and $\text{Me}_3\text{N}\rightarrow\text{BH}_2\text{Bu}^{n*}$ (ca.

* Trimethylamine-methylborane was also used as a polarity reversal

0.2 mol dm⁻³) afforded the ESR spectrum of the corresponding radical R¹C(CO₂R²)₂. The tris(ethoxycarbonyl)methyl radical, [•]C(CO₂Et)₃, was generated in the same way from triethyl methanetricarboxylate (0.3-0.4 mol dm⁻³) at 220 K; this ester was not very soluble in cyclopropane at lower temperatures. ESR parameters for these radicals are reported in Table 2.1.1, and the ESR spectrum of EtC(CO₂Et)₂ is shown in Figure 2.1.1.

In general, the (alkoxycarbonyl)alkyl radicals exhibited *g*-values (ca. 2.0040) greater than the free spin value of 2.0023. These radicals can be described as π-radicals and, as such the unpaired electron resides in a p-orbital and is partly delocalised onto oxygen, structures 2.1.2a-2.1.2b.



Using the McConnell equation (2.1.5) and taking *Q* as -23 G, we were able to calculate the unpaired spin population on the α-carbon ($\rho_{\text{C}\alpha}\pi$) (Table 2.1.2), which is essentially independent of the nature of R¹.

catalyst in some experiments but this amine-borane is less soluble in hydrocarbons than is trimethylamine-butylborane.

Table 2.1.1: ESR parameters for bis(alkoxycarbonyl)alkyl radicals in cyclopropane.

Radical	T/K	g-Factor	Hyperfine splittings/G		
			$a(1H_\alpha)$	$a(nH_\beta)^a$	Others
$\dot{H}C(CO_2Et)_2$	179	2.0039	20.35	---	1.30(4H $_\delta$)
$\dot{H}C(CO_2Bu^i)_2$	179	2.0039	20.32	---	---
$\dot{H}C(CO_2SiMe_3)_2$	177	2.0039	20.08	---	---
$\dot{H}C(CO_2CH_2Ph)_2$	178	2.0039	20.27	---	1.40(4H $_\delta$)
$Me\dot{C}(CO_2Et)_2$	183	2.0036	---	23.82(3)	0.89(4H $_\delta$)
$Et\dot{C}(CO_2Et)_2$	246	2.0035	---	13.75(2) ^b	0.37(3H $_\gamma$), 0.94(4H $_\delta$)
$Bu\dot{C}(CO_2Et)_2$	184	2.0034	---	12.85(2)	0.40(1H $_\gamma$), ^c 1.03(4H $_\delta$)
$Bu^i\dot{C}(CO_2Et)_2$	243	2.0034	---	---	0.55(9H $_\gamma$), 1.24(4H $_\delta$)
$H_2C=CH(CH_2)_3\dot{C}(CO_2Et)_2$	187	2.0035	---	12.92(2) ^d	0.98(4H $_\delta$) ^e
$\dot{C}(CO_2Et)_3$	197	2.0037	---	---	0.77(6H $_\delta$)

^a Numbers of nuclei shown in parentheses. ^b $a(2H_\beta) = 12.85$ G at 173 K. ^c Only one of the γ -protons gives resolvable splitting. ^d $a(2H_\beta) = 13.31$ G at 220 K.

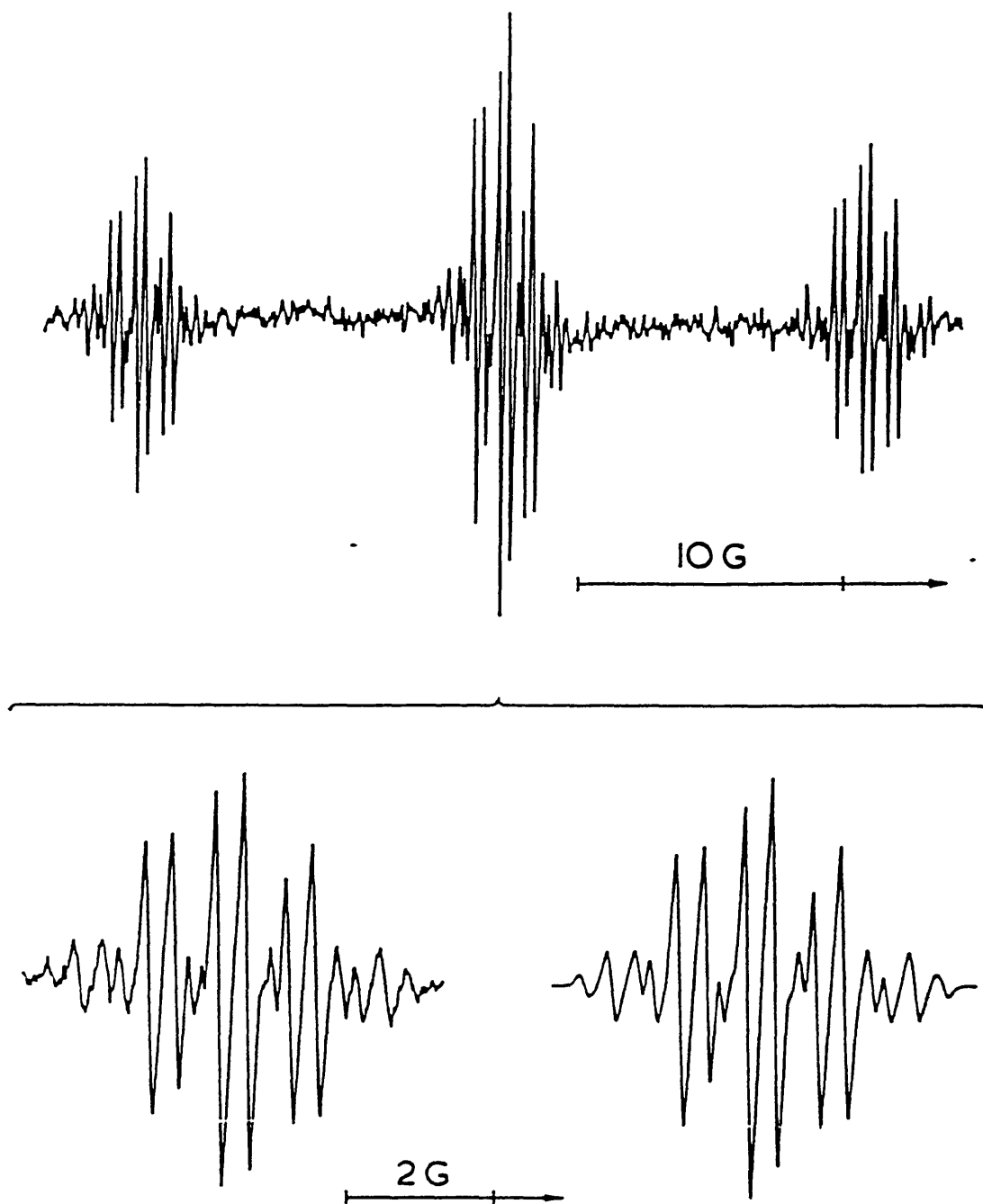


Figure 2.1.1: ESR spectrum of the radical $\text{Et}\dot{\text{C}}(\text{CO}_2\text{Et})_2$ at 234 K, produced by UV irradiation of a cyclopropane solution containing DTBP, TMBB and diethyl ethylmalonate. The central multiplet at 246 K is shown expanded alongside its computer simulation obtained using the parameters given in Table 2.1.1.

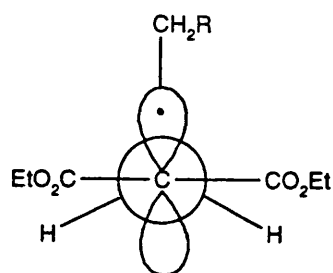
Table 2.1.2: Unpaired spin population at C_α ($\rho_{C_\alpha}^\pi$), calculated using equation (2.1.5), for some bis(alkoxycarbonyl)alkyl radicals

Radical	T/K	<i>g</i> -Factor	($\rho_{C_\alpha}^\pi$)
$\dot{H}C(CO_2Et)_2$	179	2.0039	0.89
$\dot{H}C(CO_2Bu^t)_2$	179	2.0039	0.89
$\dot{H}C(CO_2SiMe_3)_2$	177	2.0039	0.87
$\dot{H}C(CO_2CH_2Ph)_2$	178	2.0039	0.88

$$a(H\alpha) = Q\rho_{C\alpha}^{\pi} \quad (2.1.5)$$

Radicals of the type $R^1\dot{C}(CO_2R^2)_2$ are transient when $R^1 = H, Me$ or a primary alkyl group. In contrast the radical $Bu^t\dot{C}(CO_2Et)_2$ is a relatively persistent species, presumably because the radical centre is sterically hindered by the bulky t-butyl group and as such this radical is unable to undergo disproportionation. This radical was found to decay with mixed first- and second-order kinetics, with $t_{1/2} = 7$ s at 203 K.

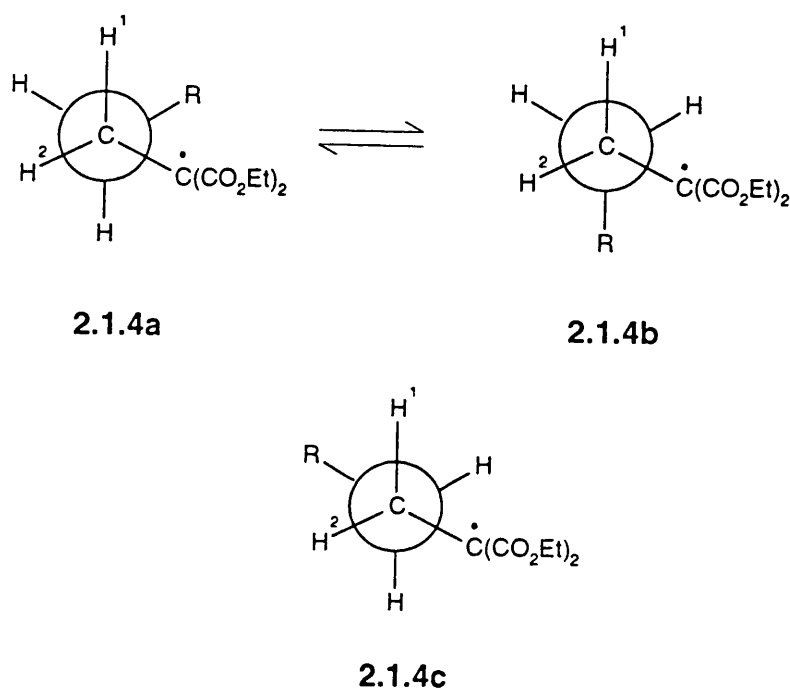
The values for $a(2H_\beta)$ for $RCH_2CH_2\dot{C}(CO_2Et)_2$ ($R = H, \text{alkyl}$) were found to be much smaller than the value for $a(3H_\beta)$ of $Me\dot{C}(CO_2Et)_2$. The value of $a(2H_\beta)$ was also found to increase with increasing temperature indicating⁹ that the preferred conformation for this type of radicals is that shown in **2.1.3**, which is what would be expected on steric grounds.



2.1.3

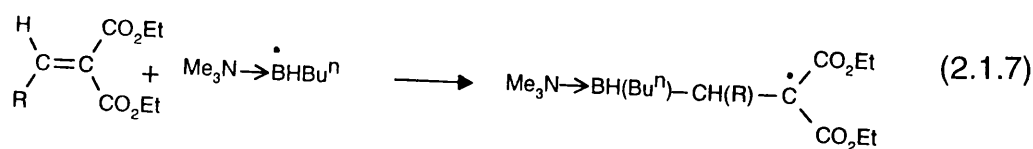
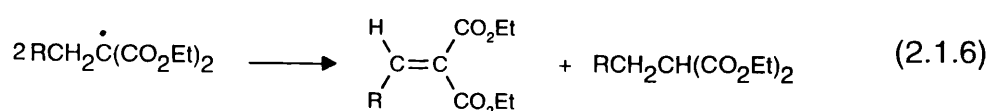
When R is other than H (see Table 2.1.1) the ESR spectra exhibited an alternating line-width effect such that the lines associated with $M_l(2H_\beta) = 0$ were selectively broadened at low temperatures. This lineshape effect was

attributed to the hindered rotation about the $C_\beta-C_\gamma$ bond, such that exchange involving conformations **2.1.4a-2.1.4b** took place on the ESR time scale. The existence of this lineshape effect requires that the conformations **2.1.4a** and **2.1.4b** must be significantly populated alongside the symmetrical conformation **2.1.4c**, and that the sum of the β -proton splittings for **2.1.4c** is similar to the sum for **2.1.4a/b**. An analogous situation exists for hindered rotation about the $C_\beta-C_\gamma$ bond in the butyl radical.¹⁰



Alongside each spectrum of $\dot{R}C(CO_2Et)_2$ ($R = \text{alkyl}$), broader less well defined lines from a relatively persistent radical were observed. This radical was barely detectable when R was methyl, but was much stronger with the larger alkyl groups. UV irradiation of a sample containing DTBP (ca. 15% v/v), $Et_2C(CO_2Et)_2$ (ca. 0.8 mol dm^{-3}) and trimethylamine-butylborane (ca.

0.3 mol dm⁻³ in cyclopropane solvent afforded the ESR spectrum of Me₃N→B[•]HBuⁿ only,² showing that the persistent radical was not derived by H-abstraction from a site other than C_α, or by addition to the ester functions. Since this persistent radical was not present immediately after the sample was first UV irradiated, this would suggest that these species may be derived from a self-reaction product of RC[•](CO₂Et)₂ and may arise from disproportionation of the alkyl malonyl radicals to form alkylidene malonates, which would be expected to react rapidly with nucleophilic radicals such as Me₃N→B[•]HBuⁿ [eqn. (2.1.6)-(2.1.7)]. The adduct radical **2.1.6** would be a relatively persistent species and exhibit a complex ESR spectrum with broad peaks since we would expect coupling to both ¹¹B (*I*=3/2) natural abundance (80%) as well as to the BH proton and H_β.



2.1.6

This is consistent with the persistent radical being least obvious with MeC(H)(CO₂Et)₂ (Figure 2.1.2), since the β-CH bonds in MeC[•](CO₂Et)₂ are expected to be strongest.

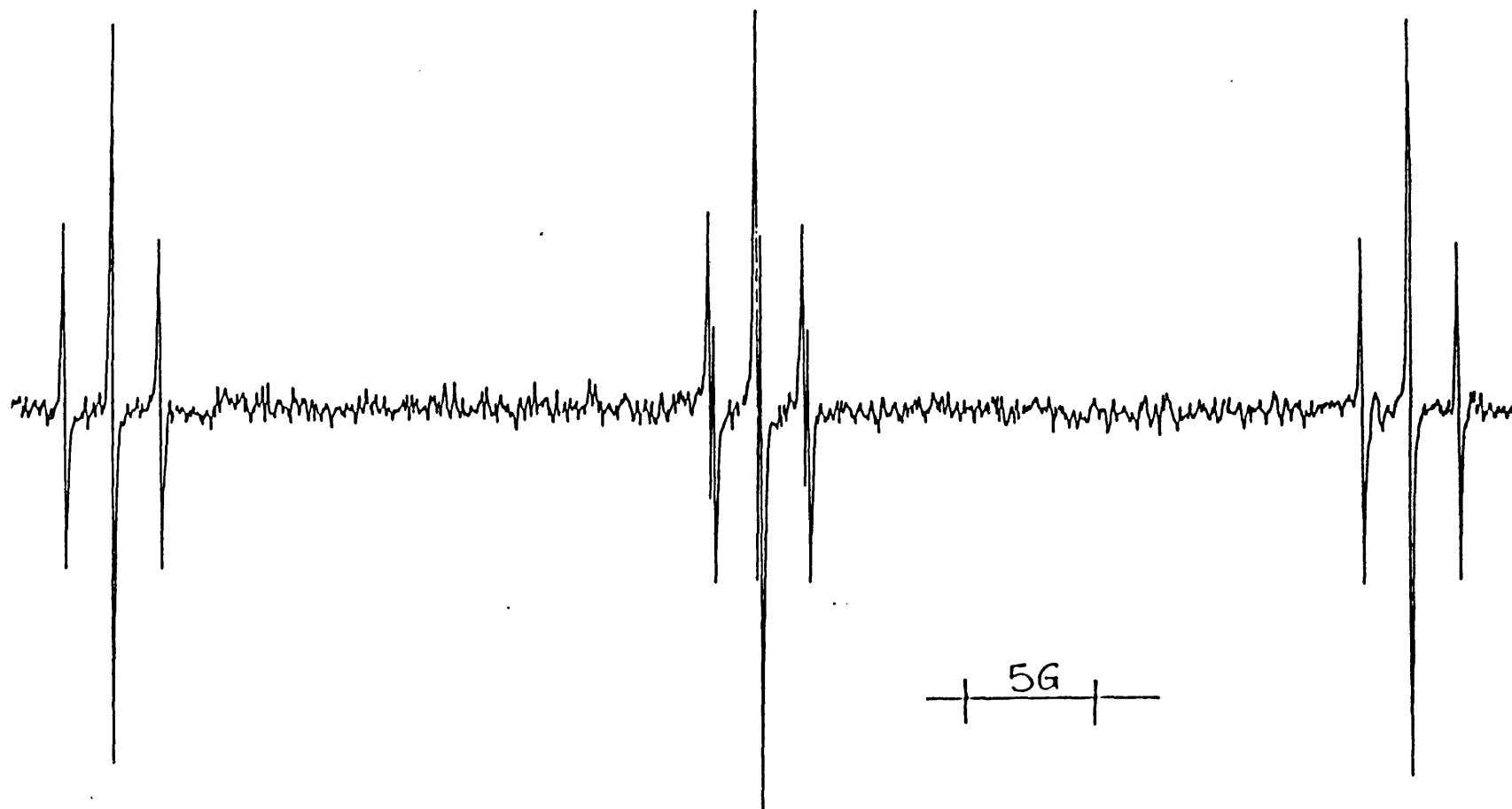


Figure 2.1.2: ESR spectrum of $\text{MeC}(\text{CO}_2\text{Et})_2$ at 187 K, produced by UV irradiation of a cyclopropane solution containing DTBP, TMBB and $\text{MeC}(\text{H})(\text{CO}_2\text{Et})_2$.

2.2. Addition of $\dot{\text{H}}\text{C}(\text{CO}_2\text{R})_2$, $\text{Me}\dot{\text{C}}(\text{CO}_2\text{Et})_2$ and $\dot{\text{C}}(\text{CO}_2\text{Et})_3$ to Alkenes

The (alkoxycarbonyl)alkyl radicals were generated as above using polarity reversal catalysis in the presence of an alkene. The ESR spectrum of the corresponding substituted alkyl radical adduct (e.g. **2.2.1**) was observed alongside the ESR spectrum of the parent (alkoxycarbonyl)alkyl radical, to an extent which increased with the concentration of alkene, increasing temperature and the nature of the addendum. In ethene solvent at ca. 180 K, the ESR spectrum of $\dot{\text{H}}\text{C}(\text{CO}_2\text{Et})_2$ was detected alongside a strong spectrum due to the adduct **2.2.1**, [(eqn. 2.2.1), (Figure 2.2.1)].



2.2.1

The ESR parameters for the adduct **2.2.1** at 189 K are reported in Table 2.2.1. The assignment of the narrow doublet splitting to the γ -proton was confirmed by recording the ESR spectrum of the γ -deuterium labelled adduct radical $[(\text{EtO}_2\text{C})_2\text{CD}-\text{CH}_2-\dot{\text{C}}\text{H}_2]$ generated from $\text{D}_2\text{C}(\text{CO}_2\text{Et})_2$.*

* In the absence of malonate, the amine-boryl radical $\text{Me}_3\text{N}\rightarrow\dot{\text{B}}\text{HBu}^n$ adds to ethene to give $\text{Me}_3\text{N}\rightarrow\text{BH}(\text{Bu}^n)\text{CH}_2\dot{\text{C}}\text{H}_2$. The β -protons are diastereotopic and the lines corresponding to $M_1(2\text{H}_\beta)$ were not observed at 180 K [$a(2\text{H}_\alpha) = 20.48$, $\bar{a}(2\text{H}_\beta) = 22.22$, $a(^{11}\text{B}) = 17.40$ G]. Corresponding addition to 2-

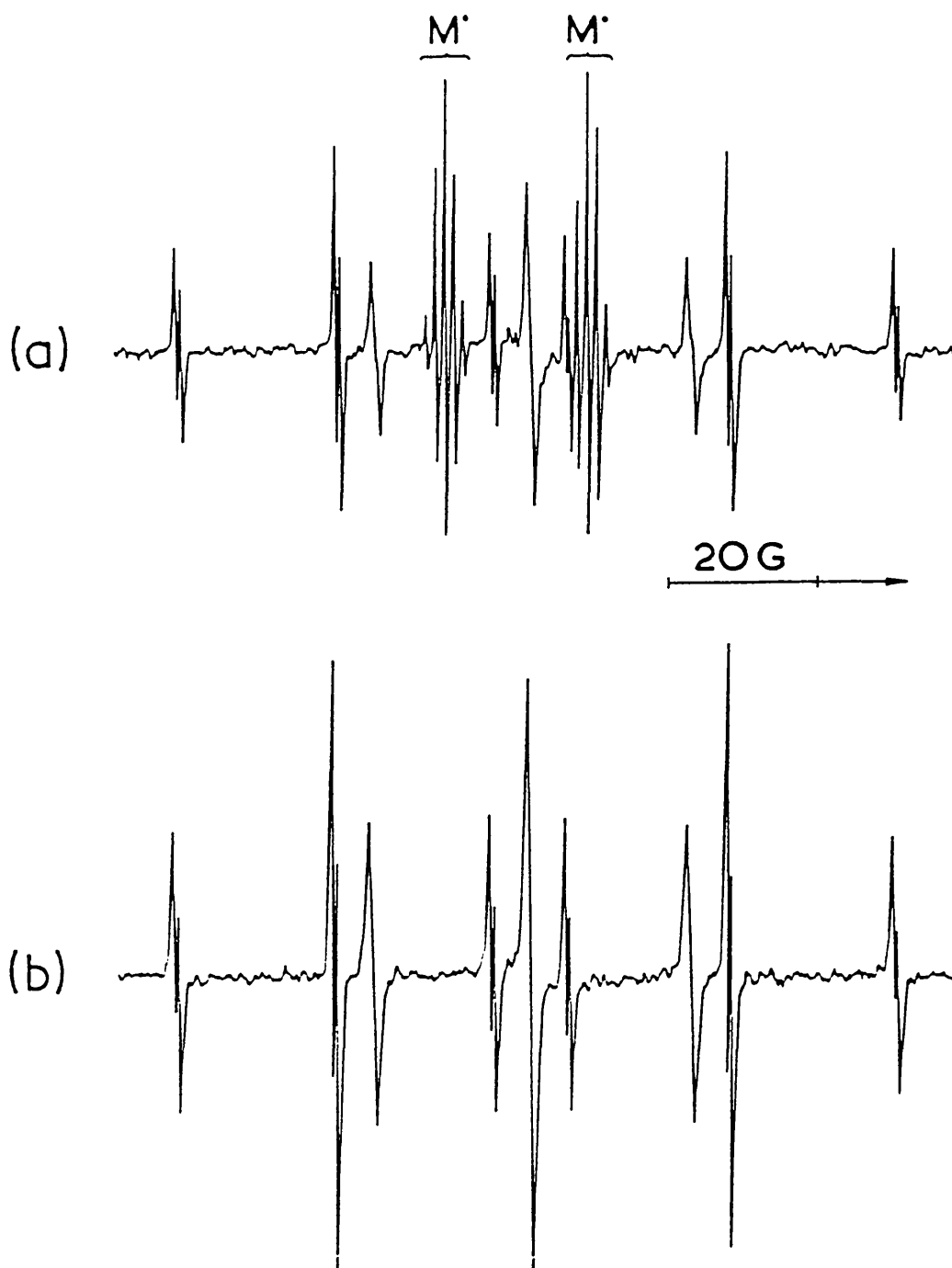
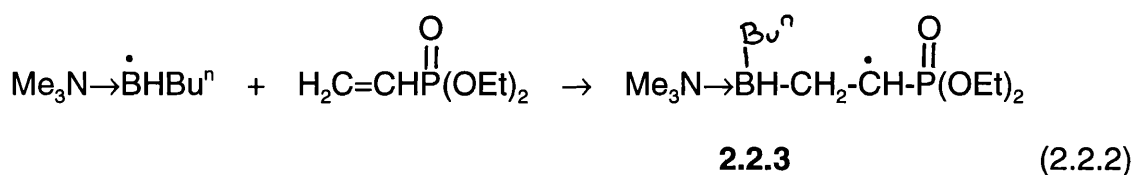


Figure 2.2.1: (a) ESR spectra of the radical $\text{HC}(\text{CO}_2\text{Et})_2$ (M^\bullet) and the adduct radical 2.2.1, obtained during generation of the former radical in ethene solvent at 180 K. (b) Spectrum of 2.2.1 in cyclopropane at 183 K, obtained by bromine-abstraction from diethyl 2-bromoethylmalonate using $\text{Me}_3\text{N} \rightarrow \text{BH}_2\text{Bu}^\bullet$.

replacement of a hydrogen atom ($I = 1/2$) by a deuterium atom ($I = 1$) results in the 1:1 doublet splitting to be replaced by a 1:1:1 triplet splitting. However, since splitting due to deuterium is 6.5 times (gyromagnetic ratios γ_H/γ_D) less than splitting due to hydrogen, the coupling from deuterium will not be observed if $a(H)$ is small. The 0.70 G doublet splitting due to the γ -hydrogen in the adduct radical **2.2.1** was absent in the ESR spectrum of the deuterated adduct radical $(EtO_2C)_2CD-CH_2-\dot{C}H_2$.

Addition of the malonyl radical to propene was faster and required a lower concentration of alkene for comparable quenching of the spectrum of the addendum; 2-methylpropene $[(CH_3)_2C=CH_2]$ was a still more reactive acceptor. Addition to the electron rich double bonds in vinyl ether and alkyltrimethylsilane also took place readily. Addition to the electron deficient double bond of diethylvinyl phosphonate was not observed; instead $Me_3N \rightarrow \dot{B}HBu^n$ added [eqn. (2.2.2)] to form the adduct **2.2.3** with $a(1H_\alpha) = 16.15$, $a(2H_\beta) = 22.50$, $a(1P_\beta) = 32.40$, $a(1B_\beta) = 19.15$ G at 220 K.



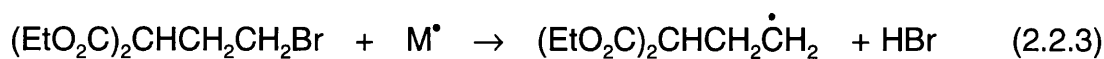
Addition of $\dot{H}C(CO_2R)_2$ ($R = Bu^t, SiMe_3$ and CH_2CF_3), $Me\dot{C}(CO_2Et)_2$ and

methylpropene could not be detected, in accord with the dominance of polar factors in influencing the rate of addition of this highly nucleophilic amine-boryl radical.

$\cdot\text{C}(\text{CO}_2\text{Et})_3$ to the above alkenes was also investigated. While $\cdot\text{C}(\text{CO}_2\text{Et})_3$ added readily, the more sterically hindered, more stabilised and less electrophilic $\text{Me}\dot{\text{C}}(\text{CO}_2\text{Et})_2$ showed no sign of addition to ethene (ca. 1.5 mol dm^{-3}) at 280 K. However, addition of this radical to propene was detected at 268 K.

These additions were all highly regioselective and only the adduct radicals formed by attachment to the least substituted end of the double bond of the alkene were detected. The ESR parameters for all the adduct radicals are collected in Table 2.2.1.

Addition of $\text{H}\dot{\text{C}}(\text{CO}_2\text{Et})_2$ to ethene was shown to be irreversible under the conditions of the ESR experiment. A sample containing diethyl 2-bromo-ethyl malonate (0.6 mol dm^{-3}), DTBP (15% v/v) and trimethylamine-butylborane (0.8 mol dm^{-3}) in cyclopropane solution was UV irradiated [eqn. (2.2.3)], and a strong spectrum of the radical **2.2.1** was observed, but no signal from $\text{H}\dot{\text{C}}(\text{CO}_2\text{Et})_2$ was detected up to 250 K, (Figure 2.2.1b).



2.2.1



All adducts exhibited *g*-factors of ca. 2.0027 which were as expected for

Table 2.2.1: ESR parameters for the radicals $(R^2O_2C)_2\dot{C}(R^1)CH_2CR^3R^4$ in cyclopropane.

						Hyperfine splittings ^a /G			
R ¹	R ²	R ³	R ⁴	T/K	g-Factor	a(2H _β)	a(R ¹) ^c	a(R ³ ,R ⁴) ^c	da(2H _β)/dT ^b (mG K ⁻¹)
H	Et	H	H	190	2.0026	27.25	0.70 (1)	22.30 (2)	-14
H	Et	H	H	182	2.0026	28.09	0.70 (1)	22.35 (2)	-22
H	Et	H	H	180	2.0027	28.17	0.72 (1)	22.35 (2)	-21
EtO ₂ C	Et	H	H	220	2.0027	22.67	---	22.37 (2)	+5
H	Et	H	Me	187	2.0027	24.60	0.80 (1)	21.95 (1), 25.10 (3)	-12
EtO ₂ C	Et	H	Me	220	2.0028	22.05	---	22.05 (1), 25.35 (3)	-3
Me	Et	H	Me	270	2.0027	23.50	---	21.75 (1), 25.12 (3)	+4
H	Et	Me	Me	181	2.0026	15.68	1.05 (1)	23.35 (6)	+10
EtO ₂ C	Et	Me	Me	221	2.0028	14.00	---	23.00 (6)	+7
Me	Et	Me	Me	240	2.0026	13.18	---	23.30 (6)	+7
H	Et	H	EtO	190	2.0032	15.30	1.05 (1)	15.00 (1), 1.80 (2)	+10
EtO ₂ C	Et	H	EtO	220	2.0032	13.85	---	15.33 (1), 2.00 (2)	+11
H	Et	H	Me ₃ SiCH ₂	218	2.0027	25.05 ^f	0.80 (1)	20.85 (1), 17.50 (2) ^f	-22, ^g +10 ^h
EtO ₂ C	Et	H	Me ₃ SiCH ₂	220	2.0027	23.35 ^f	---	20.80 (1), 17.50 (2) ^f	-16, ^g +13 ^h
Me	Et	H	Me ₃ SiCH ₂	254	2.0028	24.75 ^f	---	20.75 (1), 17.75 (2) ^f	---

^a Corrected to second-order. ^b Average temperature dependence in the region of the stated temperature. ^c Numbers of equivalent protons shown in parentheses. ^d Central lines of the β-proton triplet broaden markedly below ca. 245 K. ^e a(H_α) is temperature dependent; 14.85 G at 221 K and 14.65 G at 260 K. ^f The assignments a(2H_β) are tentative. ^g Temperature coefficient for the larger β-proton splitting.

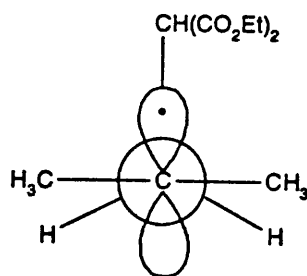
^h Temperature coefficient for the smaller β-proton splitting.

alkyl type radicals.

The magnitude and temperature dependence of the β -proton splittings for the adduct radicals, were used to deduce their conformational preferences.⁹ The Heller-McConnell equation (2.2.4)⁹ gives the relation between $a(\text{H}\beta)$ and the dihedral angle θ , formed between the C_α - $2p\pi$ orbital and the C-H bond. β -proton splitting is thus at a maximum when it is in the same plane as that of the C_α - $2p\pi$ orbital (*i.e.* when $\theta = 0$).

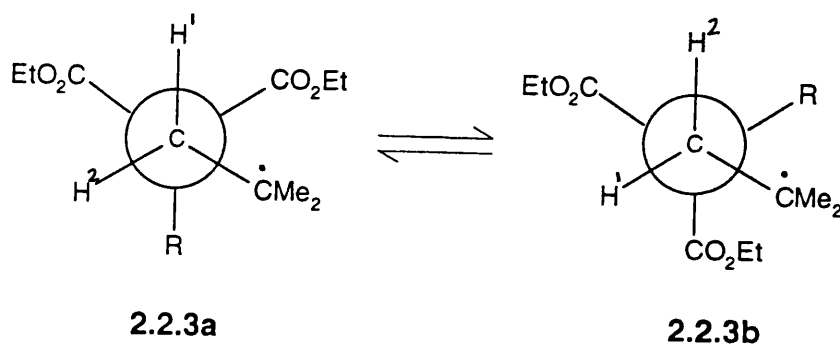
$$a(\text{H}\beta) = (A + B\cos^2\theta)\rho_{\text{C}\alpha}^\pi \quad (2.2.4)$$

The small value of $a(2\text{H}_\beta)$ and its positive temperature dependence for the 2-methyl propene adducts implies a preference for the eclipsed conformation **2.2.2**, in which the steric interactions between the addendum group $[\text{C}(\text{R})(\text{CO}_2\text{Et})_2]$ and the two α -methyl substituents are at a minimum. Most adducts to ethene show values of $a(2\text{H}_\beta)$ fairly close to the value of $a(3\text{H}_\beta)$ in the ethyl radical implying very little conformational preference.



2.2.2

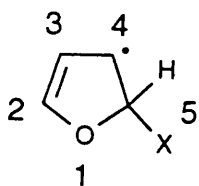
The central lines of the β -proton triplets in some adduct radicals [e.g. $(\text{EtO}_2\text{C})_2\text{CHCH}_2\dot{\text{C}}(\text{CH}_3)_2$] showed selective line broadening effects at low temperatures. This is probably due to the non-equivalence of these protons as a result of restricted rotation about the $\text{C}_\beta\text{-C}_\gamma$ bond (**2.2.3a-2.2.3b**). Rotation about the $\text{C}_\beta\text{-C}_\gamma$ bond exchanges the environments of H^1 and H^2 and, if this takes place on the ESR timescale lineshape effects will be evident in the spectrum. In no case could spectra be obtained in the slow exchange region.



Lineshape effects were particularly evident in the spectra of the 2-methylpropene adducts and the lines corresponding to $M_1(2H_\beta) = 0$ were severely broadened at low temperature. Exact agreement between the experimental spectrum and its computer simulation, correct to second-order effects, could not be obtained for the propene adduct $(\text{EtO}_2\text{C})_2\text{CHCH}_2\dot{\text{C}}\text{HCH}_3$ at very low temperature and we attributed this to higher-order effects which become important when the difference between two coupling constants becomes comparable to the associated second-order shifts.¹¹

2.3. Addition of $\dot{\text{H}}\text{C}(\text{CO}_2\text{Et})_2$, $\text{Me}\dot{\text{C}}(\text{CO}_2\text{Et})_2$ and $\dot{\text{C}}(\text{CO}_2\text{Et})_3$ to Furan

The ester derived radicals were generated using polarity reversal catalysis in cyclopropane solvent in the presence of furan (ca. 1 mol dm⁻³). Again addition of $\dot{\text{H}}\text{C}(\text{CO}_2\text{Et})_2$ and $\dot{\text{C}}(\text{CO}_2\text{Et})_3$ to furan took place readily, but addition of $\text{Me}\dot{\text{C}}(\text{CO}_2\text{Et})_2$ was much more sluggish and the corresponding adduct **2.3.3** was detectable only above ca. 270 K. The ESR spectrum of the radical **2.3.1**, which exhibits strong chemically induced dynamic electron polarisation (CIDEP) is shown in Figure 2.3.1, and the spectroscopic parameters for the adduct radicals **2.3.1-2.3.3** are reported in Table 2.3.1.



2.3.1 X = $\text{HC}(\text{CO}_2\text{Et})_2$

2.3.2 X = $\text{C}(\text{CO}_2\text{Et})_3$

2.3.3 X = $\text{MeC}(\text{CO}_2\text{Et})_2$

The *g*-factors for the adduct radicals **2.3.1-2.3.3** are 2.0031, larger than the free spin value (2.0023) and larger than the *g*-value for simple alkyl radicals (ca. 2.0027), because the unpaired electron is partly delocalised onto oxygen. In experiments where $\text{D}_2\text{C}(\text{CO}_2\text{Et})_2$ was substituted for $\text{H}_2\text{C}(\text{CO}_2\text{Et})_2$ the doublet splitting of 1.18 G due to the α -proton of the malonate was absent.

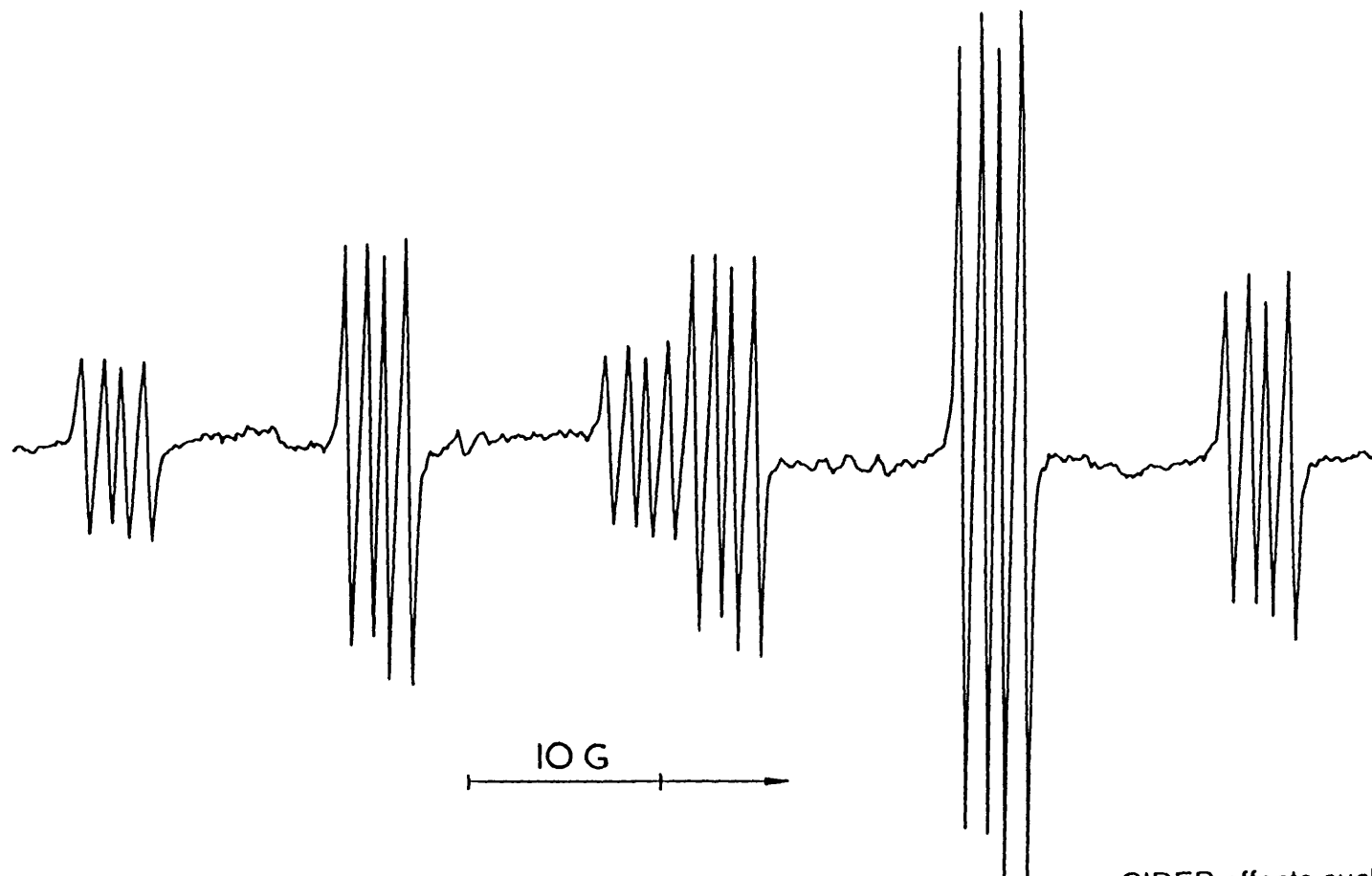


Figure 2.3.1: ESR spectrum of the radical **2.3.1** in cyclopropane at 184 K. The spectrum shows CIDEP effects such that the high-field triplet of multiplets associated with the $M_1 = -1/2$ state of H-5 are much more intense than those associated with the $M_1 = +1/2$ state (E/A polarisation)

Table 2.3.1: ESR parameters for the radicals **2.3.1-2.3.3** formed by addition to furan in cyclopropane.

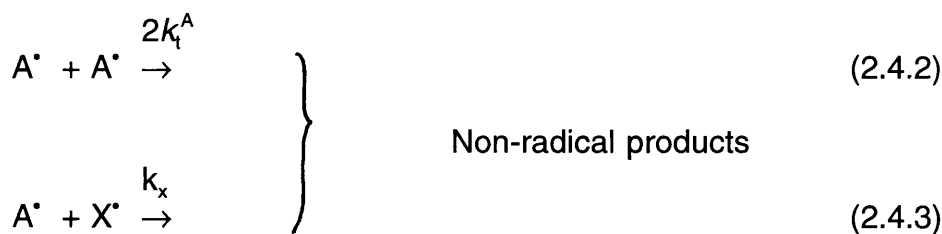
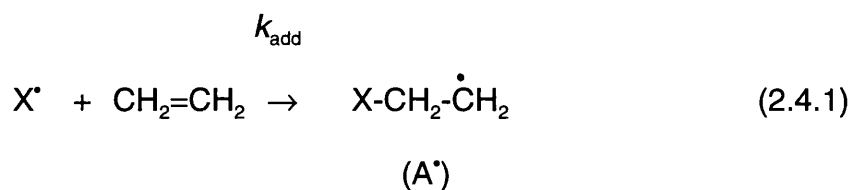
			Hyperfine splittings/G			
Radical	T/K	g-Factor	$a(5\text{-H})$	$a(2,4\text{-H})^a$	$a(3\text{-H})$	$a(1\text{H})^b$
2.3.1	185	2.0031	31.75	13.60	2.03	1.18
2.3.2	220	2.0031	34.02 ^c	13.60	2.00	---
2.3.3	286	2.0031	33.70	13.50	2.05	---

^a Splittings from 2-H and 4-H are indistinguishable within the linewidth. ^b Splitting from the α -proton of the malonate group, absent in experiments using $\text{D}_2\text{C}(\text{CO}_2\text{Et})_2$. ^c 34.08 G at 260 K.

thus verifying that assignment to the correct hydrogen.

2.4. Absolute Rate Constants for Addition of $\dot{\text{H}}\text{C}(\text{CO}_2\text{Et})_2$ and $\dot{\text{C}}(\text{CO}_2\text{Et})_3$ to Ethene

If the adduct radicals A^\bullet are formed and removed as shown in equations (2.4.1)-(2.4.3) and the assumption is made^{12,13} that $2k_t^{\text{A}} = k_x$, then the steady-state radical concentrations during continuous generation of the addendum X^\bullet will be given by equation (2.4.4).¹³ All the absolute radical concentrations were



$$(k_{\text{add}}/2k_t^{\text{A}}) = [\text{A}^\bullet]/[\text{CH}_2=\text{CH}_2] ([\text{A}^\bullet]/[\text{X}^\bullet] + 1) \quad (2.4.4)$$

measured at 221 K and extrapolated to zero UV irradiation time for initial ethene concentrations in the range 0.4-2.5 mol dm⁻³. For $\text{X}^\bullet = \dot{\text{H}}\text{C}(\text{CO}_2\text{Et})_2$ and $\dot{\text{C}}(\text{CO}_2\text{Et})_3$, the values of $(k_{\text{add}}/2k_t^{\text{A}})$ were $7.3 \pm 1.0 \times 10^{-7}$ and $1.4 \pm 0.3 \times 10^{-7}$,

respectively.

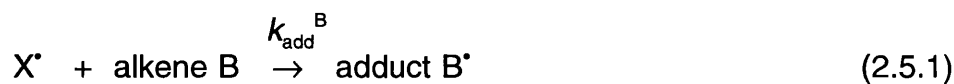
The self-reactions of small and moderately sized alkyl radicals, which are not sterically protected at the radical centre, are diffusion controlled processes for which the rate constants will all be very similar in a given medium.^{14,15} From rate constants in the literature for the self-reaction of t-butyl radicals in alkanes^{14,15} and for allyl radicals in propene-DTBP,¹⁶ we estimate that, under our conditions, $2k_t^A$ will be *ca.* $1 \times 10^{10} \text{ dm}^3 \text{ mol}^{-1} \text{ s}^{-1}$ at 221 K for both of the primary alkyl radical adducts $(\text{EtO}_2\text{C})_2\text{CHCH}_2\dot{\text{C}}\text{H}_2$ and $(\text{EtO}_2\text{C})_3\text{CCH}_2\dot{\text{C}}\text{H}_2$. Using this value of $2k_t^A$, approximate rate constants for addition of $\text{H}\dot{\text{C}}(\text{CO}_2\text{Et})_2$ and $\dot{\text{C}}(\text{CO}_2\text{Et})_3$ to ethene at 221 K are 7.3×10^3 and $1.4 \times 10^3 \text{ dm}^3 \text{ mol}^{-1} \text{ s}^{-1}$, respectively. If we take^{17,18} the Arrhenius *A*-factor for these addition reactions to be $10^{7.5} \text{ dm}^3 \text{ mol}^{-1} \text{ s}^{-1}$, the corresponding activation energies would be 15.4 and 18.4 kJ mol^{-1} , respectively. Both additions are appreciably more rapid than addition of the nucleophilic t-butyl radical to ethene¹⁸ ($k_{\text{add}} = 24 \text{ s}^{-1}$ at 221 K) and the large difference is attributable mainly to polar effects.

Addition of $\text{H}\dot{\text{C}}(\text{CO}_2\text{Et})_2$ to propene is 19 times faster than its addition to ethene at 221 K (see below) and thus the absolute rate constant for addition to propene is *ca.* $1.4 \times 10^5 \text{ dm}^3 \text{ mol}^{-1} \text{ s}^{-1}$. This value is appreciably larger than the rate constant for addition of the less electrophilic $\dot{\text{C}}\text{H}_2\text{CO}_2\text{Bu}^t$ to butene ($5.6 \times 10^3 \text{ dm}^3 \text{ mol}^{-1} \text{ s}^{-1}$ at 221 K, extrapolated from data obtained at 296 K) determined by Beranek and Fischer,¹⁹ again in accord with rate-controlling polar

effects.

2.5. Relative Rates of Addition to Alkenes

When an addendum radical X^\bullet is generated continuously in the presence of two different alkenes B and C, the relative concentrations of adduct radicals under steady-state conditions will be given by equation (2.5.3), provided that the two adducts are removed by self- and cross-reactions which have equal (diffusion-controlled) rate constants.^{12,13,20} The relative rate constants at 221 K were determined by double integration and/or computer simulation of appropriate lines in the adduct ESR spectra for at least two different alkene



$$(k_{\text{add}}^{\text{B}}/k_{\text{add}}^{\text{C}}) = [\text{adduct B}^\bullet][\text{alkene C}]/[\text{adduct C}^\bullet][\text{alkene B}] \quad (2.5.3)$$

concentration ratios, as described previously.^{12,13,20} The results are given in Table 2.5.1.

Polar effects are important in determining the relative rates of addition of the electrophilic radicals $\text{HC}(\text{CO}_2\text{Et})_2^\bullet$ and $^\bullet\text{C}(\text{CO}_2\text{Et})_3$, as can be seen by

Table 2.5.1: Relative rates of addition of (alkoxycarbonyl)alkyl radicals to alkenes in cyclopropane at 220 K.

Alkene	Relative rates of addition			Alkene ionisation energy/eV ^b
	$\text{H}\dot{\text{C}}(\text{CO}_2\text{Et})_2$	$\dot{\text{C}}(\text{CO}_2\text{Et})_3$	$\text{Me}\dot{\text{C}}(\text{CO}_2\text{Et})_2$ ^a	
$\text{H}_2\text{C}=\text{CH}_2$ ^c	(10)	(1)	---	10.51
$\text{MeCH}=\text{CH}_2$	19	18	(1)	9.73
$\text{Me}_2\text{C}=\text{CH}_2$	261	281	4.6	9.24
$\text{Me}_3\text{SiCH}_2\text{CH}=\text{CH}_2$	444	900	5.4	9.0 ^d

^a Relative rates at 275 K. ^b Data from G. Bieri, F. Burger, E. Heilbronner and J.P. Maier, *Helv. Chim. Acta*, 1977, **60**, 2213, unless noted otherwise. ^c Molar reactivities are reported; in ethene the two ends of the double are equally reactive. ^d U. Weidner and A Schweig, *J. Organomet. Chem.*, 1972, **39**, 261.

comparing propene and allyltrimethylsilane for which steric effects and reaction enthalpies will be similar. Addition of either radical to the electron-rich double bond in the silane (ionisation energy: $E_i = 9.0$ eV) is much more rapid than its addition to propene ($E_i = 9.73$ eV). The rate differences are smaller for the less electrophilic and less reactive $\text{Me}\dot{\text{C}}(\text{CO}_2\text{Et})_2$, although these data were obtained at higher temperature where the chemoselectivity would be expected to be reduced. A computer simulation of the overlapping spectra at 275 K of $\text{Me}\dot{\text{C}}(\text{CO}_2\text{Et})_2$ (X^\bullet) and its adduct to propene (A^\bullet), gave $[\text{A}^\bullet]/[\text{X}^\bullet] = 0.33$. The initial concentration of propene in that experiment was 2 mol dm^{-3} , and assuming that $[\text{A}^\bullet] + [\text{X}^\bullet] = 5 \times 10^{-7} \text{ mol dm}^{-3}$ and $2k_t = 1 \times 10^{10} \text{ dm}^3 \text{ mol}^{-1} \text{ s}^{-1}$. It is possible to calculate the rate constant for addition of $\text{Me}\dot{\text{C}}(\text{CO}_2\text{Et})_2$ to propene at 275 K, using the rate equation (2.4.4) and replacing ethene by propene, then k_{add} is ca. $8 \times 10^2 \text{ dm}^3 \text{ mol}^{-1} \text{ s}^{-1}$.

2.6. Cyclisation of the 1,1-Bis(ethoxycarbonyl)hex-5-enyl Radical

The title radical **2.6.1** was generated from diethyl pent-4-enylmalonate under conditions of polarity reversal catalysis using trimethylamine-butylborane catalyst (The ESR parameters for the radical **2.6.1** were reported in Table 2.1.1) and its cyclisation was monitored by ESR spectroscopy between 190 and 250 K (see Figure 2.6.1). The persistent radicals which were detected alongside the alkyl malonyl radicals (discussed in section 2.1.1) were not detected at temperatures sufficiently high for significant concentrations of the

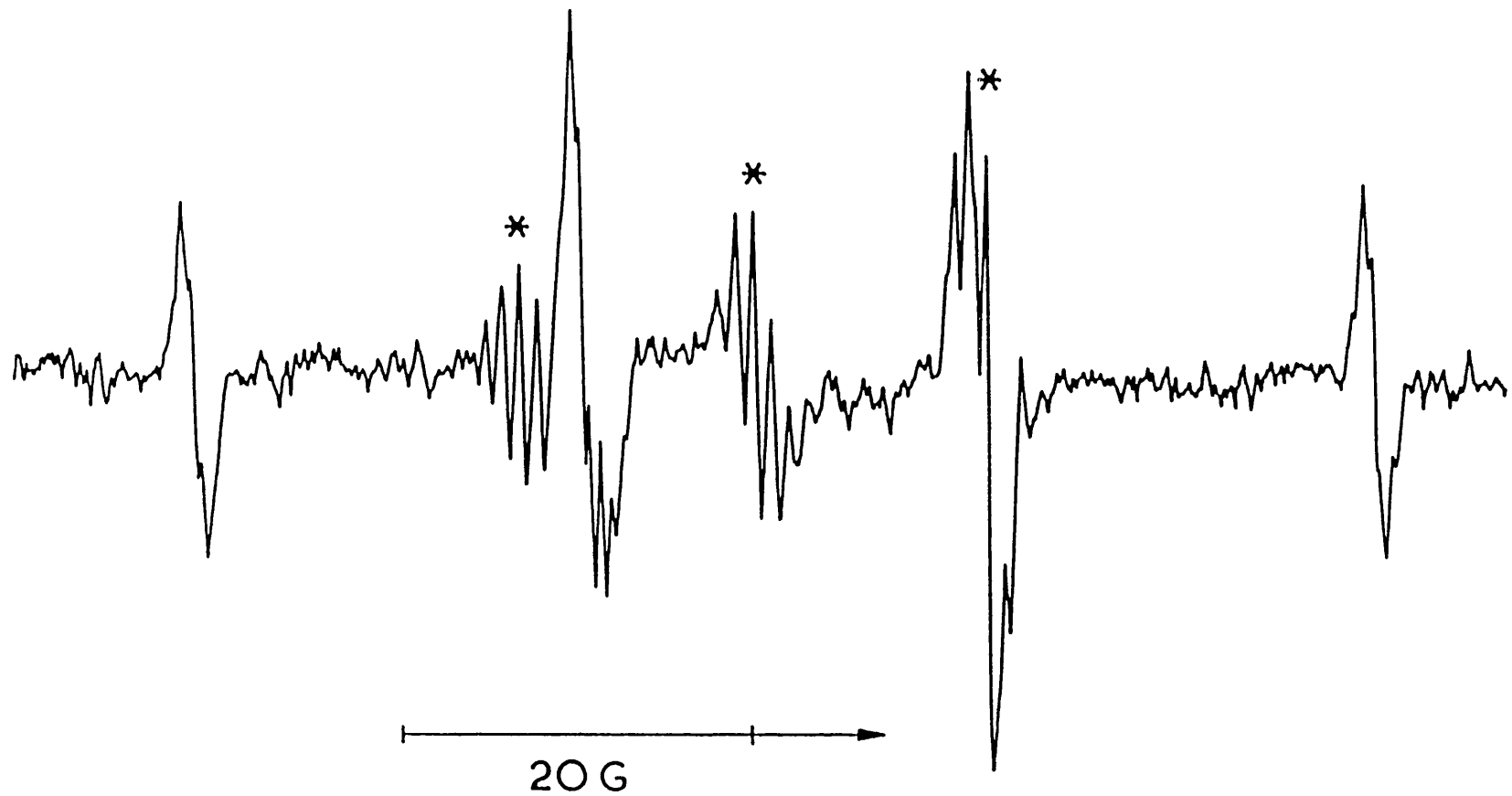
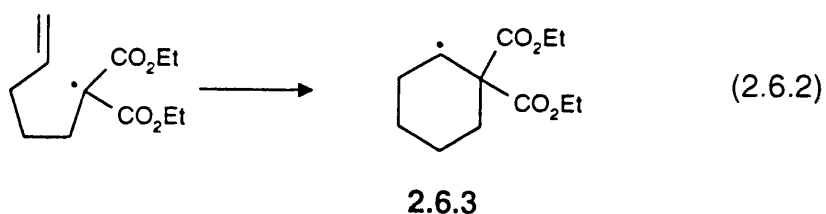
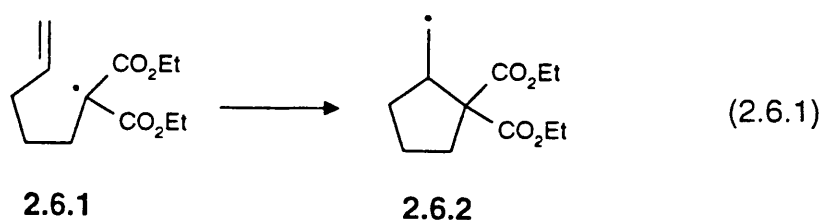


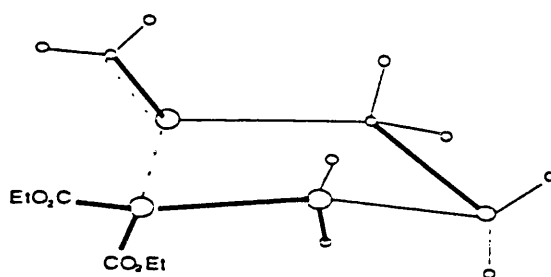
Figure 2.6.1: ESR spectrum of the radical 2.6.2 alongside that of the uncyclised radical 2.6.1 (multiplets marked with asterisks) in cyclopropane at 221 K.

cyclised radical **2.6.2** to be present along with **2.6.1** [eqn. (2.6.1)]. Only the 5-*exo*-cyclisation of **2.6.1** to give the radical **2.6.2** with the following ESR parameters [$a(2H_\alpha) = 22.13$, $a(1H_\beta) = 23.25$ and $a(4H_{\gamma\delta}) = 0.55$ G at 225 K] was detected and no spectrum attributable to the more stable radical **2.6.3** [eqn. (2.6.2)] was observed up to 270 K, at which temperature **2.6.1** was no longer detectable. These results are in accord with the cyclisation occurring irreversibly under our conditions, as expected.²¹ From product isolation experiments,²¹ carried out under conditions of kinetic control, it is known that the relative rates of 5-*exo*- and 6-*endo*-cyclisation of the dimethyl ester analogue of **2.6.1** are in the ratio 89 : 11 at 358 K. Assuming that the rate difference is wholly attributable to the difference in activation energies, this ratio would become *ca.* 94 : 6 at 270 K, consistent with our inability to detect **2.6.3** in the temperature range 190-270 K.



The selectivity for the 5-*exo*-cyclisation can be understood in terms of

stereoelectronic factors. The ideal SOMO-LUMO overlap for alkyl radical addition to a double bond is better accommodated in the 5-*exo*-transition state, structure 2.6.4, than that which would lead to 6-*endo*-cyclisation. In addition, the amount of torsional strain for the transition state shown in 2.6.4 is less as it resembles that in a 6-membered ring.²¹⁻²⁴



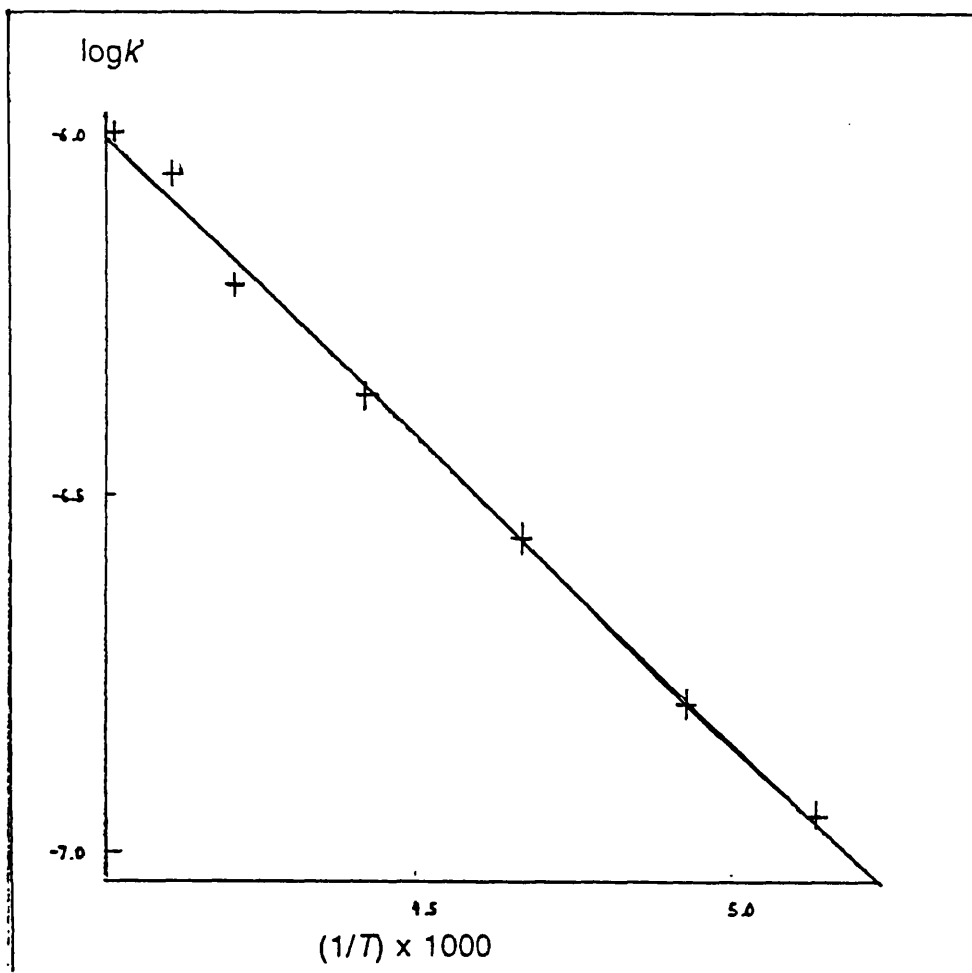
2.6.4

The rate constant for 5-*exo*-cyclisation of 2.6.1 was determined relative to that ($2k_t$) for self-reaction of 2.6.2 using equation (2.6.3), which is derived by assuming that the rate constant for (diffusion-controlled) reaction between 2.6.1 and 2.6.2 is equal to $2k_t$.²⁵

$$(k_{\text{cyc}}/2k_t) = [2.6.2]([2.6.2]/[2.6.1] + 1) \quad (2.6.3)$$

The results gave a good fit to the Arrhenius rate expression (2.6.4) (see Figure 2.6.2), in which $\theta = 2.303 RT$. If we take $2k_t$ to be the same as that for self-reaction of the cyclopentylmethyl radical 2.6.5 in cyclopropane, which is given by equation (2.6.5),²⁷ then we obtain the rate expression (2.6.6).

$$\log_{10}(k_{\text{cyc}}/2k_t) = -(2.56 \pm 0.20) - (16.42 \pm 1.50)/\theta \quad (2.6.4)$$



Reference =

1/T

log k'

5.1300E-03	-6.950
4.9300E-03	-6.790
4.6700E-03	-6.560
4.4200E-03	-6.360
4.2200E-03	-6.210
4.1200E-03	-6.055

a0 = -2.5580046049E+00

a1 = -8.5765632487E+02

standard deviation = 2.5562764538E-02

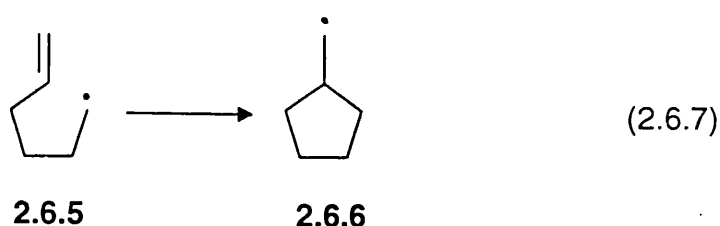
corr. coef. = 9.9778614926E-01

Figure 2.6.2: Graph fitting the Arrhenius equation (2.6.4).

$$\log_{10}(2k_f/\text{dm}^3 \text{ mol}^{-1} \text{ s}^{-1}) = 11.85 - 7.1/\theta \quad (2.6.5)$$

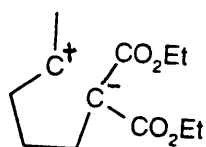
$$\log_{10}(k_{\text{cyc}}/\text{s}^{-1}) = (9.3 \pm 0.3) - (23.5 \pm 2.0)/\theta \quad (2.6.6)$$

The rate constant (k_{cyc}) for 5-*exo*-cyclisation of the unsubstituted hex-5-enyl radical **2.6.5** to give **2.6.6** is given by equation (2.6.8).^{24,26}



$$\log_{10}(k_{\text{cyc}}/\text{s}^{-1}) = (10.35 \pm 0.35) - (28.29 \pm 1.89)/\theta \quad (2.6.8)$$

At 200 K the rate constants for cyclisation of **2.6.1** and **2.6.5** are similar ($1.5 \times 10^3 \text{ s}^{-1}$ and $9.2 \times 10^2 \text{ s}^{-1}$, respectively), even though cyclisation of **2.6.1** is presumably less exothermic and the radical centre in **2.6.1** is more crowded than that in **2.6.5**. The lower activation energy for cyclisation of **2.6.1** is probably a polar effect, reflecting charge transfer stabilisation of the transition state as indicated in structure **2.6.7**. The lower *A*-factor for cyclisation of **2.6.1** may reflect a less flexible transition structure, because of steric effects and the probable requirement for rigid orientation of the CO_2Et groups.

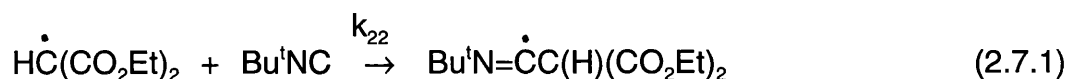


2.6.7

2.7. Radical Addition to Alkyl Isocyanides

We examined the addition reactions of radicals derived from esters of the type $R^1C(H)(CO_2R^2)_2$ (ca. 1.0 mol dm^{-3}) to t-butyl isocyanide Bu^tNC in cyclopropane solvent. The ester derived radicals were generated using polarity reversal catalysis as before in the presence of Bu^tNC (ca. 1.2 mol dm^{-3}).

When $\dot{H}C(CO_2Et)_2$ was generated from diethyl malonate, in the presence of t-butyl isocyanide (ca. 1.2 mol dm^{-3}) at 180 K, overlapping ESR spectra of the addendum and the imidoyl radical **2.7.1** were observed (see Figure 2.7.1). t-Butoxyl radicals react with amine-alkylboranes very rapidly²⁷ and are known to add to Bu^tNC to give $Bu^tN=\dot{C}OBu^t$, but no competing addition^{28,29} to the isocyanide was detected when $[Bu^tNC]/[TMBB^*]$ was ca. 4.



2.7.1

The spectrum of **2.7.1** appears as a 1:2:2:1 quartet because the ^{14}N and β -proton splittings are almost equal and, this was confirmed by experiments with $D_2C(CO_2Et)_2$. The ESR spectrum of the deuterated imidoyl radical consisted of a 1:1:1 triplet (2.65 G) due to coupling with the β -nitrogen ($I = 1$). The concentration ratio $[2.7.1] : [\dot{H}C(CO_2Et)_2]$ increased with increasing temperature, as expected since the rate of addition to Bu^tNC will increase with increasing

* TMBB: Trimethylamine-butylborane.

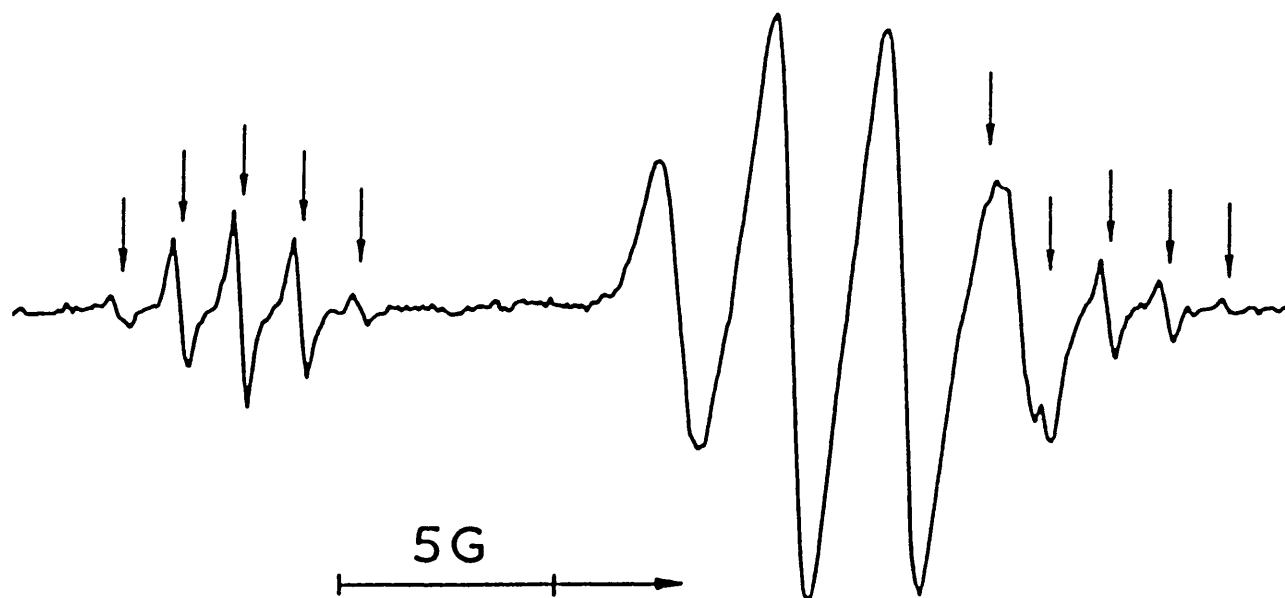
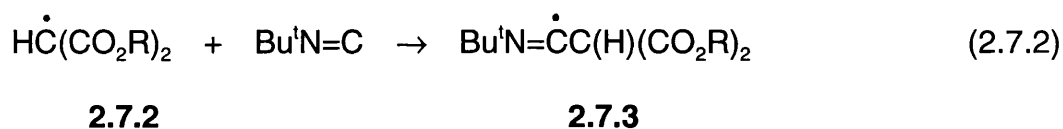


Figure 2.7.1: ESR spectra in cyclopropane at 173 K of $\text{Bu}'\text{N}=\dot{\text{C}}\text{C}(\text{H})(\text{CO}_2\text{Et})_2$. The lines originating from $\text{H}\dot{\text{C}}(\text{CO}_2\text{Et})_2$ are marked with arrows.

temperature. The spectrum of the imidoyl radical decayed within the fall-time of the spectrometer (0.2 s) when UV photolysis was interrupted, showing that the increase in concentration of **2.7.1** was not due to build-up of that radical.

When solutions containing $\text{H}_2\text{C}(\text{CO}_2\text{R})_2$ [(R = Bu^t, CH₂Ph, SiMe₃); (ca. 1.0 mol dm⁻³)], DTBP (18% v/v), Me₃N→BH₂Buⁿ (ca. 0.2 mol dm⁻³) and Bu^tNC (ca. 1.2 mol dm⁻³) in cyclopropane solvent were photolysed in the cavity of the ESR spectrometer [eqn. (2.7.2)], again the ESR spectra of both imidoyl radical and malonyl radical **2.7.2** were observed alongside each other at low



temperature (ca. 175 K). The concentration ratios of the imidoyl **2.7.3** to malonyl **2.7.2** radical increased with increasing temperature for all Rs. This was verified quantitatively, by integration of the overlapping spectra of **2.7.3** and **2.7.2** with R = Bu^t at 175 K and 220 K (see Table 2.7.1). The ESR spectrum of these imidoyl radicals consisted of a 1:2:2:1 quartet with $a(1\text{N}_\beta) \sim a(1\text{H}_\beta)$.

With radicals of the type $\text{RC}(\text{CO}_2\text{Et})_2$ a significant decrease in the rate of addition to Bu^tNC was noted as the steric bulk at C_α increased from R = H to R = Buⁿ with the exception of $\overset{\cdot}{\text{C}}(\text{CO}_2\text{Et})_3$ which added readily to give the corresponding imidoyl radical **2.7.3**. This adduct radical gave rise to a 1:1:1

Table 2.7.1: Concentration ratio of imidoyl $\text{Bu}^t\dot{\text{N}}\text{C}(\text{H})(\text{CO}_2\text{Bu}^t)_2$ (I^\bullet) to malonyl radical $\dot{\text{H}}\text{C}(\text{CO}_2\text{Bu}^t)_2$ (R^\bullet).

T/K	$[\text{I}^\bullet]/[\text{R}^\bullet]$
180	43
220	91

triplet overlapping a binomial septet due to $\cdot\text{C}(\text{CO}_2\text{Et})_3$. The ESR spectrum of the more electrophilic $\cdot\text{C}(\text{CO}_2\text{Et})_3$ was almost completely replaced by that of the corresponding imidoyl adduct in the presence of Bu^1NC (1.2 mol dm^{-3}) at 230 K. This adduct radical is relatively persistent and its spectrum decayed with mixed first- and second-order kinetics when photolysis was interrupted (first half-life *ca.* 15 s at 200 K for an initial concentration of *ca.* $10^{-6} \text{ mol dm}^{-3}$). Because of this, it is not possible to make a semi-quantitative estimate of the rate of addition based on the relative concentrations of the adduct and $\cdot\text{C}(\text{CO}_2\text{Et})_3$. On the other hand, addition of $\text{Me}\dot{\text{C}}(\text{CO}_2\text{Et})_2$ to Bu^1NC (*ca.* 1.2 mol dm^{-3}) was much slower and an imidoyl adduct was detected only above *ca.* 260 K. Steric, polar and enthalpic factors are presumably responsible for this difference. As R is replaced from hydrogen to n-butyl the steric hindrance at the α -carbon increases and, the electrophilicity of the ester radical decreases, since alkyl groups are mildly electron donating. Though, $\cdot\text{C}(\text{CO}_2\text{Et})_3$ should exhibit similar steric requirements at C_α as the alkyl malonyl radicals, $\cdot\text{C}(\text{CO}_2\text{Et})_3$ is much more electrophilic, because of the presence of a third alkoxy group.

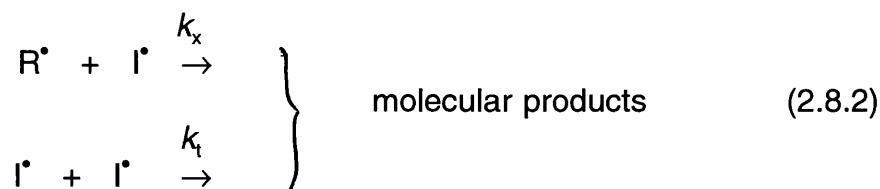
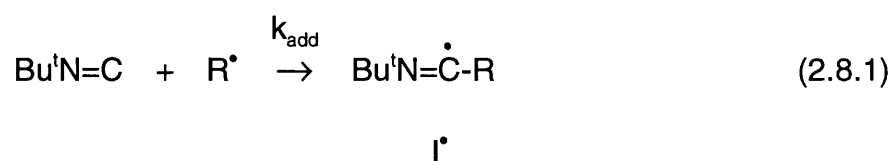
Again the persistent radicals which accompany the higher alkylated malonyl radicals, appeared to be much weaker when Bu^1NC was present, as was the case with ethene.

Similar addition took place to methyl isocyanide and the spectrum of the

imidoyl adduct $\text{MeN}=\dot{\text{C}}\text{-C(H)(CO}_2\text{Et)}_2$ is shown in Figure 2.7.2a and Figure 2.7.2b is a computer simulation of Figure 2.7.2a; the ESR spectrum of the imidoyl radical consisted of 1:2:2:1 quartet with $a(1\text{N}_\beta) \sim a(1\text{H}_\beta)$, further split into 1:3:3:1 quartets due to coupling with the 3 γ -hydrogens of the methyl group. Addition of $\text{Me}\dot{\text{C}}(\text{CO}_2\text{Et)}_2$ to $\text{CH}_3\text{N}=\text{C}$ was not detected even at 285 K. The spectroscopic parameters for all the imidoyl radicals are collected in Table 2.7.2.

2.8. Relative Rates of Addition to Alkyl Isocyanide

Assuming radicals are removed by diffusion controlled self- and cross-reactions, a series of ESR spectra were recorded in order to determine the relative rates of addition to t-butyl isocyanide. The general scheme is given below, in which R^\bullet is an (alkoxycarbonyl)alkyl radical and I^\bullet is the imidoyl adduct.



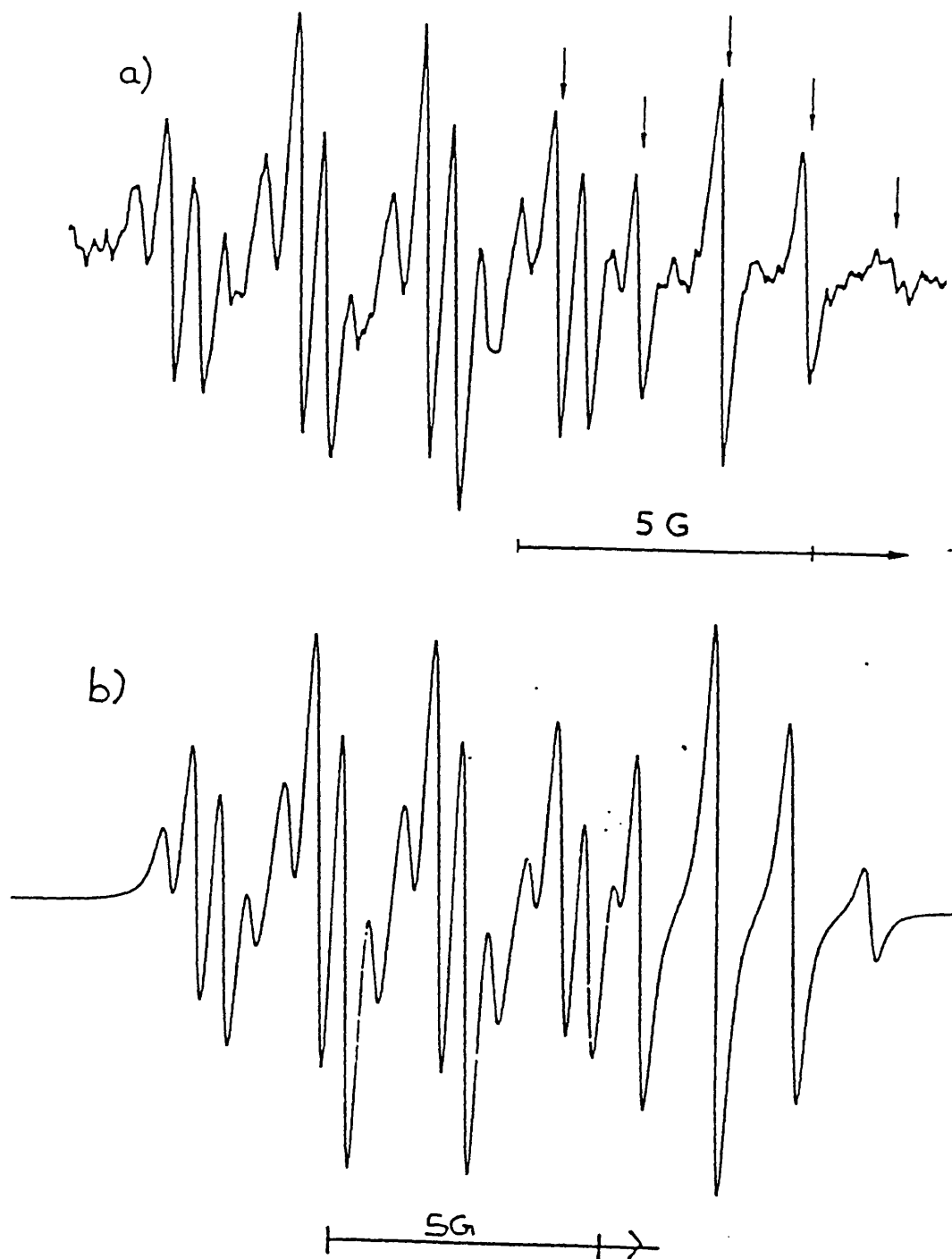


Figure 2.7.2: (a) ESR spectra in cyclopropane at 173 K of $\text{MeN}=\dot{\text{C}}\text{C}(\text{H})(\text{CO}_2\text{Et})_2$. The lines originating from $\text{H}\dot{\text{C}}(\text{CO}_2\text{Et})_2$ are marked with arrows. (b) Computer simulation of the above spectrum.

Table 2.7.2: ESR parameters for imidoyl radicals $\text{RN}=\dot{\text{C}}\text{X}$ in cyclopropane.

				Hyperfine splittings/G	
R	X	T/K	<i>g</i> - Factor	$a(\text{N}_\beta)$	Others
Bu ^t	HC(CO ₂ Et) ₂	180	2.0014	2.67 ^a	2.70 ^a (1H _β)
Bu ^t	DC(CO ₂ Et) ₂	180	2.0014	2.69	---
Bu ^t	HC(CO ₂ Bu ^t) ₂	180	2.0015	2.50	2.65(1H _β)
Bu ^t	HC(CO ₂ SiMe ₃) ₂	180	2.0014	2.53	2.38(1H _β)
Bu ^t	HC(CO ₂ CH ₂ Ph) ₂	178	2.0013	2.67	2.72(1H _β)
Bu ^t	MeC(CO ₂ Et) ₂	286	2.0014	2.50	---
Bu ^t	EtC(CO ₂ Et) ₂	220	2.0014	2.55	---
Bu ^t	C(CO ₂ Et) ₃	200	2.0014	2.50	---
Me	HC(CO ₂ Et) ₂	180	2.0013	2.20	2.35(1H _β),0.51(3H _γ)
Me	HC(CO ₂ SiMe ₃) ₂	180	2.0014	2.40	2.16(1H _β),0.38(3H _γ)
Me	C(CO ₂ Et) ₃	217	2.0014	2.53	0.70(3H _γ)

^a At 212 K, $a(\text{N}_\beta) = 2.75$ G and $a(1\text{H}_\beta) = 3.35$ G.

When a steady-state is reached during continuous generation of R^\bullet , equation (2.8.3) will hold.

$$d[I^\bullet]/dt = k_{\text{add}}[\text{Bu}^t\text{NC}][R^\bullet] - 2k_t[I^\bullet]^2 - k_x[R^\bullet][I^\bullet] = 0 \quad (2.8.3)$$

If $2k_t$ is equal to k_x , that is they are both diffusion controlled, then we have equation (2.8.4).

$$k_{\text{add}} = 2k_t[I^\bullet]\{[I^\bullet][R^\bullet]\}^\dagger / [\text{Bu}^t\text{NC}][R^\bullet] \quad (2.8.4)$$

In experiments with different addenda R^\bullet the total radical concentration should be constant (since the rate of primary radical production is constant at constant light intensity) and hence, for samples containing the same isocyanide concentration, equation (2.8.5) should hold approximately.

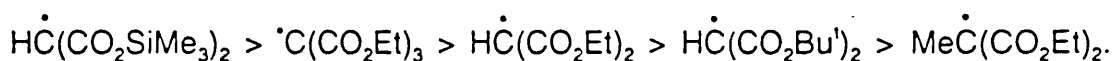
$$k_{\text{add1}}/k_{\text{add2}} = [I_1^\bullet]/[R_1^\bullet] \times [R_2^\bullet]/[I_2^\bullet] \quad (2.8.5)$$

The radical concentration ratios and values of $(k_{\text{add1}}/k_{\text{add2}})$ are given in Table 2.8.1.

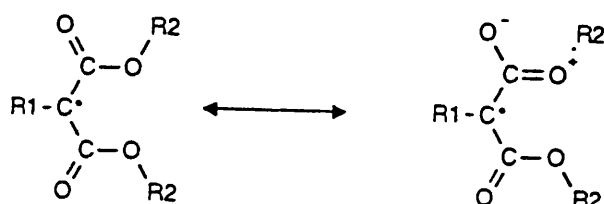
The rate of radical addition to Bu^tNC decreased in the following order:

Table 2.8.1: Radical concentration ratios for imidoyl radicals $\text{Bu}^t\text{N}=\dot{\text{C}}\text{X}$ (I^\bullet) and bis(alkoxycarbonyl)alkyl radicals (R^\bullet) and values of $(k_{\text{add1}}/k_{\text{add2}})$.

X	T/K	$[\text{I}^\bullet]/[\text{R}^\bullet]$	$k_{\text{add1}}/k_{\text{add2}}$
$\text{HC}(\text{CO}_2\text{Et})_2$	180	59	(1)
$\text{HC}(\text{CO}_2\text{Bu}^t)_2$	180	43	0.7
$\text{HC}(\text{CO}_2\text{SiMe}_3)_2$	180	150	2.5

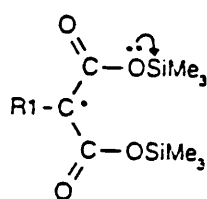


This order can be understood in terms of a balance between polar and steric effects. BuⁱNC is relatively electron rich and as such it should react more readily with the most electrophilic R¹Ċ(CO₂R²)₂. Conjugative interactions between the alkoxy and carbonyl groups should decrease the electrophilicity of the (alkoxycarbonyl)alkyl radical, structure 2.8.2. By making R² more electron withdrawing the contribution from structure 2.8.2 would decrease and, the electrophilicity of that radical would be enhanced. When R² = SiMe₃, silicon was able to use its low lying 3d orbital in order to stabilise the pπ-lone pair on oxygen, structure 2.8.3, which would reduce the contribution from 2.8.2.



2.8.1

2.8.2



2.8.3

Competition experiments were carried out to determine the relative rate of addition of $\dot{\text{H}}\text{C}(\text{CO}_2\text{Et})_2$ to BuⁱNC and to ethene. UV irradiation of a cyclopropane solution containing ethene (3.4 mol dm⁻³), BuⁱNC (0.70 mol dm⁻³), diethyl malonate, DTBP and TMBB at 220 K afforded an ESR spectrum which

showed the presence of both adducts and, computer simulation gave $[\text{Bu}^t\dot{\text{N}}\text{C}(\text{H})(\text{CO}_2\text{Et})_2]/[\text{H}_2\dot{\text{C}}\text{H}_2\text{CHC}(\text{CO}_2\text{Et})_2] = 3.3$. Hence, the rate constant for addition to Bu^tNC is about 16 times that for addition to ethene and thus k_{add} the rate of addition of the malonyl radical to Bu^tNC is ca. $1 \times 10^5 \text{ dm}^3 \text{ mol}^{-1} \text{ s}^{-1}$ at 220 K. Addition of methyl radicals to Bu^tNC was not detected by ESR spectroscopy²⁹ and clearly polar factors are very important in determining the rate of addition of carbon radicals to isocyanides.

As judged from the relative concentrations of α -(ethoxycarbonyl)alkyl radicals and imidoyl adducts, addition to MeNC is significantly slower than corresponding addition to Bu^tNC (in which the *N*-alkyl group is *more* bulky). Addition of $\text{Me}\dot{\text{C}}(\text{CO}_2\text{Et})_2$ to MeNC could not be detected up to 285 K so the difference between the isocyanides may be attributed to polar effects resulting from the greater nucleophilicity of Bu^tNC .³⁰

2.9. Imidoyl radicals derived from $\text{Bu}^t\text{N}=\text{}^{13}\text{C}$

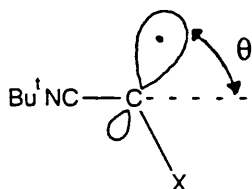
Imidoyl radicals of the general type **2.9.1** are usually bent at C_α and the angle θ increases as the electronegativity of the substituent increases.²⁹ We used isotopically-enriched *t*-butyl isocyanide (ca. 33 atom% $^{13}\text{C}_\alpha$), to measure the values of $a(^{13}\text{C}_\alpha)$ for **2.9.1** in which $\text{X} = -\text{C}(\text{H})(\text{CO}_2\text{Et})_2$, $-\text{C}(\text{H})(\text{CO}_2\text{SiMe}_3)_2$, $-\text{C}(\text{Me})(\text{CO}_2\text{Et})_2$ and $-\text{C}(\text{CO}_2\text{Et})_3$ (see Table 2.9.1).

Table 2.9.1: ^{13}C Hyperfine coupling constants for $\text{Bu}^i\text{N}=\overset{\cdot}{\text{C}}\text{X}$ in cyclopropane.

X	T/K	$a(^{13}\text{C}_\alpha)/\text{G}$
$\text{HC}(\text{CO}_2\text{Et})_2$	180	86.7
$\text{HC}(\text{CO}_2\text{SiMe}_3)_2$	215	85.9 ^a
$\text{C}(\text{CO}_2\text{Et})_3$	200	92.8 ^b
$\text{MeC}(\text{CO}_2\text{Et})_2$	286	85.3

^a At 250 K, $a(^{13}\text{C}_\alpha) = 86.0$ G. ^b At 250 K $a(^{13}\text{C}_\alpha) = 93.0$ G

The magnitude of $a(^{13}\text{C}_\alpha)$ is a sensitive measure of the contribution of the α -C2s atomic orbital to the SOMO and is thus a measure of the deviation from linearity at C_α in the imidoyl radical, structure **2.9.1**. These imidoyl radicals are evidently strongly bent at C_α and the extent of bending increases with the number of CO_2Et groups attached to C_β , as expected from consideration of group electronegativities. The values of $a(^{13}\text{C}_\alpha)$ were found to be larger than the value for $\text{Bu}^i\text{N}=\dot{\text{C}}\text{SBu}^i$ (76.0 G), but smaller than that for $\text{Bu}^i\text{N}=\dot{\text{C}}\text{OBu}^i$ (108.0 G).²⁹ For example, the radical $\text{Bu}^i\text{N}=\dot{\text{C}}\text{SiEt}_3$ shows $a(^{13}\text{C}_\alpha) = 29.8$ G and is believed to be linear at C_α , such that the SOMO is essentially a C-2p orbital and the $a(^{13}\text{C})$ arises through spin polarisation. (cf. CH_3^\bullet which shows $a(^{13}\text{C}_\alpha) = 36.6$ G). In contrast, $\text{Bu}^i\text{N}=\dot{\text{C}}\text{OBu}^i$ shows $a(^{13}\text{C}_\alpha) = 108.0$ G, corresponding to ca. 10% unpaired electron at the C_α -2s atomic orbital, and is strongly bent at C_α .



2.9.1

In conclusion, these results indicate that the exploitation of polar effects to influence the rate of addition of carbon-centred radicals to isocyanides could provide a basis for useful procedures for chain extension and ring formation.³¹⁻³³ Similar principles might be applicable to radical addition to carbon monoxide.³⁴ Substituent effects which act to increase the nucleophilicity of the carbon atom in the NC function might be used to advantage.

2.10. References to Chapter 2

- 1 W. Lung-Mun and H. Fischer, *Helvetica Chimica Acta*, 1983, **66**, 138
- 2 P. Kaushal, P.L.H. Mok and B.P. Roberts, *J. Chem. Soc., Perkin Trans. 2*, 1990, 1663.
- 3 V. Paul, B.P. Roberts and C.R. Willis, *J. Chem. Soc., Perkin Trans. 2*, 1989, 1953.
- 4 V. Paul and B.P. Roberts, *J. Chem. Soc., Perkin Trans. 2*, 1988, 1183.
- 5 V. Paul, B.P. Roberts and C.A.S. Robinson, *J. Chem. Res. (S)*, 1988, 264.
- 6 R. P. Allen, B.P. Roberts and C.R. Willis, *J. Chem. Soc., Chem. Commun.*, 1989, 1387.
- 7 J.N. Kirwan, B.P. Roberts and C.R. Willis, *Tetrahedron Lett.*, 1990, **31**, 5093.
- 8 S.J Cole, J.N. Kirwan, B.P. Roberts and C.R. Willis, *J. Chem. Soc., Perkin Trans. 2*, 1991, 103.
- 9 J.K. Kochi, *Adv. Free Radical Chem.*, 1975, **5**, 189.
- 10 S. Brumby, *J. Phys. Chem.*, 1983, **87**, 1917.
- 11 P. Burkhard and H. Fischer, *J. Magn. Reson.*, 1980, **40**, 335.
- 12 A.G. Davies, D. Griller and B.P. Roberts, *J. Chem. Soc. B*, 1971, 1823
- 13 D. Griller and K.U. Ingold, *Acc. Chem. Res.*, 1980, **13**, 193.
- 14 H. Shuh and H. Fischer, *Internat. J. Chem. Kinetics*, 1976, **8**, 341
- 15 H. Shuh and H. Fischer, *Helv. Chim. Acta*, 1978, **61**, 2130.

- 16 H.J. Heffer, C.-H.S. Wu and G.S. Hammond, *J. Am. Chem. Soc.*, 1973, **95**, 851.
- 17 K. Münger and H. Fischer, *Internat. J. Chem. Kinetics*, 1985, **17**, 809.
- 18 F. Jent, H. Paul, E. Roduner, M. Heming and H. Fischer, *Internat. J. Chem. Kinetics*, 1986, **18**, 113.
- 19 I. Beranek and H. Fischer, in *Free Radicals in Synthesis and Biology*, ed. F. Minisci, NATO, ASI Series C, vol. 260, Kluwer Academic Publishers, Dordrecht, 1989, pp 303-315.
- 20 J.A. Baban and B.P. Roberts, *J. Chem. Soc., Perkin Trans. 2*, 1981, 161.
- 21 D.P. Curran and C.-T. Chang, *J. Org. Chem.*, 1989, **54**, 3140.
- 22 D.P. Curran, E. Bosh, J. Kaplan and M. Newcomb, *J. Org. Chem.*, ~~1989~~ **54**, 1826.
- 23 D.P. Curran, M.-H. Chen, E. Spletzer, C.-M. Seong and C.-T. Chang, *J. Am. Chem. Soc.*, 1989, **111**, 8872.
- 24 A.L.J. Beckwith and S. Glover, *Aust. J. Chem.*, 1978, **40**, 157.
- 25 D. Lal, D. Griller, S. Husband and K.U. Ingold, *J. Am. Chem. Soc.*, 1974, **96**, 6355.
- 26 C. Chatgililoglu, K.U. Ingold and J.C. Scaiano, *J. Am. Chem. Soc.*, 1981, **103**, 7739.
- 27 V. Paul, B.P. Roberts and C.R. Willis, *J. Chem. Soc., Perkin Trans. 2*, 1989, 1953.
- 28 P.M. Blum and B.P. Roberts, *J. Chem. Soc., Chem. Commun.*, 1976, 535.

- 29 P.M. Blum and B.P. Roberts, *J. Chem. Soc., Perkin Trans. 2*, 1978, 1313.
- 30 K.B. Wiberg, *J. Org. Chem.*, 1991, **56**, 544
- 31 M.D. Bachi and D. Denenmark, *J. Org. Chem.*, 1990, **55**, 3442.
- 32 M.D. Bachi and D. Denenmark, *J. Am. Chem. Soc.*, 1989, **111**, 1886.
- 33 D.P. Curran and H. Liu, *J. Am. Chem. Soc.*, 1991, **113**, 2127.
- 34 I. Ryu, K. Kusano, M. Hasegawa, N. Kambe and N. Sonoda, *J. Chem. Soc., Chem Commun.*, 1991, 1018.

Chapter 3: EXPERIMENTAL

3.1. ESR Spectroscopy and Computer Simulations

ESR spectra were recorded during continuous UV irradiation of samples positioned in a standard variable temperature insert in the microwave cavity of a Varian E-109 or a Bruker ESP-300 spectrometer operating at 9.1-9.4 GHz. The light source was a 500 W mercury discharge lamp (Osram HBO 500 W/2) in an Oriel 1 KW housing equipped with an f0.7 Aspherab fused silica condensing lens. The slightly converging beam from this was focused using a fused silica lens (focal length 10 cm, diameter 7.5 cm) and directed onto the sample through a 3 cm pathlength water-cooled cell filled with a aqueous solution containing $\text{NiSO}_4 \cdot 7\text{H}_2\text{O}$ (0.38 mol dm^{-3}), $\text{CoSO}_4 \cdot 7\text{H}_2\text{O}$ (0.07 mol dm^{-3}) and sulfuric acid (0.04 mol dm^{-3}). The temperature of the sample during photolysis was determined, using the method described previously,¹ by careful measurement of the value of $a(\text{H}_\beta)$ (in gauss) for the isobutyl radical in cyclopropane. The temperature dependence of this splitting constant is given by equation (3.1). The heating effect at full light intensity varied between 5 and 7 K depending on conditions.

$$T/K = 2.70394 a(\text{H}_\beta)^2 - 198.419 a(\text{H}_\beta) + 3763.56 \quad (3.1)$$

Samples were prepared using a vacuum line and were sealed in evacuated Suprasil quartz tubes (2 or 3 mm i.d., 0.5 mm wall, depending on the dielectric properties of the contents).

The microwave frequency was measured using a frequency counter (Hewlett-Packard 5350B) and the magnetic field was measured using an NMR gaussmeter calibrated to account for the field difference between the sample and the NMR probe using the pyrene radical anion (g 2.00271) as standard.^{2,3} Where necessary, second-order corrections⁴ were applied to g -factors and hyperfine splittings.

Computer simulations of spectra were obtained using a modified version of ESRSPEC2,⁵ extended to handle composite spectra from up to four radicals with different centres, second-order shifts for coupling to single nuclei with $I > \frac{1}{2}$, and lineshapes continuously variable between 100% Gaussian and 100% Lorentzian.

Relative radical concentrations were determined by double integration of appropriate lines in each spectrum and/or by computer simulation of the composite spectrum. On the timescale of most measurements, extrapolation of radical concentration ratios to zero photolysis time gave negligible corrections. The ESR spectra of some radicals exhibited CIDEP effects such that corresponding hyperfine lines to low- and high-field of the spectrum centre

were of unequal intensity (E/A polarisation).⁶⁻⁸ In those circumstances, relative radical concentrations were determined by taking the average intensity of corresponding low- and high-field lines.⁶⁻⁸ Absolute radical concentrations were measured by comparison with the spectrum obtained from a standard solution of *N,N*-diphenyl-*N*-picrylhydrazyl in carbon tetrachloride, using the signal from a piece of synthetic ruby (fixed permanently inside the microwave cavity) as an internal standard.¹

3.2. NMR Spectroscopy

NMR spectra (CDCl₃ solvent) were obtained with a Varian VXR-400 instrument (400 MHz for ¹H), using tetramethylsilane as an internal standard (¹H) or BF₃·OEt₂ as an external standard (¹¹B).

3.3. Materials

Di-*t*-butyl peroxide (98%, Aldrich) was passed down a column of basic alumina (activity 1) and distilled (b.p. 46-47 °C at 76 Torr) before use. Diethyl pent-4-enylmalonate⁹ and methyl isocyanide¹⁰ were prepared as described in the literature. Trimethylamine-butylborane (TMBB) was prepared using the method of Hawthorne,¹¹ with a slight modification as described below for trimethylamine-methylborane.

Trimethylamine-methylborane.^{12,13} - Lithium aluminium hydride (13.7 g, 0.36 mol) was added to dry diethyl ether (250 cm³) and the mixture was stirred under reflux for 1 h under argon. The resulting solution was cooled in an ice-bath, the reaction flask was equipped with a condenser containing solid CO₂-acetone slush, and trimethylamine (45 cm³, 0.50 mol) was allowed to evaporate into the solution. The mixture was stirred and warmed under reflux during dropwise addition of trimethylboroxine (10.2 g, 0.08 mol; Aldrich) in diethyl ether (40 cm³). After the addition was complete, the mixture was heated under reflux for 1.5 h, then cooled using an ice-salt bath during *cautious* dropwise addition of water (30.5 cm³). Anhydrous MgSO₄ (ca. 20 g) was added and the mixture was left to stand at room temperature overnight. The mixture was filtered under argon, the filtrate was dried further (MgSO₄), Et₂O was removed under reduced pressure and the residue was distilled to yield trimethylamine-methylborane (14.4 g, 70%), b.p. 60 °C at 16 Torr. δ_{H} -0.20 (br.t, 3H, MeB), 1.80 (q, 2H, *J* 95 Hz, BH₂), and 2.52 (s, 9H, MeN). δ_{B} -3.8 (t, *J* 95 Hz).

Diethyl 2-bromoethylmalonate.¹⁴ - Diethyl 1,1-cyclopropanedicarboxylate (10.32 g, 0.055 mol; Aldrich) was weighed into a dry, argon-filled, two-necked, flat-bottomed flask and a magnetic stirrer bar was added. One neck was connected through an air condenser to a bubbler and the other neck was fitted with a gas inlet tube through which either argon or dry HBr gas could be passed. The flask was immersed in a water bath and the contents stirred while

HBr gas was bubbled slowly through the liquid. The weight gain was determined periodically after flushing out the flask with argon. When HBr (4.22 g, 0.052 mol) had been absorbed (5-10 min bubbling) analysis by ^1H NMR spectroscopy showed the presence only of residual cyclopropanedicarboxylate (5%) and diethyl 2-bromoethylmalonate (95%); δ_{H} 1.28 (t, 6H, Me), 2.44 (q, 2H, CH_2C), 3.46 (t, 2H, CH_2Br), 3.66 (t, 1H, CH) and 4.22 (q, 4H, CH_2O). This mixture was used without purification.

Bis(2,2,2-trifluoroethyl) malonate. - Malonyl dichloride (12.85 g, 0.09 mol) in diethylether (80 cm³) was added dropwise to a solution of trifluoroethanol (18.10 g, 0.18 mol) and triethylamine (20.39 g, 0.20 mol) in diethyl ether. The mixture was heated under reflux for 3 h, allowed to cool to room temperature, the amine hydrochloride precipitate was removed by filtration, and the ether was removed under reduced pressure. The crude product was redissolved in Et₂O (50 cm³) and washed with sulfuric acid (2 x 25 cm³, 2 mol dm⁻³), then with saturated sodium chloride solution (25 cm³) and dried (MgSO₄). Diethyl ether was removed under reduced pressure and the residual oil was distilled to yield the malonate (9.05 g, 64%), b.p. 60-62 °C at 0.9 Torr. δ_{H} 4.56 (q, 4H, J_{HF} 8.23), 3.61 (s, 2H); δ_{C} 40.10, 61.08, 124.02, 164.07. ($J_{\text{C-F}}$ 37.2)

^{13}C -Labelled *t*-butyl isocyanide.^{15,16} - ^{13}C -Labelled *t*-butyl isocyanide was prepared according to the method of Nef^{15,16}, from *t*-butyl iodide and labelled silver cyanide, itself prepared from K¹³CN (Aldrich; 99% atom % ^{13}C , 0.25 g)

diluted with normal KCN (0.75 g).

3.4. References to Chapter 3

- 1 J.A. Baban and B.P. Roberts, *J. Chem. Soc., Perkin Trans. 2*, 1981, 161.
- 2 B. Segal, M. Kaplan and G.K. Fraenkel, *J. Chem. Phys.*, 1965, **43**, 4191.
- 3 R. Allendorfer, *J. Chem. Phys.*, 1971, **55**, 161.
- 4 R.W. Fessenden, *J. Chem. Phys.*, 1962, **37**, 747.
- 5 P.J. Krusic, *QCPE*, Program no. 210.
- 6 J.K.S. Wan and A.J. Elliot, *Acc. Chem. Res.*, 1977, *10*, 161.
- 7 P.J. Hore, C.G. Joslin and K.A. McLauchlan, *Chem. Soc. Rev.*, 1979, **8**, 29.
- 8 M. Anpo, K.U. Ingold and J.K.S. Wan, *J. Phys. Chem.*, 1983, **87**, 1674.
- 9 R.G. Salomon, D.J. Coughlin, S. Ghosh and M.G. Zagorski, *J. Am. Chem. Soc.*, 1982, **104**, 998.
- 10 R.E. Schuster, J.E. Scott and J. Casanova, *Org. Synth.*, 1966, **46**, 75.
- 11 M.F. Hawthorne, *J. Am. Chem. Soc.*, 1961, **83**, 831.
- 12 P. Kaushal, P.L.H. Mok and B.P. Roberts, *J. Chem. Soc., Perkin Trans. 2*, 1990, 1663.
- 13 H.I. Schlesinger, N.W. Flodin and A.B. Burg, *J. Am. Chem. Soc.*, 1939, **61**, 1078.
- 14 A.C. Knipe and C.J.M. Stirling, *J. Chem. Soc. (B)*, 1968, 67. A.C. Knipe, personal communication.

- 15 P.M. Blum and B.P. Roberts, *J. Chem. Soc., Perkin Trans. 2*, 1978, 1313.
- 16 I.U. Nef, *Justus Liebig's Ann. Chem.*, 1899, **309**, 126.

**SECTION B: ENANTIOSELECTIVE HYDROGEN-ATOM ABSTRACTION
BY OPTICALLY ACTIVE AMINE-BORYL RADICALS**

Chapter 4: INTRODUCTION

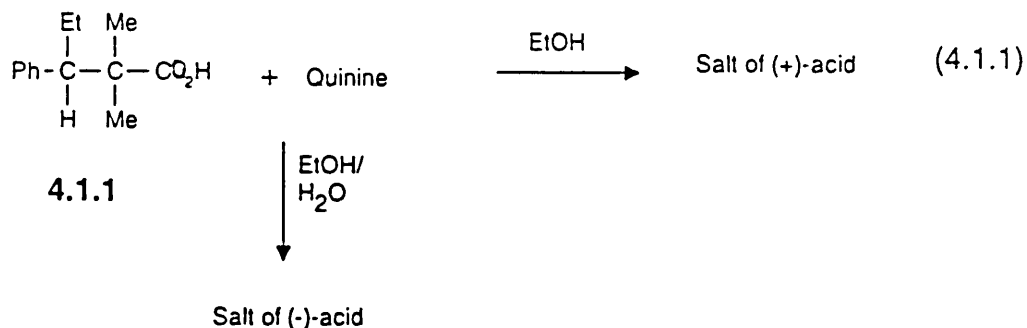
Chirality is a prominent feature of most biological processes, and the enantiomers of bioactive molecules often give different biological effects.¹ In recent years interest in the synthesis of pure enantiomers has gained new impetus as a result of the increasing awareness of the importance of optical purity in the context of biological activity.² Optical activity can be introduced by resolving a racemate or by asymmetric synthesis. The latter refers to the use of a chiral reagent on a prochiral substrate to produce an excess of one enantiomer in a chemical process. In the absence of a chiral reagent a racemic product would be produced.

4.1. Methods for Resolution

The important practical methods for the separation of enantiomers from a racemic mixture are described below.^{3,4}

Resolution via diastereoisomer formation. This method involves the combination of a racemate with a chiral reagent, followed by the separation of the diastereoisomeric products. This technique constitutes one of the most practical methods for resolution. For example, the reaction of a racemate with an optically active acid or base to form a mixture of diastereoisomeric salts which is separated by crystallisation,⁵ such as the resolution of the acid **4.1.1**

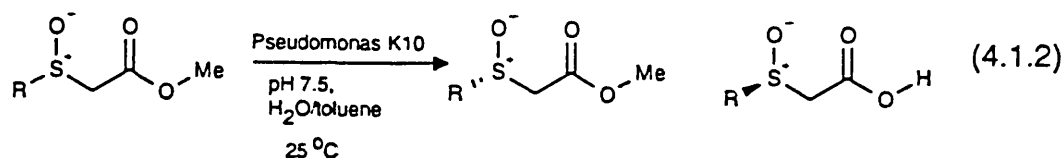
using quinine [eqn. (4.1.1)].



*Differential absorption.*⁶ If a chromatographic column is packed with a chiral substance then, when a racemic mixture is placed on that column, the enantiomers will move along the packing at different rates. Chiral columns and chiral additives have made a major impact on chromatographic analysis and purification of enantiomers.

Mechanical separation. This process relies upon the spontaneous or induced crystallisation of optically active compounds from racemic solutions. The enantiomers are able to crystallise as mechanical mixtures of crystals containing only the (*R*) or the (*S*) enantiomer in the unit-cell, and it is then possible to separate them manually.⁵ Some racemic amino acids and their derivatives are known to separate in this way,⁷ such as asparagine, histidine, thionine, glutamic acid and aspartic acid. Other amino acids have also been resolved in the form of aromatic sulfonates and these include alanine, leucine and lysine.⁷

Biochemical processes.^{8,9} Enzymes and living organisms such as bacteria are used to digest one of the enantiomers for use in biosynthesis. An example is provided by the biocatalytic resolution of sulfinylalkanoates using crude lipase prepared from *Pseudomonas sp.* to mediate the hydrolysis of these esters in an aqueous environment [eqn. (4.1.2)].¹⁰ When R was 4-ClC₆H₄, the ester was recovered in 48% yield and 95% enantiomeric excess (e.e.), and the acid in 38% yield and 91% e.e.

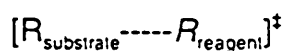


*Kinetic resolution.*¹¹ Enantiomers react with chiral compounds at different rates, so it is sometimes possible to affect a separation by stopping the reaction before completion. This process is discussed in more detail below.

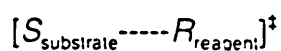
4.2. Kinetic Resolution

The enantiomers of a racemic mixture [50% (*R*)-enantiomer, 50% (*S*)-enantiomer], react at different rates with an optically active reagent [e.g. 100% (*R*)-enantiomer]. This difference in rate occurs because the transformation is mediated by a chiral reagent, and the two possible transition states for the reaction 4.2.1 and 4.2.2 are diastereomeric. Therefore, the transition state

energies will be different for each enantiomer, and thus the rate of reaction will be different. Hence, the reaction will be enantioselective, with one enantiomer being removed more rapidly.

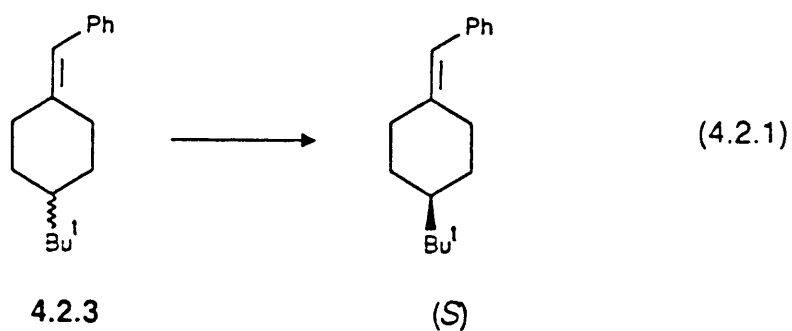


4.2.1



4.2.2

The first successful example of a chemical kinetic resolution, was the partial esterification of racemic mandelic acid by (-)-menthol under homogenous conditions.¹² Another example, is the kinetic resolution of alkenes *via* asymmetric dihydroxylation,¹³ using an osmium tetroxide-cinchona alkaloid catalyst; when the ligand was 1,4-bis(9-*O*-dihydroquinine)phthalazine the alkene 4.2.3 was recovered with an e.e. of 66% after 50% consumption.



The success of a kinetic resolution relies on the fact that the two enantiomers react at different rates with a chiral reagent, and the usefulness of a kinetic resolution for a given percentage consumption is measured by the value of the e.e. for the unreacted substrate. These quantities are directly

related by eqn. (4.2.2) to the enantioselectivity-factor s which is the ratio of the rates of reaction for the faster and slower reacting enantiomer (*i.e.* k_R/k_S or k_S/k_R).¹¹

$$s = \frac{\ln[(1 - C)(1 - EE)]}{\ln[(1 - C)(1 + EE)]} \quad (4.2.2)$$

EE , is the fractional e.e.

C , is the fractional consumption.

Sharpless and co-workers published computed curves showing the evolution of e.e. as a function of the conversion for various values of s (Figure 4.2.1).¹⁴ It is important to note that a relative rate difference of 100 is nearly as effective as a relative rate difference of infinity. Even small rate differences (*e.g.* 5-10) can provide useful amounts of a substance with high enantiomeric purity. For example, when $s = 5$, after 75% consumption the remaining substrate shows an e.e. in excess of 95%, and 25% yield is not unreasonable since 50% is the maximum yield expected in a perfect kinetic resolution. Therefore, it is possible to obtain products with as high an e.e. as desired if losses of material can be tolerated. Most of the chemical kinetic resolutions described in the literature involve s -values lower than 10.¹¹ The Sharpless epoxidation of racemic allylic alcohols with a given tartrate-titanium isopropoxide combination, provides us with a very successful example of kinetic resolution, with s -values ranging from 15-140.¹⁴ For example, during the oxidation of the

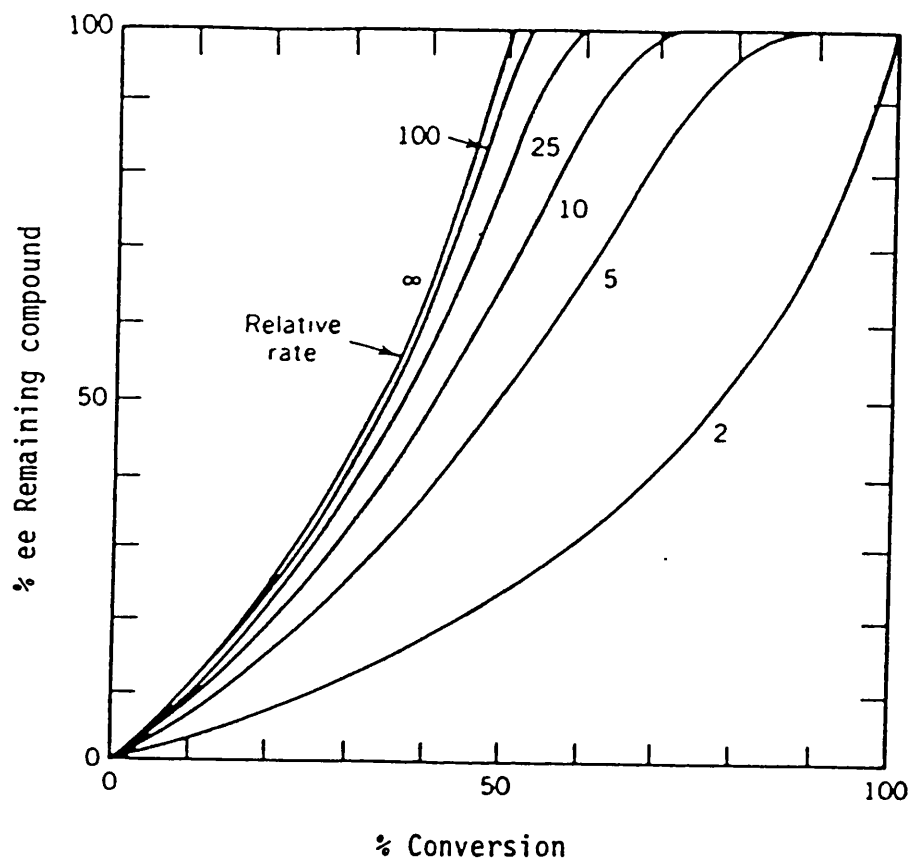
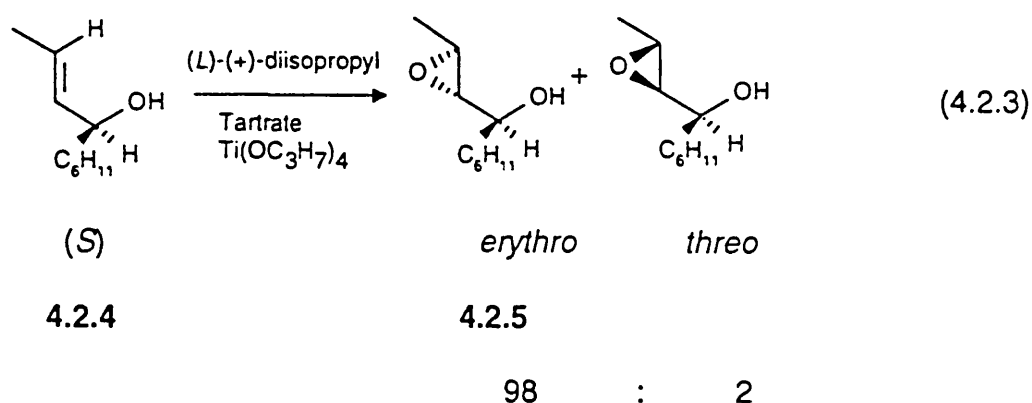


Figure 4.2.1:¹⁴ Dependence of e.e. on relative rates of reaction of two enantiomers.

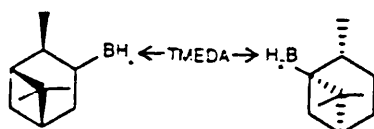
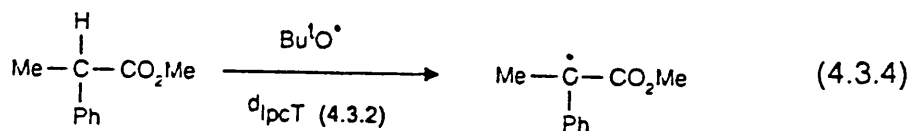
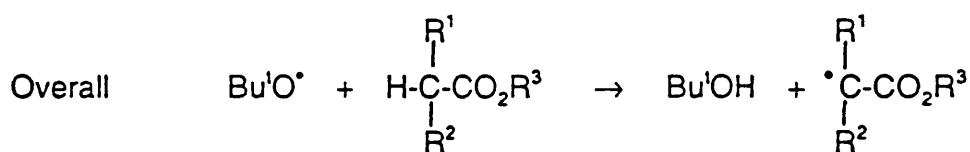
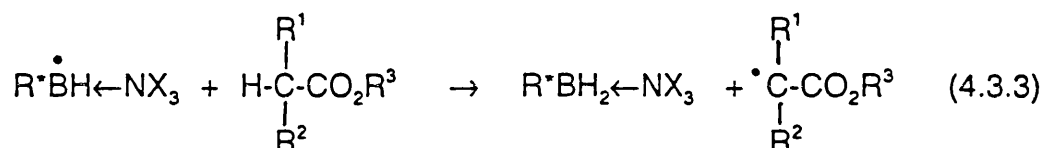
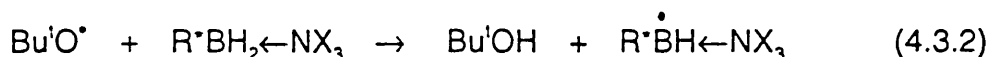
racemic alcohol 4.2.4 using *L*-(+)-diisopropyl tartrate, the (*S*)-enantiomer reacts about a hundred times faster than the (*R*)-enantiomer, leading preponderantly to the *erythro*-epoxide 4.2.5. After 55% consumption, the (*R*)-alcohol is recovered with an e.e. > 96% [eqn. (4.2.3)].



4.3. Enantioselective Hydrogen-Atom Abstraction

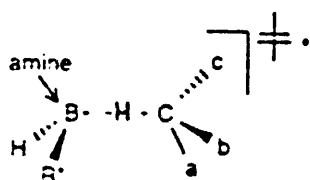
It is known that abstraction of electron deficient hydrogen from substrates such as esters, ketones and nitriles is subject to polarity reversal catalysis by amine-alkylboranes.¹⁵⁻¹⁸ Work done by Pearl Mok,¹⁵⁻²¹ showed that if the amine-boryl radical is optically active (*e.g.* if the amine moiety or the *B*-alkyl group is chiral) and the ester is also chiral, then, the hydrogen-atom abstraction step can be enantioselective, and the overall hydrogen-atom transfer to Bu[•]O[•] also becomes enantioselective [eqn. (4.3.1)-(4.3.3)]. This has been used for the kinetic resolution of racemic esters [e.g. eqn. (4.3.4), shows the kinetic resolution of methyl-2-phenylpropanoate using the amine-borane

4.3.2 at -67 °C. The unreacted ester was recovered in 30.2% e.e. after 54.5% consumption].²¹



4.3.2

It was suggested that steric interactions between the groups attached to boron and those attached to the α -carbon atom of the substrate in a transition state of the general structure 4.3.3, could account for the selectivities observed.²¹

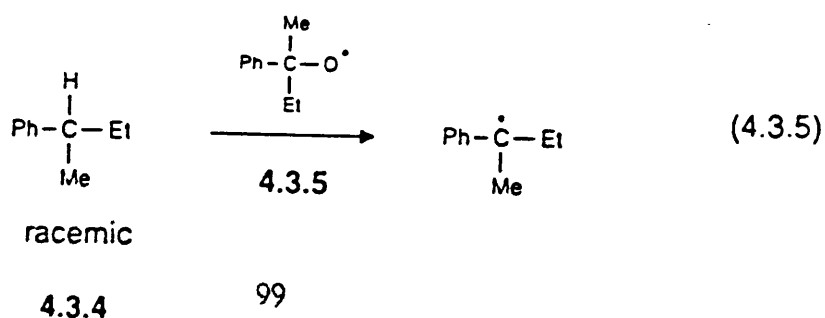


4.3.3

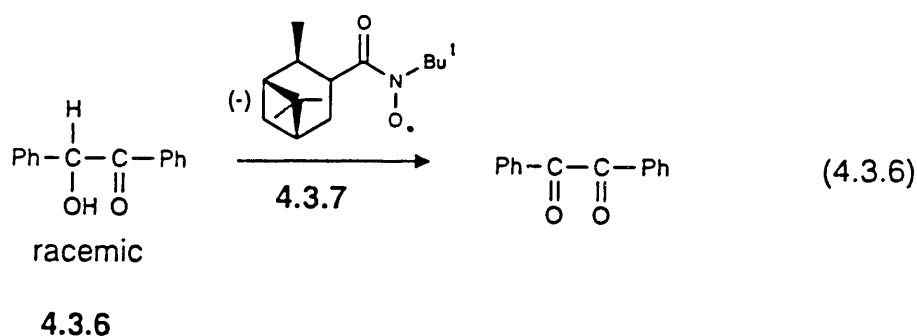
However, the enantioselectivities achieved were not large, and it was noted that factors other than steric strain will probably also be important in determining the relative stabilities of the diastereoisomeric transition states. An aim of the work described in this section was to carry out further studies of the enantioselective hydrogen-atom abstraction reactions of chiral amine-boryl radicals with a variety of substrate containing electron deficient C-H groups α to a carbonyl function, in attempt to define more precisely the factors which influence chiral discrimination.

Though, many examples of stereoselective free radical reactions are known, there are comparatively few examples of enantioselective radical reactions, and enantioselective atom-transfer reactions are particularly uncommon.

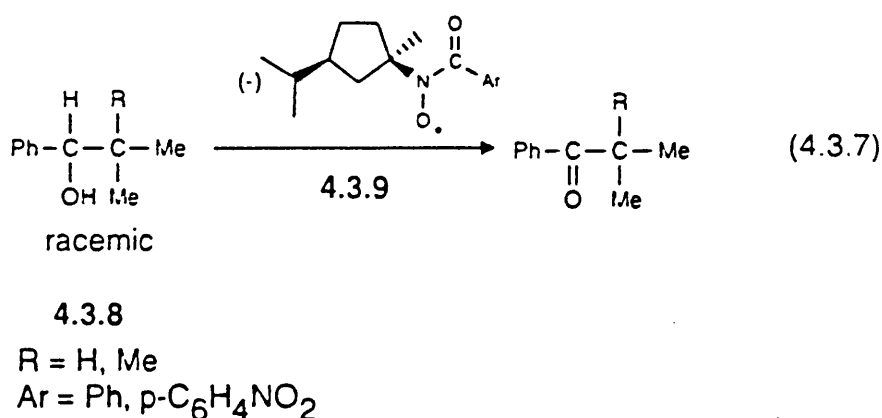
The first example of an enantioselective H-atom transfer to be reported was the partial resolution of racemic 2-phenylbutane **4.3.4** with the optically active 2-phenyl-2-butoxyl radical **4.3.5** (optical purity 86.2%) at 293 K [eqn. (4.3.5)]. After 50% consumption of 2-phenylbutane, the unreacted alkane recovered was found to be enriched with 15.4% of the (+)-enantiomer.²²



A second example of enantioselective H-atom abstraction is the oxidation of racemic benzoin **4.3.6** by the pinanecarbonyl aminoxy radical **4.3.7** [eqn. (4.3.6)] at room temperature. The unreacted benzoin showed $[\alpha]^{25}_D$ (CHCl_3) = $+14^\circ$, corresponding to an e.e. of 7% after 60% consumption of benzoin.²³

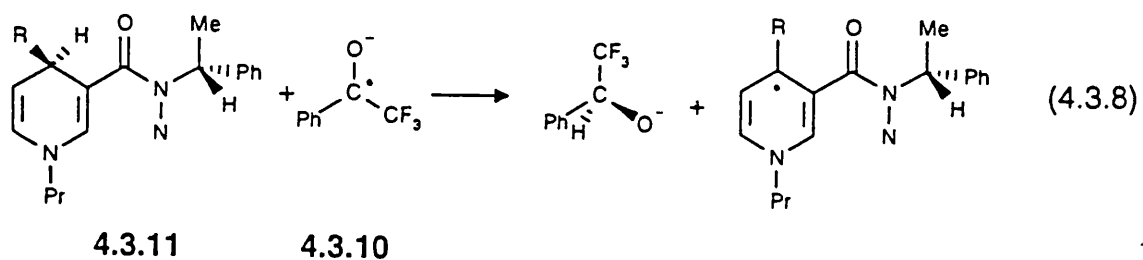


This process was further extended to the oxidation of α -phenylalcohols **4.3.8** using acyl fenchyl aminoxy radicals **4.3.9** [eqn. (4.3.7)], but enantioselectivities remained very small.²⁴



A third example of enantioselective H-atom transfer is provided by the reduction of prochiral α,α,α -trifluoroacetophenone by enantiomerically enriched

dihyronicotinamides **4.3.11** [eqn. (4.3.8)]. The radical anion **4.3.10** derived from the trifluoroacetophenone reacts with the dihyronicotinamide (R = H or Me) to give to give the (*S*)-alkoxide with an e.e. of 22 and 67% respectively.²⁵



4.4. References to Chapter 4

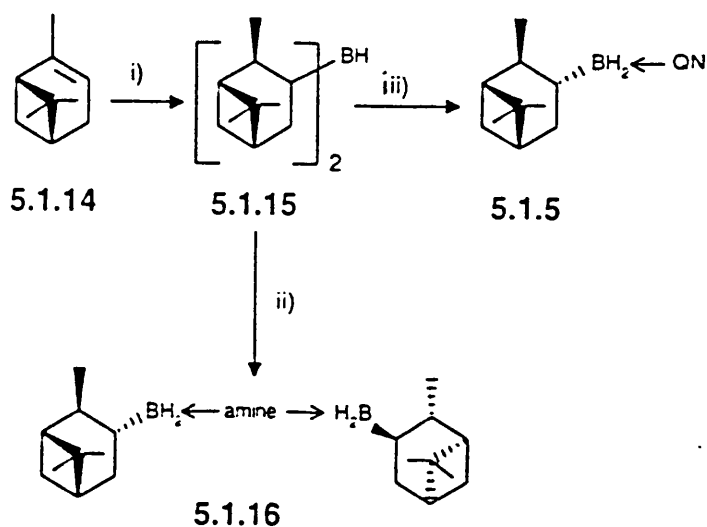
- 1 J. Carey, *Chem. in Britain*, 1993, **29**, 1053.
- 2 R. Sheldon, *Chem. and Industry*, 1990, 212.
- 3 J. March, in *Advanced Organic Chemistry*, 3rd ed., ch. 4, 102.
- 4 S.H. Wilen, in *Topics in stereochem.*, **6**, 108.
- 5 S.H. Wilen, A. Collet and J. Jacques, *Tetrahedron*, 1977, **33**, 2725.
- 6 P. Camilleri, V de Biasi and A. Hutt, *Chem. in Britain*, 1994, **30**, 43.
- 7 S. Yamada, M. Yamamoto and I. Chibata, *J. Org. Chem.*, 1973, **38**, 4408.
- 8 A.J.M. Jansen, A.J.H. Klunder and B. Zwanenburg, *Tetrahedron*, 1991, **47**, 7645.
- 9 A.M. Klibanov, *Acc. Chem. Res.*, 1990, **23**, 114.
- 10 K. Burgess, I. Henderson and K.-K. Ho, *J. Org. Chem.*, 1992, **57**, 1290.
- 11 H.B. Kagan and J.C. Fiaud, in *Topics in Stereochem.*, 1988, **18**, 249.
- 12 W. Marckwald and A. McKensie, *Chem. Ber.*, 1899, **32B**, 2130.
- 13 M.S. Van Nieuwenhze and K.B. Sharpless, *J. Am. Chem. Soc.*, 1993, **115**, 6237.
- 14 V.S. Martin, S.S. Woodward, T. Katsuki, Y. Yamada, M. Ikeda and K.B. Sharpless, *J. Am. Chem. Soc.*, 1981, **103**, 6237.
- 15 P. Kaushal, P.L.H. Mok and B.P. Roberts, *J. Chem. Soc., Perkin Trans. 2*, 1990, 1663.
- 16 V. Paul and B.P. Roberts, *J. Chem. Soc., Chem. Commun.*, 1987, 1322.

- 17 V. Paul and B.P. Roberts, *J. Chem. Soc., Perkin Trans. 2*, 1988, 1183.
- 18 V. Paul, B.P. Roberts and C.R. Willis, *J. Chem. Soc., Perkin Trans. 2*, 1989, 1953.
- 19 P.L.H. Mok and B.P. Roberts, *J. Chem. Soc., Chem. Commun.*, 1991, 150.
- 20 P.L.H. Mok and B.P. Roberts, *Tetrahedron Lett.*, 1992, 7249.
- 21 P.L.H. Mok, B.P. Roberts and P.T. McKetty, *J. Chem. Soc., Perkin Trans. 2*, 1993, 665.
- 22 J.H. Hargis and H.-H Hsu, *J. Am. Chem. Soc.*, 1977, **99**, 8114.
- 23 C. Berti and M.J. Perkins, *Angew. Chem., Internat. Ed. Engl.*, 1979, **29**, 864.
- 24 D.J. Brooks, M.J. Perkins, S.L. Smith, D.M. Goodhall and D.K. Lloyd, *J. Chem. Soc., Perkin Trans. 2*, 1992, 393.
- 25 D.D. Tanner and A. Kharrat, *J. Am. Chem. Soc.*, 1988, **110**, 2968.

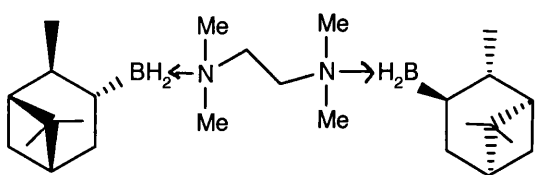
Chapter 5: RESULTS AND DISCUSSION

5.1. Synthesis of Catalysts

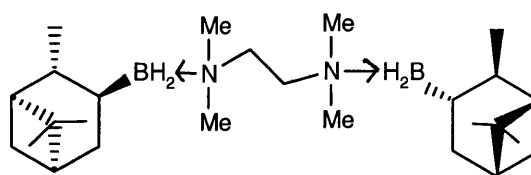
The chiral amine-borane complexes used in this section are shown in structures 5.1.1-5.1.13. The isopinocampheylborane complexes 5.1.1, 5.1.3 and 5.1.5 with *N,N,N',N'*-tetramethylethylenediamine (TMEDA),¹⁻⁵ 1,4-diazabicyclo[2.2.2]octane (DABCO),⁶ and quinuclidine (QN), respectively, are those derived from (1*R*)-(+)- α -pinene 5.1.14 by hydroboration, followed by reaction of diisopinocampheylborane (Ipc₂BH) 5.1.15 with the appropriate amine (see Scheme 5.1.1). The enantiomeric forms 5.1.2, 5.1.4 and 5.1.6 were obtained from (1*S*)-(-)- α -pinene.



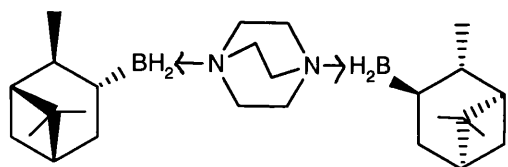
Scheme 5.1.1: Reagents and conditions: i) BMS, Et₂O reflux; ii) 0.5 mol eq. TMEDA or DABCO; iii) 1 mol eq. QN.



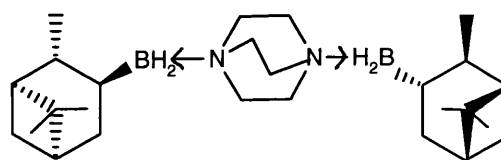
5.1.1
d_{IpcT}



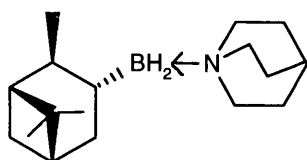
5.1.2
l_{IpcT}



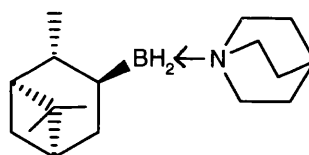
5.1.3
d_{IpcD}



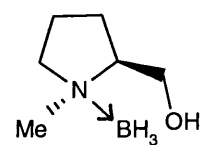
5.1.4
l_{IpcD}



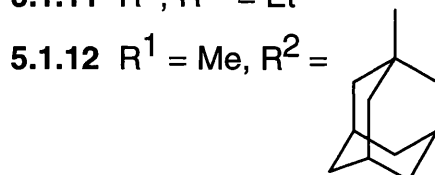
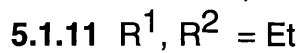
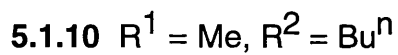
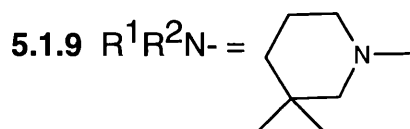
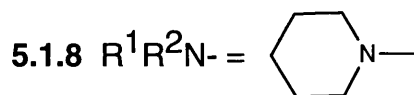
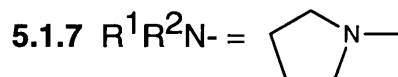
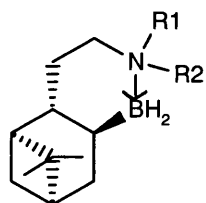
5.1.5
d_{IpcQ}



5.1.6
l_{IpcQ}



5.1.13

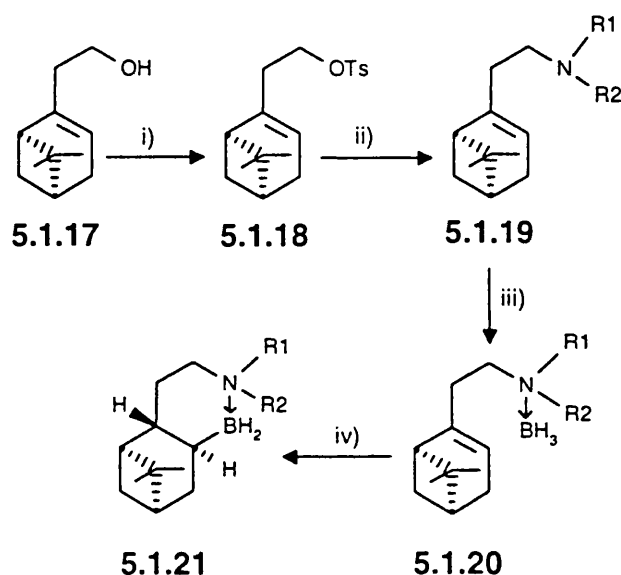


Treatment of a two-fold excess of **5.1.14** (or its enantiomer) with one molar equivalent of borane-dimethyl sulfide (BMS) in refluxing diethyl ether rapidly gives Ipc_2BH **5.1.15** (or its enantiomer). Subsequent addition of amine (0.5 eq. TMEDA or DABCO; 1 eq. QN) gives the crystalline complexes **5.1.1**, **5.1.3** and **5.1.5** (or their enantiomers **5.1.2**, **5.1.4** and **5.1.6**, respectively) by displacement of α -pinene. The superscript *d* or *l* is used with the acronyms shown to indicate whether the starting pinene (which was essentially optically pure) was *dextro*- or *laevo*-rotatory, following the convention adopted by Brown *et al.*⁷⁻¹⁰ *Syn*-hydroboration takes place from the least hindered face of the pinene (opposite from the 6,6-dimethyl bridge) to give a product of defined stereochemistry.^{8,11}

Unlike IpcT , IpcD does not enrich its optical purity upon crystallisation.²⁻⁶ It was therefore, necessary to synthesise this complex using optically pure α -pinene (>99% e.e.). The IpcD complex, like IpcT , was found to melt with obvious decomposition¹ (m.p. = 124-147 and 120-145 °C, respectively), the complex started to melt at 124 °C with visible evolution of gas (presumably hydrogen) and some solid was still visible at 147 °C. This is contrary to reports in the literature where melting points of 160-161 °C for IpcD and 140-141 °C for IpcT are reported.²⁻⁵ We conclude that IpcT and IpcD are thermally unstable at or below their melting points. IpcQ was found to melt between 74-76 °C without decomposition. The IpcD and IpcQ complexes were slightly more soluble in oxirane than IpcT and the former were shown to be relatively stable

in air. Thus, no changes in the ^1H NMR spectra of these complexes were noted after exposure of the crystalline compounds to the atmosphere for more than 24 h. IpcT is known to be stable under the same conditions for more than 12 h.¹

The polycyclic amine-boranes **5.1.7-5.1.11** were prepared from (1*R*)-(-)-nopol **5.1.17** (91% e.e.), as shown in Scheme 5.1.2.

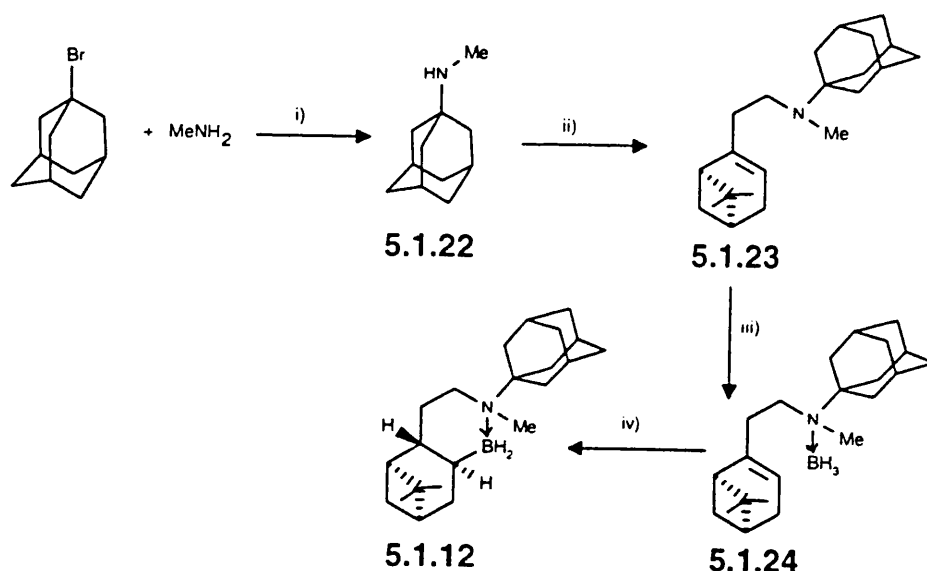


Scheme 5.1.2: *Reagents and conditions:* i) TsCl in pyridine at 0-5 °C; ii) amine (R¹R²NH) in THF, reflux; iii) BMS in Et₂O at -20 °C; iv) Toluene, reflux.

The (1*R*)-(-)-nopol **5.1.17** was treated with tosyl chloride in pyridine at ca. 5 °C to give (1*R*)-(-)-nopyl tosylate **5.1.18**. The tosylate leaving group was then displaced by the appropriate amine in refluxing tetrahydrofuran (THF) to give **5.1.19**. The complex **5.1.20** was formed by treating **5.1.19** with BMS at

-20 °C, followed by cyclisation of **5.1.20** to give **5.1.21** in refluxing toluene.

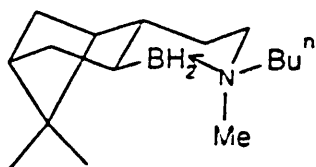
The complex **5.1.12** was prepared from *N*-adamantylmethylamine **5.1.22**, itself prepared by the reaction of adamantyl bromide with methylamine in a pressure vessel at 215 °C and *ca.* 70 bar; presumably an S_N1 mechanism is involved. The amine was treated with (1*R*)-nopyl tosylate in refluxing dioxan to give the tertiary amine **5.1.23**; the yield of this amine was lower than for the previously-synthesised nopyl amines **5.1.19**, presumably because of steric hindrance from the bulky adamantyl group. The amine **5.1.23** was then treated with BMS in diethyl ether at -20 °C to give **5.1.24**, followed by cyclisation of this complex in refluxing dioxan to give **5.1.12** (Scheme 5.1.3). Dioxan was used in preference to toluene, because with the latter solvent unidentified aromatic secondary reaction products were obtained alongside the desired product.



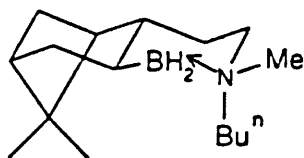
Scheme 5.1.3: *Reagents and conditions:* i) bromoadamantane and methylamine at 215 °C; ii) nopyl tosylate in dioxan, reflux; iii) BMS in Et₂O at -20 °C; iv) dioxan, reflux.

The relative ease with which the unsaturated amine-borane complexes **5.1.20** and **5.1.24** undergo cyclisation increases with the bulk of the *N*-alkyl groups along the series $(\text{CH}_2)_4\text{N} \sim (\text{CH}_2)_5\text{N} < \text{MeBu}^n\text{N} \sim \text{Et}_2\text{N} < (\text{Me})_2\text{C}(\text{CH}_2)_4\text{N} < \text{AdMeN}$ (Ad = adamantyl). This order suggests that thermally induced cleavage of the N→B bond in **5.1.20** and **5.1.24** precedes *syn*-hydroboration by free BH_3 at the least hindered face of the double bond. Cyclisation takes place to form the more stable *trans*-ring junction.

The ^1H and ^{13}C NMR of **5.1.10** showed it to consist of a 1 : 1 mixture of two isomers **5.1.10a** and **5.1.10b** (see Figures 5.1.1a-b), in which the *n*-butyl group occupies either the equatorial or the axial position, respectively. It is possible to separate the two isomers by high performance liquid chromatography (HPLC, Nucleosil 100 5 μm silica gel stationary phase, hexane-ethyl acetate, 99 : 1 v/v eluent). The first isomer to elute is a low melting solid (m.p. = 29-30 °C) and the second isomer is a viscous liquid. We were unable at this stage to assign the isomers to their respective configurations.



5.1.10a



5.1.10b

In principle, **5.1.9** and **5.1.12** could also exist as mixtures of axial and equatorial

Mixture of isomers

a)

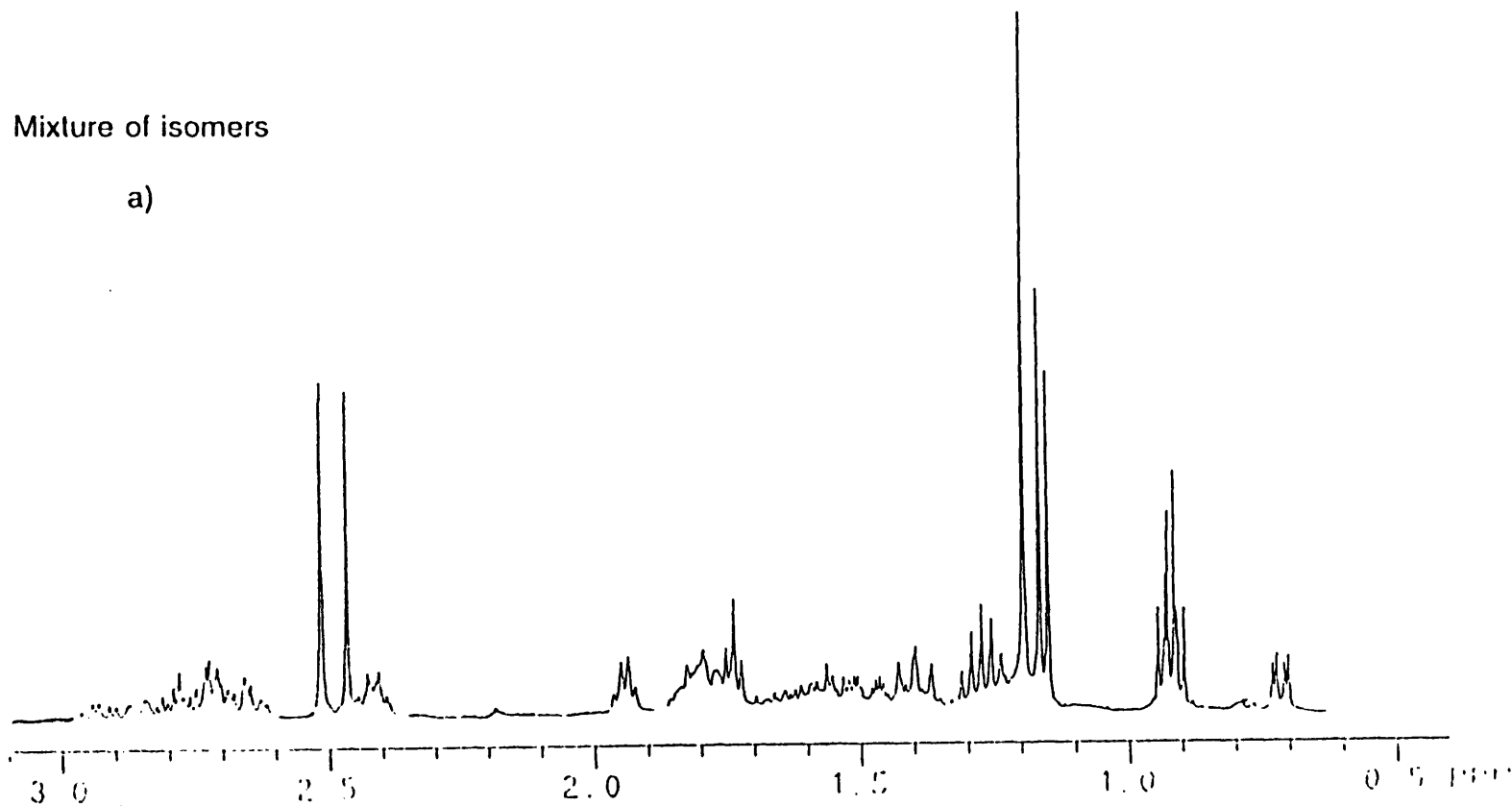
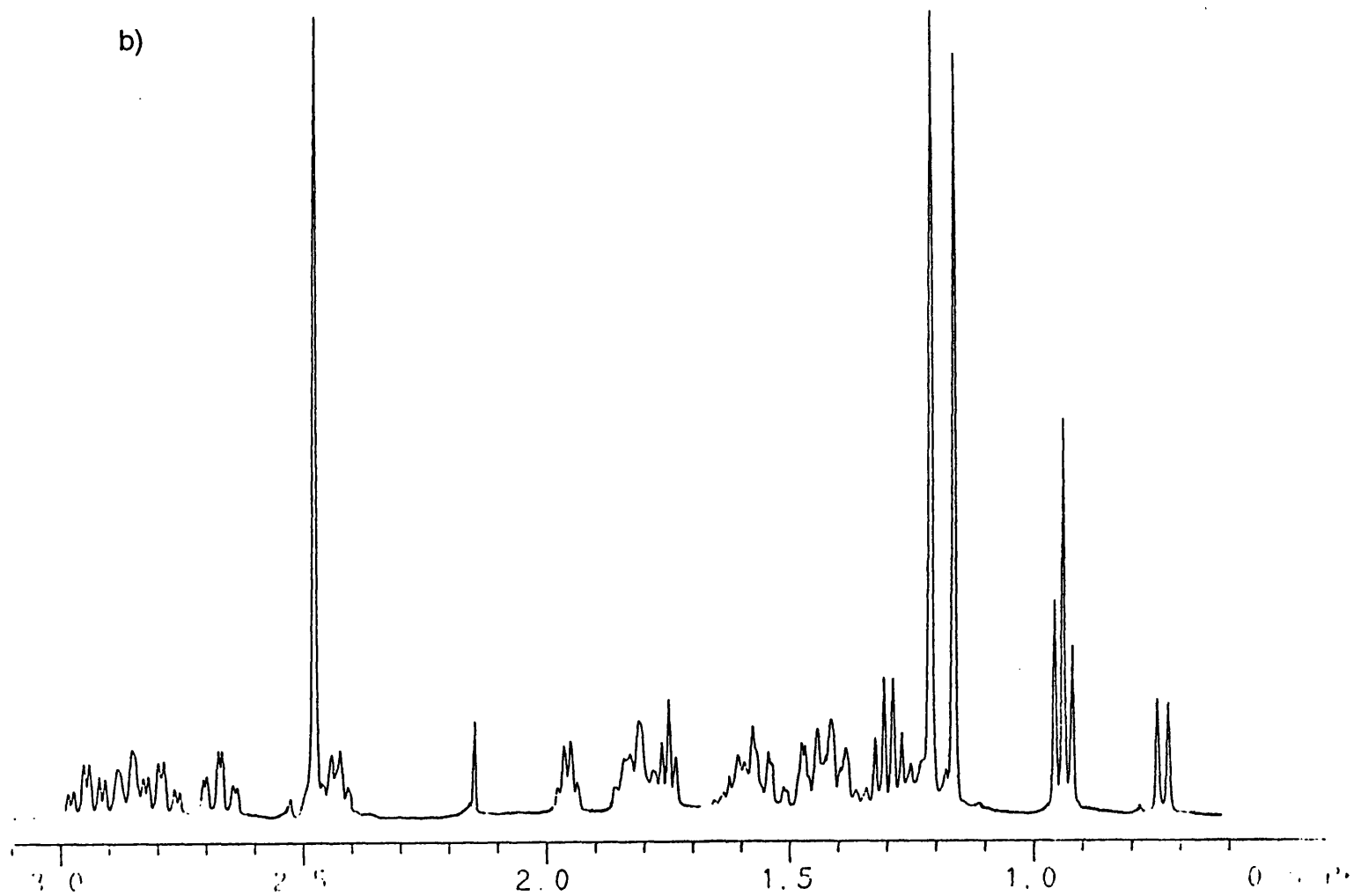


Figure 5.1.1: ¹H NMR spectra of 5.1.10; a) showing the mixture of the two isomers; b) of the isomer which eluted first by HPLC; c) of the isomer which eluted second by HPLC.

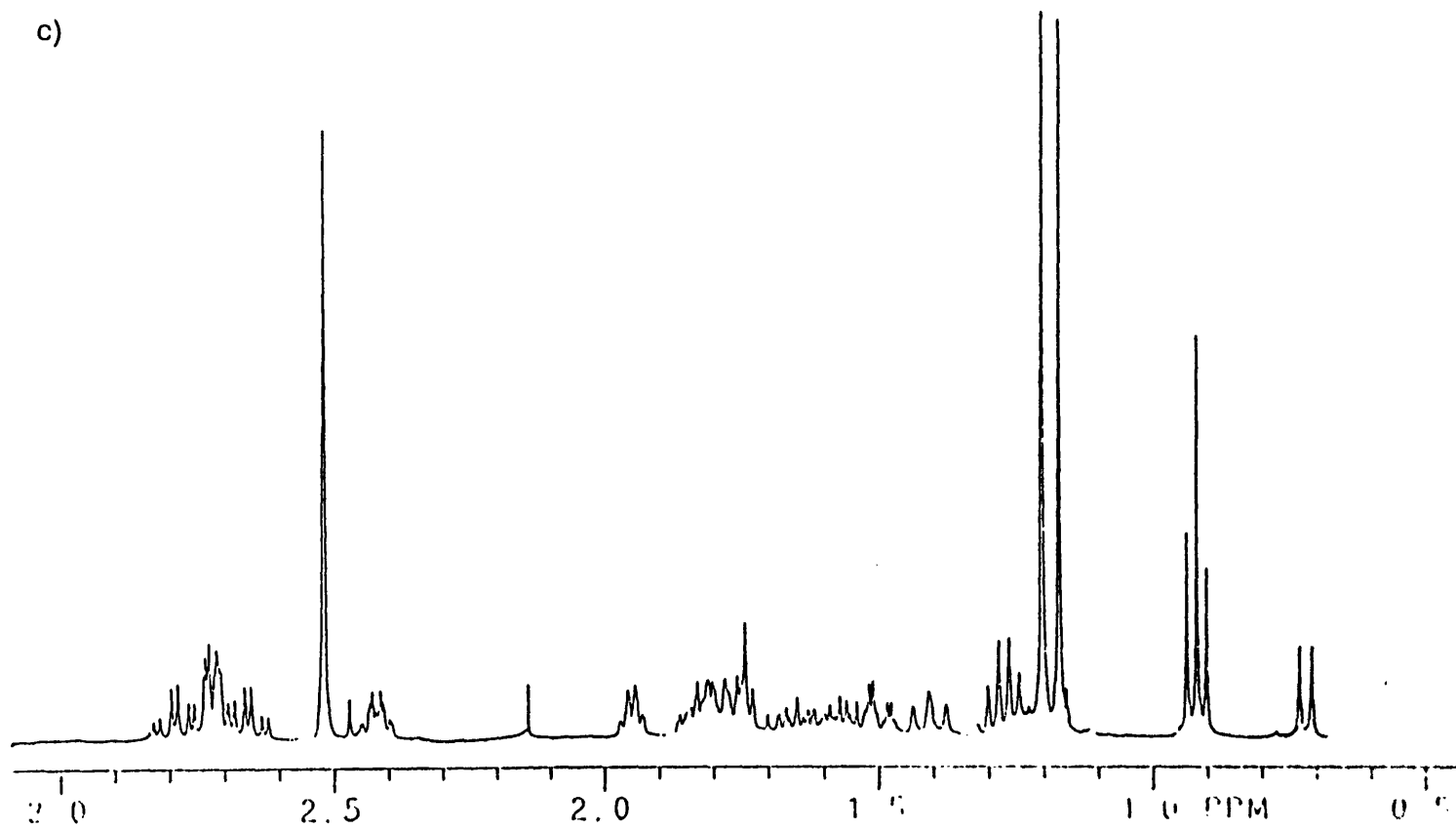
First eluting isomer

b)



Second eluting isomer

c)



isomers, but the ^1H and ^{13}C NMR spectra of these complexes show that only one isomer is formed during the reaction. It is not unreasonable to assume, on steric grounds, that the isomers formed are the ones having the bulky 3,3-dimethylpiperidine group and the adamantyl group, respectively, in an equatorial position.

With the exception of **5.1.9** (m.p. 112-125 °C, decomp.), the polycyclic amine-boranes melted sharply with no sign of decomposition. These complexes were also shown to be relatively air-stable for periods of up to 48 h, by comparison of the ^1H NMR spectra recorded before and after exposure of the pure materials to the atmosphere. In particular, the complexes **5.1.7**, **5.1.8** and **5.1.10** appear to be indefinitely stable, as no decomposition was observed even after 14 days standing in air. The general observation is that these complexes show high thermal stability as well as stability towards hydrolysis; presumably both are results of incorporating the N→B linkage into a six-membered ring. These catalysts are also more soluble in ethers and hydrocarbons than the lpc-amine-boranes **5.1.1-5.1.6**, with the exception of **5.1.9** which is relatively insoluble in both ethers and hydrocarbons.

X-ray crystal structures were obtained for the complexes **5.1.6** and **5.1.7**, these are shown in Section 5.5 (Figures 5.5.1-5.5.3). The X-ray structure for **5.1.1**, previously determined by Soderquist *et al*² is shown for reference alongside the structures for **5.1.6** and **5.1.7**. These clearly show that *syn*-

hydroboration has taken place from the least-hindered face of the double bond.

Oxirane solutions containing n-butyl chloride (1 mol dm^{-3}), DTBP (18% v/v) and an amine-borane (1 mol dm^{-3}) were UV irradiated in the cavity of the ESR spectrometer, in order to investigate the ability of the derived amine-boryl radicals to abstract halogen from carbon. In the absence of amine-borane, only the oxiranyl radical can be detected and thus the t-butoxyl radical is more reactive towards oxirane than the alkyl chloride. In the presence of an amine-borane, abstraction of chlorine by the amine-boryl radical takes place to give the n-butyl radical, and this was observed for all the complexes **5.1.1-5.1.13** even at $-84 \text{ }^\circ\text{C}$. This confirms that in the presence of the amine-borane, $\text{Bu}^t\text{O}^\bullet$ reacts with this in preference to oxirane and produces an amine-boryl radical, which then goes on to abstract the chlorine atom from n-butyl chloride.

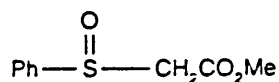
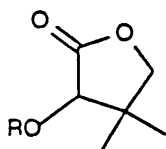
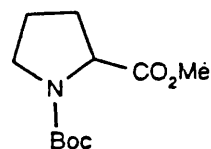
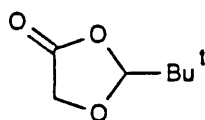
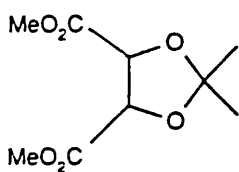
In order to verify that each of these amine-boranes functions as a polarity reversal catalyst, oxirane solutions containing ethyl acetate (*ca.* 1 mol dm^{-3}), DTBP (18% v/v), and the amine-borane (*ca.* 0.3 mol dm^{-3}) were UV irradiated in the cavity of the ESR spectrometer at $-78 \text{ }^\circ\text{C}$. In each case, only a strong signal due to $\text{H}_2\overset{\bullet}{\text{C}}\text{CO}_2\text{CH}_2\text{CH}_3$ was observed.* Therefore, $\text{Bu}^t\text{O}^\bullet$ reacts more rapidly with the amine-borane than with ethyl acetate, as required for an

* ESR parameters for $\text{H}_2\overset{\bullet}{\text{C}}\text{CO}_2\text{CH}_2\text{CH}_3$ are $a(\text{H}_\alpha)$ 21.35, $a(\text{H}_\beta)$ 21.50, $a(\text{H}_\delta)$ 1.59 G and g 2.0036 in oxirane at $-78 \text{ }^\circ\text{C}$.

efficient polarity reversal catalyst.

5.2. Kinetic Resolution of Substrates Using IpcT

The substrates 5.2.1-5.2.8 were examined and, for all these compounds, amine-boryl radicals are expected to abstract a hydrogen atom rapidly from a C-H group α to a carbonyl function.^{1,13-18}



5.2.5 R = Me₃Si

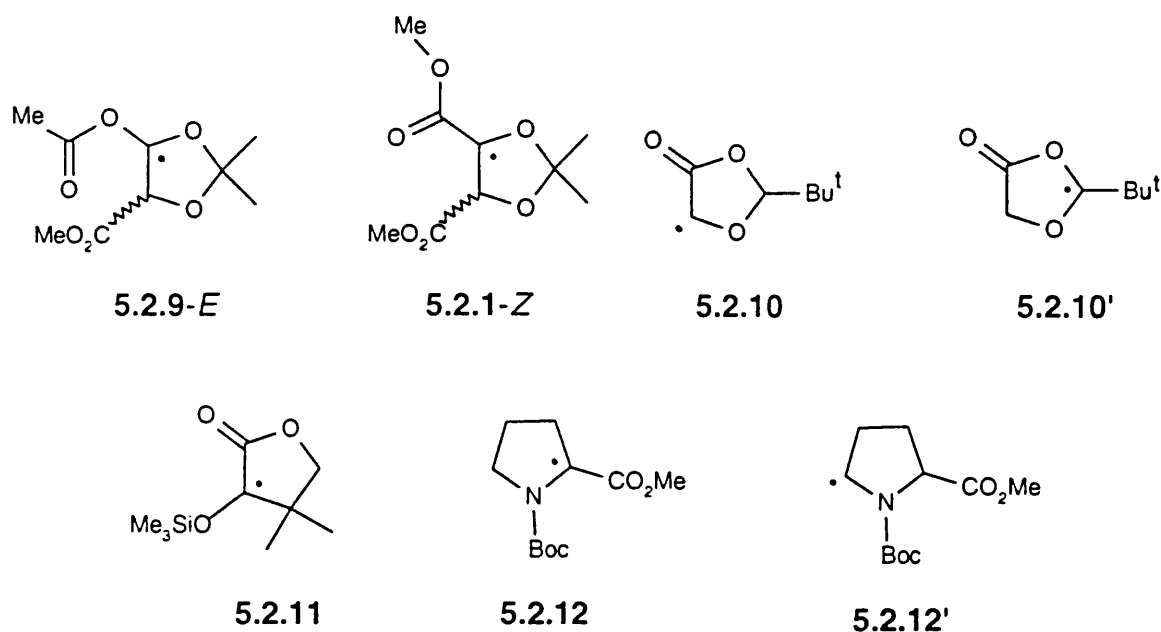
5.2.6 R = Me₂Bu^t

5.2.7 R = Et₃Si

5.2.8 R = ⁱPr₃Si

When oxirane solutions containing 5.2.1, trimethylamine-butylborane catalyst and DTBP were UV irradiated in the cavity of the ESR spectrometer at 188 K, the only signals observed were from the radicals 5.2.9-*E* and 5.2.9-*Z*. However, in the absence of an amine-borane catalyst, the oxiranyl radical is detected along with 5.2.9-*E/Z*.¹⁸ When similar experiments were carried out

at 199 K with **5.2.2** and **5.2.5** (in the presence of an amine-borane catalyst), the only radicals detected were **5.2.10**, and **5.2.11**, derived by abstraction of hydrogen from a C-H group α to a carbonyl function. In the absence of catalyst, for **5.2.2** the oxiranyl radical was detected alongside the radicals **5.2.10** and **5.2.10'**²² and for **5.2.5** the oxiranyl radical was detected alongside **5.2.11**. In the case of **5.2.3**, different ESR spectra were obtained in the presence of quinuclidine-butylborane catalyst than in its absence. Spectra were too complex to analyse, but it is fair to assume that in the presence of an amine-borane the signal was due entirely to **5.2.12**, while in the absence of catalyst, signals due to both **5.2.12** and **5.2.12'** alongside that of the oxiranyl radical were observed.



Typical samples for kinetic resolution consisted of the racemic substrate (1.0 mol dm^{-3}), amine-borane catalyst (0.3 mol dm^{-3}), DTBP (28% v/v) and t-butyl-benzene ($0.2\text{-}0.4 \text{ mol dm}^{-3}$) as an unreactive internal concentration standard. Oxirane was chosen as the solvent because amine-boranes have adequate solubilities at low temperatures, and because of its relatively low reactivity (for an ether containing $\alpha\text{-C-H}$ groups) towards hydrogen-atom abstraction by alkoxy radicals. Samples were sealed in evacuated quartz tubes and irradiated with unfiltered light from a 160 W medium-pressure mercury discharge lamp. The sample was immersed in a solid CO_2 /ethanol bath and the experimental arrangement is shown in Figure 5.2.1. The temperature during photolysis was estimated to be *ca.* $-74 \text{ }^\circ\text{C}$ by inserting a thermocouple inside an open quartz tube filled with DTBP, an amine-borane and an ester in diethyl ether as for kinetic resolutions and recording the temperature during photolysis.¹ The t-butoxy radicals, generated by photochemical cleavage of DTBP, reacted rapidly with the amine-borane catalyst to form an amine-boryl radical which then abstracted a hydrogen from a position α to a carbonyl in the substrate [Scheme (5.2.1)]. After partial consumption of the substrate, the amount remaining was determined using gas liquid chromatography (GLC), by comparing the intensity of the peaks arising from the substrate and t-butyl-benzene before and after photolysis. The remaining substrate was recovered by column chromatography on silica gel and its e.e. was determined either by ^1H NMR spectroscopy using a chiral shift reagent or by chiral-stationary-phase HPLC (see Figure 5.2.2). Assignments

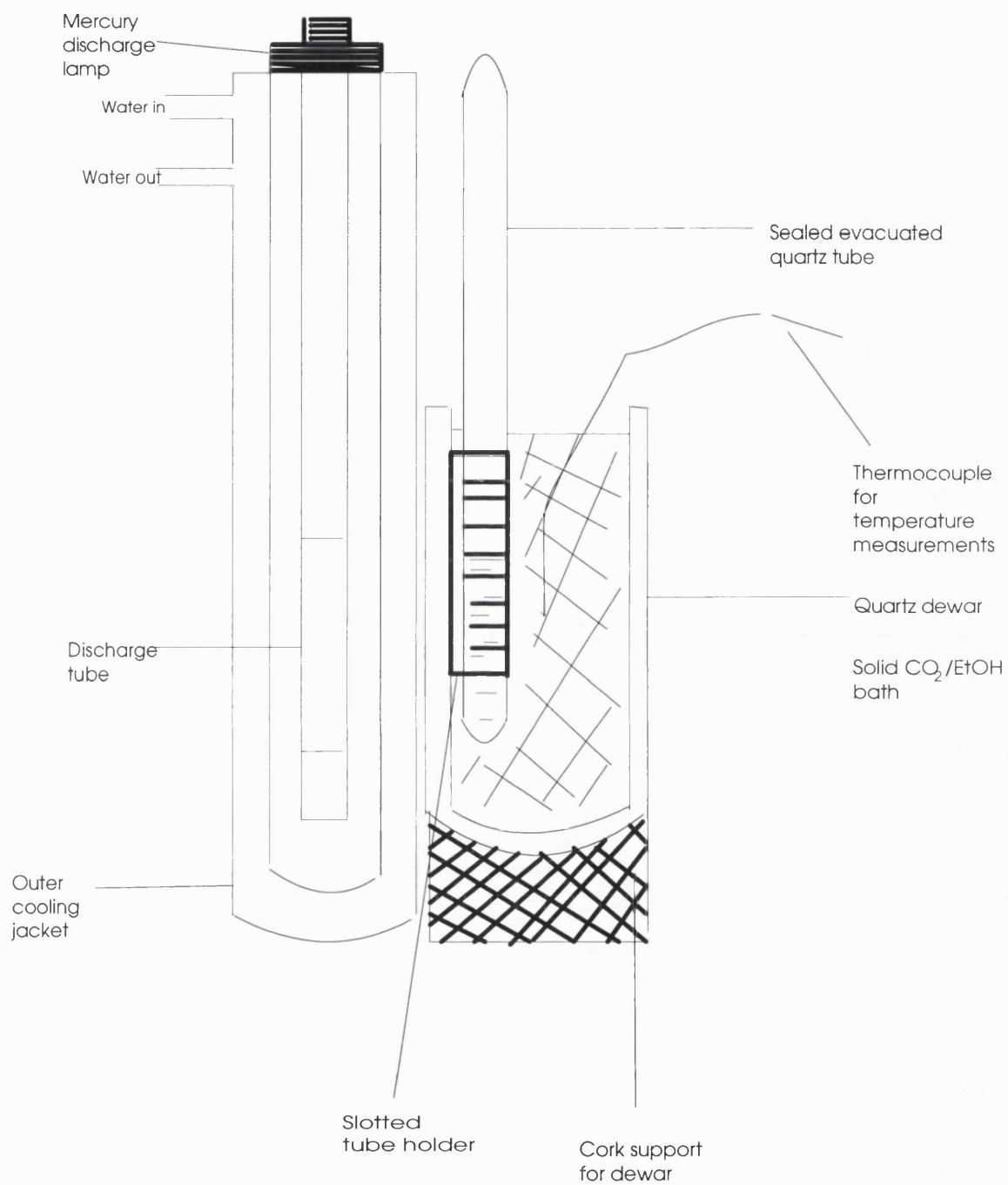


Figure 5.2.1: Experimental arrangement for kinetic resolution at -78 °C

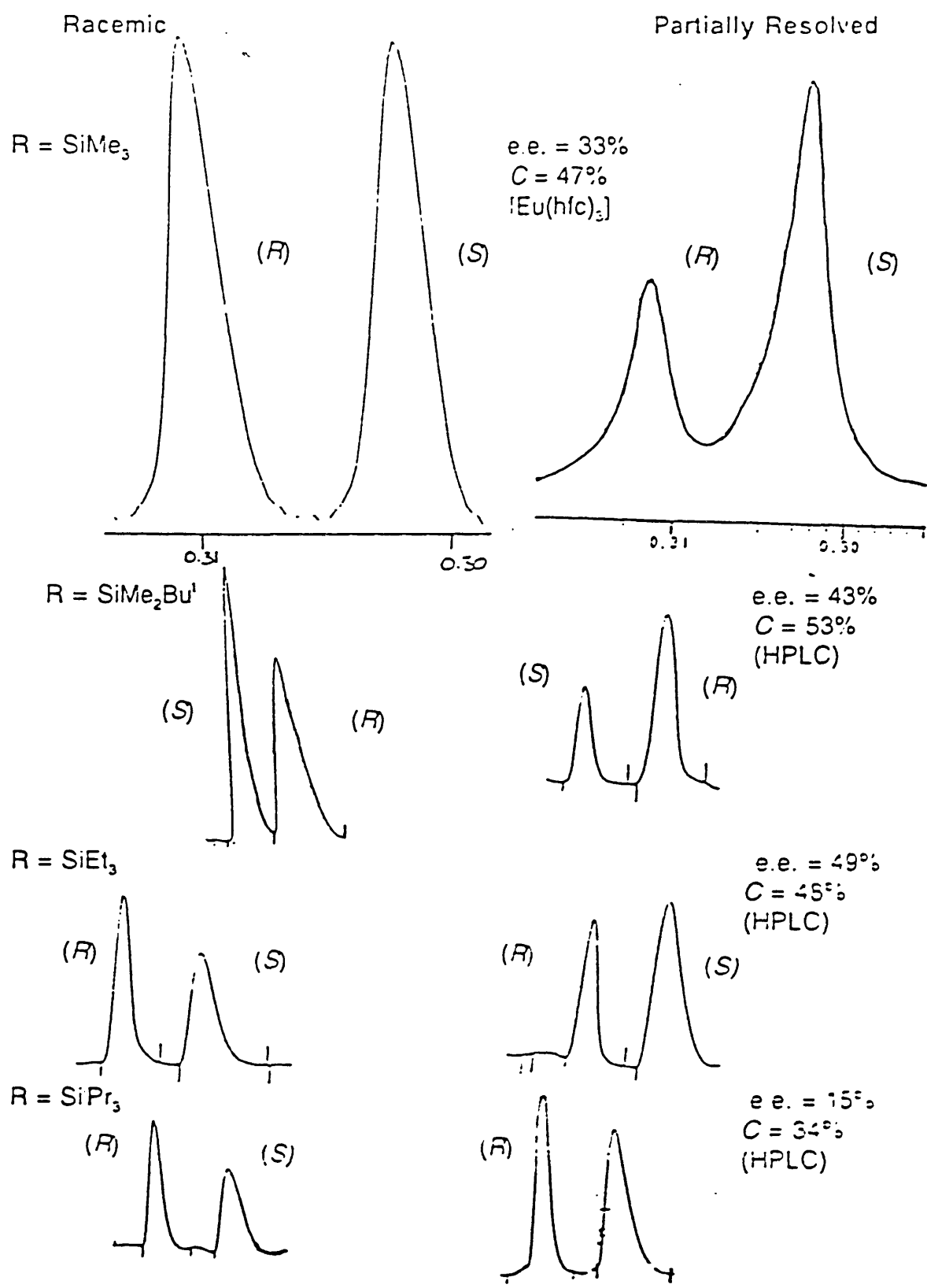
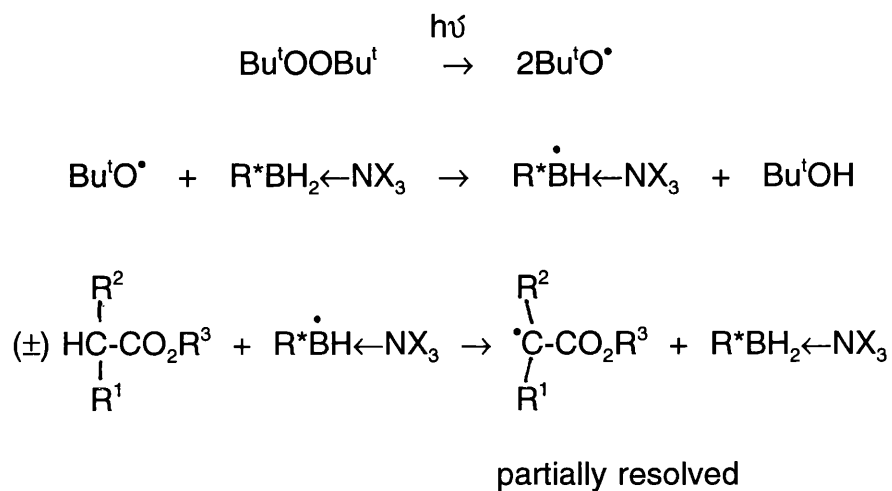


Figure 5.2.2: Peaks for the two enantiomers of the substrates 5.2.5-5.2.8, before (racemic) and after kinetic resolution (partially resolved) using 5.1.9 as a catalyst. The method for determination of the e.e. is shown in parentheses.

of enantiomers were made by comparison with authentic substrates of known absolute configuration.



R* = chiral alkyl group

Scheme 5.2.1

The radicals derived from the substrates **5.2.1-5.2.8** would be expected to be removed mainly *via* coupling reactions¹⁹ to form dimers. If none of the α -carbonyl(alkyl) radicals produced go on to abstract hydrogen unselectively and thus regenerate racemic substrate, the enantioselectivity factor s will be given by equation (5.2.1).^{20,21} However, it appears probable that some of the α -carbonyl(alkyl) radicals will decay by hydrogen-atom abstraction, probably mainly radical-radical disproportionation reactions, and thus application of equation (5.2.1) will give a lower limit for s .¹ Results of kinetic resolutions using ^dIpcT **5.2.1** as catalyst are presented in Table 5.2.1.

Table 5.2.1: Kinetic resolutions of racemic substrates using ^dlpcT **5.2.1** catalyst^a in oxirane at -74 °C.

Substrate	UV irradiation time (min)	Substrate consumption (%)	More reactive enantiomer	E.e. of residual substrate (%) ^b	Method for determination of e.e. ^c	Enantioselectivity factor <i>s</i> ^d	Steric chirality of more reactive enantiomer ^e
5.2.1	50	52	<i>S,S</i>	62 (<i>R,R</i>)	A	6.8 ^f	ρ
5.2.2	45	44	<i>g</i>	8 ^h	B	1.3	—
5.2.3	120	20	<i>R</i>	10(<i>S</i>)	C	2.6	(σ)
5.2.4	105	57	<i>R</i>	8(<i>S</i>)	B,D,E	1.2 ⁱ	—
5.2.5	110	31	<i>R</i>	15(<i>S</i>)	A	2.3 ^j	σ
5.2.6	140	29	<i>S</i>	13(<i>R</i>)	B	2.1	ρ
5.2.7	130	27	<i>R</i>	4(<i>S</i>)	B	1.3	ρ
5.2.8	240	39	<i>R</i>	9(<i>S</i>)	B	1.4	ρ

^a Catalyst concentration 0.20 mol dm⁻³. ^b Enantiomer present in excess shown in parentheses. ^c A = ¹H NMR spectroscopy in the presence of Eu(hfc)₃, B = HPLC using Chiralcel OD stationary phase, C = ¹H NMR spectroscopy in the presence of Eu(tfc)₃, D = optical rotation, E = ¹H NMR in the presence of (*S*)-(+)-DNBB. ^d Calculated using equation (5.2.2). ^e See text. Assignments in parentheses are very tentative. ^f With ^llpcT catalyst *s* = 7.4; the (*R,R*)-enantiomer is more reactive. ^g Enantiomer eluting first. ^h Enantiomer eluting second. ⁱ With the ^llpcT catalyst *s* = 1.2; the (*S*)-enantiomer is more reactive. ^j With the ^llpcT catalyst *s* = 2.1; the (*S*)-enantiomer is more reactive.

$$s = (k_A/k_B) = \ln[(1 - C)(1 - EE)]/\ln[(1 - C)(1 + EE)] \quad (5.2.1)$$

The s -values reported in Table 5.2.1 are rather small, with the exception of the results obtained for the substrate **5.2.1**. However, these enantioselectivities would undoubtedly increase at lower temperatures. The temperature dependence of s can be described by the Arrhenius equation (5.2.2), in which E is the activation energy, A is the Arrhenius pre-exponential factor and T is the absolute temperature.¹ If (A_A/A_B) is taken to be one, then s -values of 2-20 at 199 K would correspond to activation energy differences of 1.1-4.9 kJ mol⁻¹ and the values of s will increase at lower temperatures. If a kinetic resolution is to yield useful amounts of material with high e.e., the values of s must be ≥ 5 .^{20,21}

$$s = (k_A/k_B) = (A_A/A_B) \exp(E_B - E_A)/RT \quad (5.2.2)$$

When ^lIpcT was used as catalyst for kinetic resolutions, the magnitude of s was similar to that observed with ^dIpcT, but the selectivity was reversed (e.g. kinetic resolution of **5.2.4** with ^dIpcT, $s = 1.25$ and the (*R*)-enantiomer is the more reactive enantiomer; with ^lIpcT, $s = 1.24$ and the (*S*)-enantiomer is the more reactive).

A control experiment carried out by Pearl Mok¹ using optically pure (4*S*,5*S*)-**5.2.1** in order to assess the extent of substrate racemisation under the

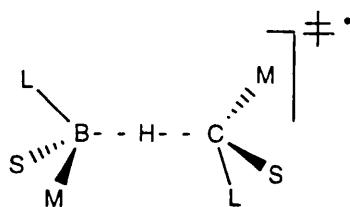
conditions of the experiments, showed that after 20 min irradiation at -90 °C, 51% of the ester had been consumed, and the residual ester contained a barely-detectable amount (0.3%) of the (4*R*,5*R*)-enantiomer; its formation requires inversion at both asymmetric centres, which would presumably take place *via* the intermediacy of the *cis*-(*meso*)-isomer.¹⁸ Also, in a preparative run at -90 °C, (4*R*,5*R*)-**5.2.1** was isolated in 25% yield, with an e.e. of 97%.¹

When samples containing the sulfoxide **5.2.4**, *t*-butyl-benzene as internal standard for GLC analyses and DTBP in oxirane solution were photolysed at 199 K for 100 min, it was found that 85 % of **5.2.4** was consumed, the unreacted starting material was shown to have an e.e. of *ca.* 0%. Therefore, the Bu¹O[•] reacts with the sulfoxide directly in a non-enantioselective process, as expected and thus if this reaction occurs in the presence of the amine-borane, the observed value of *s* will be a lower limit. In the absence of DTBP the substrate consumption was *ca.* 0 and the e.e. was also *ca.* 0. Therefore, in the presence of an amine-borane catalyst the e.e. observed arise from enantioselective hydrogen-atom abstraction by optically active amine-boryl radicals.

5.3. The Steric Strain Model for Enantioselective Hydrogen-Atom Abstraction

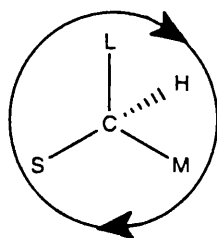
The transition state for hydrogen atom transfer from a 4-coordinate

carbon to an amine-boryl radical, has for electronic and steric reasons, the $B\cdots H\cdots C$ fragment near to linear. It was previously suggested that if long-range torsional/steric interactions (front strain) between the substituents on the boron atom of the catalyst-derived radical and those at C_α of the substrate are dominant in determining the geometry of the TS, then this should be the staggered conformation **5.3.1**, in which the symbols L, M and S refer to groups of large, medium and small effective bulk.¹



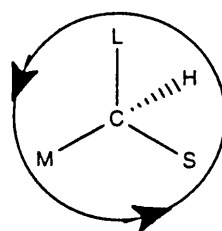
5.3.1

Steric chiralities have been defined by analogy to the Cahn-Ingold-Prelog rules²³ for describing absolute stereochemistry, using the priority sequence $L > M > S$ (see structures **5.3.2a/b**, $E = B$ or C).



ρ

5.3.2a

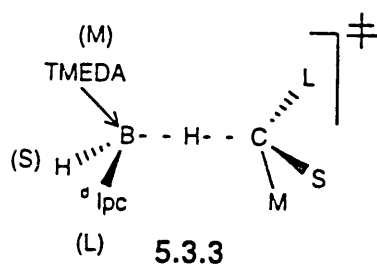


σ

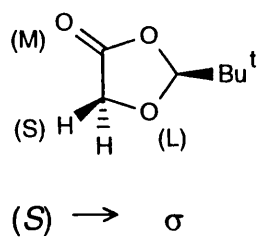
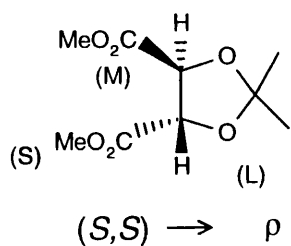
5.3.2b

A boron-centre of steric chirality σ will give a more stable transition state, when associated with a carbon-centre of steric chirality ρ than with one having

steric chirality σ . The steric chirality at the boron-centre in a TS for hydrogen-atom abstraction by the amine-boryl radical derived from $^{\sigma}\text{IpcT}$ is probably σ , and thus the more reactive enantiomer of a substrate should have steric chirality ρ , as shown in 5.3.3.

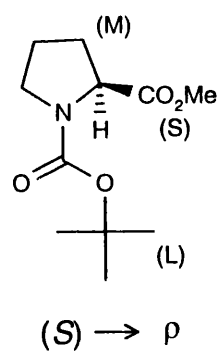
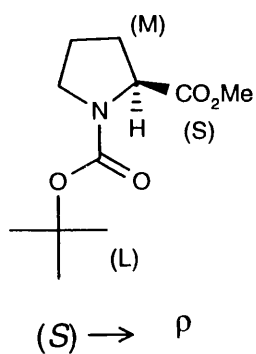


The steric chirality of the more reactive (*S,S*)-enantiomer of the isopropylidene tartrate 5.2.1 can be predicted with the aid of molecular models and indeed appears to be ρ (Structure 5.3.4), as required if steric effects are dominant. It is often difficult to deduce the effective helicity of the steric environment around the α -C-H bond in a substrate and the energy differences between diastereoisomeric transition states are very small for all substrates 5.2.1-5.2.8. The (*R*)-enantiomers of 5.2.5 and 5.2.6 have steric chirality σ (see 5.3.7a) if the effective sizes of the groups attached to C_{α} in the transition state are taken to decrease in the order $-\text{CMe}_2- > -\text{CO}_2\text{CH}_2- > -\text{OR}$. Then the (*S*)-enantiomer (steric chirality ρ) should be the more reactive enantiomer towards the amine-boryl radical derived from $^{\sigma}\text{IpcT}$ catalyst. This is indeed what is observed with 5.2.6, but with 5.2.5 it is the (*R*)-enantiomer which appears to be more the reactive towards $^{\sigma}\text{IpcT}$. The (*R*)-enantiomers of 5.2.7 and 5.2.8 both have steric chirality ρ (see 5.3.7b), since



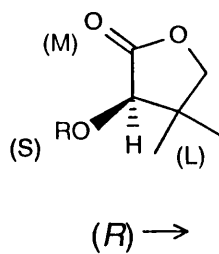
5.3.4

5.3.5

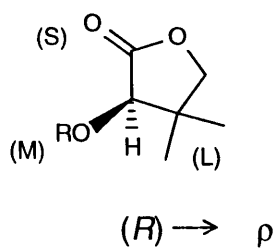


5.3.6a

5.3.6b



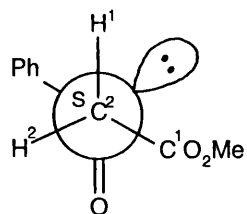
R = Me₃Si, Me₂Bu^tSi



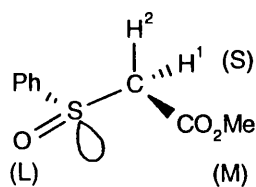
R = Et₃Si, ⁱPr₃Si

5.3.7a

5.3.7b



5.3.8



5.3.9

when the alkyl groups on silicon are larger than methyl the group priority would appear from molecular models to change to $-\text{CMe}_2- > -\text{OR} > -\text{CO}_2\text{CH}_2-$. Therefore, according to the steric strain model, the (*R*)-enantiomer of these substrates should react more rapidly with $^d\text{lpcT}$, which is indeed what is observed. The trends in the enantioselectivities observed with the pantolactone derivatives **5.2.5-5.2.8** were further investigated and are discussed in Section 5.4. For **5.2.2** it is assumed that attack by the amine-boryl radical takes place from the side opposite the *t*-butyl group and that the hydrogen atom which is transferred preferentially is that *trans* to the bulky *t*-butyl group (see **5.3.5**). Therefore, if steric interactions are dominant in the transition state, the (*R*)-enantiomer should have steric chirality ρ , and should react more rapidly with the amine-boryl radical derived from $^d\text{lpcT}$. This would mean that the (*R*)-enantiomer is the enantiomer eluting first by HPLC, and the (*S*)-enantiomer would be that eluting second. By inspection of molecular models, it is very difficult to decide on the steric chirality around the $\alpha\text{-C-H}$ bond in **5.2.3**. Taking the effective sizes of the groups attached to C_α in the transition state to decrease in the order $\text{Boc(R)N} > \text{RCH}_2 > \text{MeO}_2\text{C}$ for both amide rotamers **5.3.6a-5.3.6b**, then the (*S*)-enantiomer has steric chirality ρ . However, it is the (*R*)-enantiomer which is the more reactive when $^d\text{lpcT}$ is the catalyst. The relative importance of steric interactions between groups near the reaction centre compared with those between groups more distant from it could vary with the structure of the amine-boryl radical for such finely balanced systems, and a simplistic model based on transferable steric chiralities of the

reactants is quite likely to prove inadequate.

The preferred conformation about the α -C-S bond in the sulfoxide **5.2.4** would be predicted on steric grounds to be that shown in **5.3.8** for the (*R*)-enantiomer. The conformation adopted by **5.2.4** in the solid state was shown by X-ray crystallography to be close to the idealised structure **5.3.9** (see Figure 5.3.1), with dihedral angles $C^1-C^2-S=O$ and $C^1-C^2-S-C_{Ar}$ equal to 65.1 and 174.2°, respectively. If we assume that this conformation is maintained in the transition state for α -hydrogen-atom abstraction in solution, then provided that steric effects dominate, the less hindered H^1 should be transferred preferentially to boron and the steric chirality of the (*R*)-enantiomer would be σ . However, if stereoelectronic effects are dominant,* the more reactive α -C-H bond could be that antiperiplanar to the sulfur lone pair front-lobe (maximum back-lobe interaction)²⁴ and H^2 will then be transferred. Now the steric chirality of the (*R*)-enantiomer is ρ (see structure **5.3.9**) and this enantiomer would be predicted to react more rapidly with the amine-boryl radical derived from ^dlpcT, as observed.

* This could happen because of a captodative interaction between the sulfur lone pair and the carbonyl group, with the latter orientated for maximum π -overlap with the developing singly-occupied orbital on C_α in the transition state.

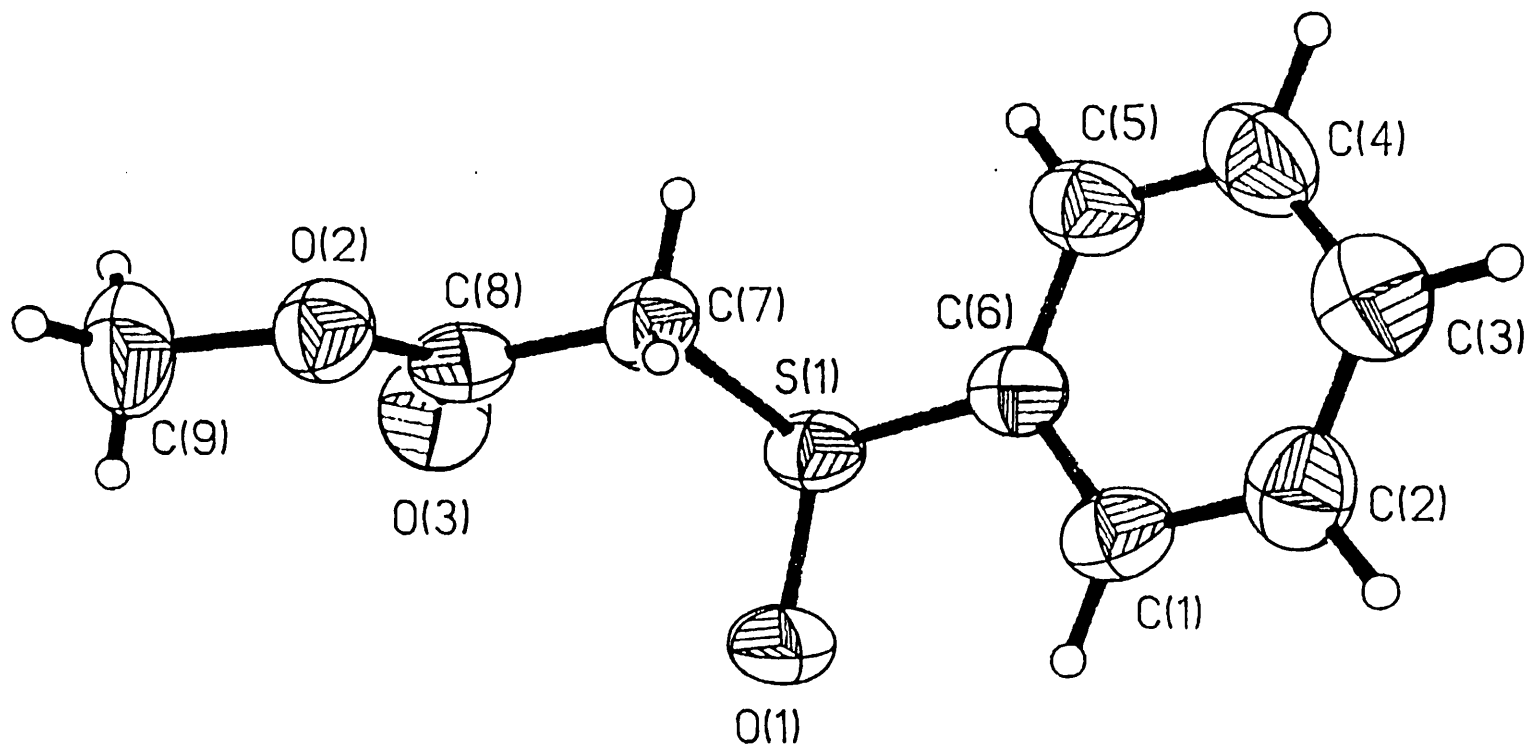


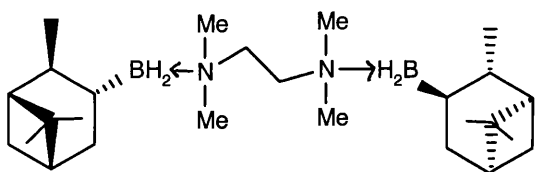
Figure 5.3.1: Crystal structure of PhS(O)CH₂CO₂Me 5.2.4. The dihedral angles C¹-C²-S=O and C¹-C²-S-C_{Ar} are 65.1 and 174.2°, respectively.

5.4. Kinetic Resolutions Using 5.1.3-5.1.13.

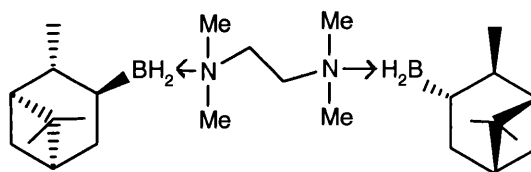
The efficiency of catalysts 5.1.1-5.1.7, 5.1.11 and 5.1.13 for kinetic resolutions of 5.2.1-5.2.5 were compared and the results are presented in Table 5.4.1. The isopropylidene tartrate 5.2.1 showed the greater *s*-values. The most encouraging results were obtained with ^dlpcT 5.1.1 and the polycyclic amine-boranes 5.1.7 and 5.1.11, which gave the highest enantioselectivities and were readily prepared and handled (^dlpcT and ^llpcT are commercially available; 5.1.7 and 5.1.11 exhibit high thermal and air stability). A preparative run was carried out, starting with 3 mmol of racemic substrate 5.2.5 and using 5.1.11 as catalyst, and (*S*)-*O*-trimethylsilylpantolactone having an e.e. of 84% was isolated after 71% substrate consumption (*s* = 4.9).²⁵

Molecular models indicate that the steric asymmetry around boron is somewhat smaller for lpcD and lpcQ than for lpcT, in accord with the greater enantioselectivities found with the latter as a catalyst. It is also possible that the unreacted lpcBH₂ group could interact in the transition state for hydrogen-atom abstraction by the amine-boryl radical derived from lpcT* to increase enantioselectivity in a way not possible when the two boron moieties are rigidly held apart as in lpcD. The enantioselectivities realised with the quinuclidine complex ^llpcQ 5.1.6, which contains only one lpcBH₂ group, are similar to that

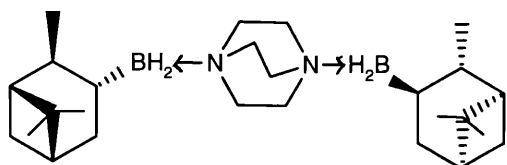
* The structure of ^dlpcT has been determined by X-ray crystallography.¹²



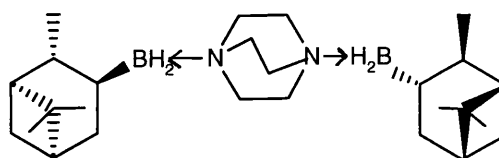
5.1.1
d₁ipcT



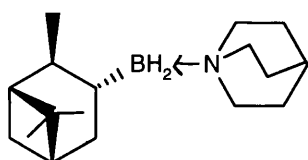
5.1.2
l₁ipcT



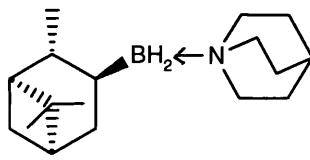
5.1.3
d₁ipcD



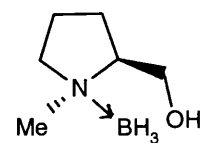
5.1.4
l₁ipcD



5.1.5
d₁ipcQ



5.1.6
l₁ipcQ



5.1.13

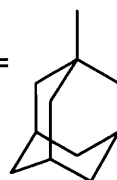
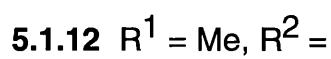
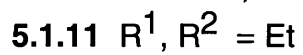
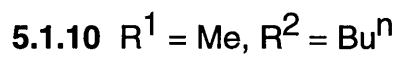
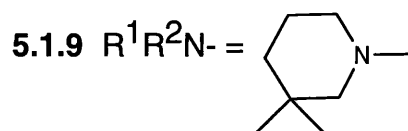
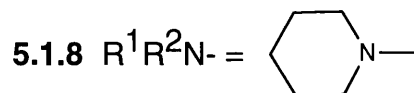
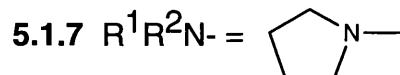
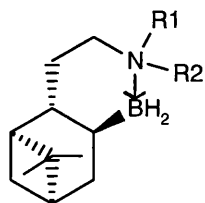


Table 5.4.1: Kinetic resolutions of racemic substrates using **5.1.1-5.1.7**, **5.1.11** and **5.1.13** as catalysts at -74 °C.

Enantiselectivity factor s^b					
Substrates					
Catalysts ^a	5.2.1	5.2.2	5.2.3	5.2.4	5.2.5
5.1.1	6.7(<i>S,S</i>)	1.3 ^c	2.6(<i>R</i>)	1.2(<i>R</i>)	2.3(<i>R</i>)
5.1.4	3.0(<i>R,R</i>)	—	1.4(<i>S</i>)	1.1(<i>S</i>)	—
5.1.6	3.2(<i>R,R</i>)	—	1.4(<i>S</i>)	1.1(<i>S</i>)	—
5.1.7	1.8(<i>S,S</i>)	1.6 ^c	1.5(<i>R</i>)	—	1.9(<i>S</i>)
5.1.11	2.1(<i>S,S</i>)	—	—	—	5.2(<i>S</i>)
5.1.13	2.0(<i>S,S</i>)	1.2 ^c	2.2(<i>S</i>)	—	1.4(<i>S</i>)

^a Typical catalyst concentrations were *ca.* 0.3-0.4 mol dm⁻³. ^b More reactive enantiomer is shown in parentheses.

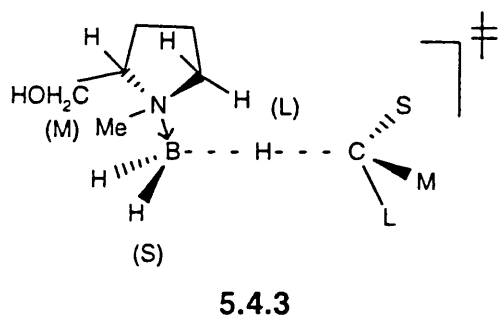
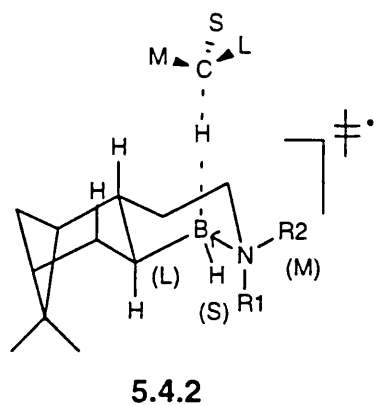
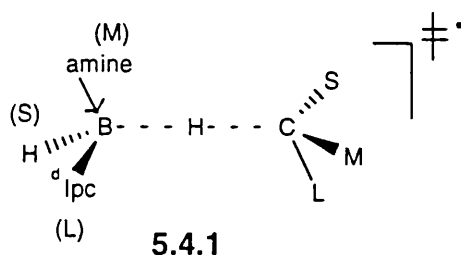
^c Enantiomer eluting first by HPLC using the Chiralcel OD column.

obtained with ¹lpcD **5.1.4**.

Examination of molecular models indicates that the steric chiralities of the amine-borane residues in the transition state for reactions mediated by **5.1.3**, **5.1.5**, **5.1.7**, **5.1.11** and **5.1.13** are all σ (see **5.4.1-5.4.3**), as for reactions involving ^dlpcT. Hence, if steric effects are dominant, the more reactive enantiomer of all substrates should be ρ . The substrate **5.2.1** does indeed appear to follow the model's prediction quite well. For **5.2.3** and **5.2.4** the enantioselectivities observed are consistently the opposite of the enantioselectivities predicted on the basis of dominant steric effects in the transition state. In the case of **5.2.4** this was previously explained in terms of captodative interactions in the transition state.

As mentioned earlier, it is sometimes difficult to deduce the effective size of the groups attached to C _{α} . The fact that the groups attached to C _{α} do not differ substantially in size probably accounts for the low enantioselectivities observed and, in the case of **5.2.3**, it is possible that the size order of the groups attached to C _{α} is Boc(R)N > MeO₂C > RCH₂ rather than Boc(R)N > RCH₂ > MeO₂C. If this is true, then the (*R*)-enantiomer would have a steric chirality of ρ and, would be predicted to react faster with the amine-boryl radicals derived from **5.1.1**, **5.1.3**, **5.1.5** and **5.1.7**, which would be in agreement with our observations. The steric chirality of the (*S*)-enantiomer of **5.2.5** was predicted to be ρ , this means that it should react faster with the

radical derived from $^d\text{lpcT}$, $^d\text{lpcD}$, $^d\text{lpcQ}$, **5.1.7** and **5.1.12**, which is in agreement with experimental observations, with the exception of the result obtained with $^d\text{lpcT}$.



The amine-borane **5.1.13** was examined in the hope that the CH_2OH group might be involved in hydrogen bonding with the substrate in the transition state **5.4.3**, leading to enhanced enantioselectivity. However, no such increases are evident from the results in Table 5.4.1. The direction of the small enantioselectivities observed can be rationalised in terms of the steric strain model for the substrates **5.2.1-5.2.3** and **5.2.5**. Now, in accord with the original ordering of group sizes about C_u , the (*S*)-enantiomer of **5.2.3** is more reactive than its antipode, in contrast with previous results obtained with other catalysts (see Table 5.4.1).

The effect of changing the alkyl groups at silicon in the pantolactone derivatives, as well as the effect of varying the amino group of the polycyclic amine-boranes, were investigated by comparing the results obtained from kinetic resolutions of the substrates **5.2.5-5.2.8** with **5.1.1** and **5.1.7-5.1.12** as catalysts. The isopropylidene tartrate **5.2.1** was also included as a substrate, because the most encouraging results were obtained with this substrate, and it also appears to obey the steric strain model well. These results are presented in Table 5.4.2.

Examination of molecular models indicates that the steric chiralities of the catalysts **5.1.7-5.1.12** in the transition state are all σ , as for the reactions involving $d^1\text{IpcT}$. This argument assumes that the hydrogen transferred occupies a position in the transition state similar to that of the more exposed axial hydrogen attached to boron in the parent amine-boranes (see structure **5.4.2**). Hence, if steric effects are dominant the more reactive enantiomer of all substrates should have steric chirality ρ (as observed), with the exception of the substrate **5.2.5** where the direction of enantioselectivity is reversed with $d^1\text{IpcT}$. At first, it was expected that the *O*-trialkylsilylpantolactone derivatives would all show the same direction of enantioselectivity, but further inspection of molecular models showed that the compounds **5.2.5** and **5.2.6** have different steric chirality to **5.2.7** and **5.2.8** (see structures **5.3.7a/b**). For **5.2.7** and **5.2.8**, the bulky OSiEt_3 and OSi^iPr_3 groups are better at shielding the hydrogen which is abstracted. The silicon group now

Table 5.4.2: Kinetic resolutions of racemic substrates with **5.2.1**, **5.1.7-5.1.12** at $-74\text{ }^{\circ}\text{C}$

		Enantioselectivity factor s^b				
		Substrates				
Catalysts ^a	5.2.1	5.2.5	5.2.6	5.2.7	5.2.8	
5.1.1	6.7(<i>S,S</i>)	2.3(<i>R</i>)	2.1(<i>S</i>)	1.3(<i>R</i>)	1.4(<i>R</i>)	
5.1.7	1.8(<i>S,S</i>)	1.7(<i>S</i>)	1.3(<i>S</i>)	2.2(<i>R</i>)	1.4(<i>R</i>)	
5.1.8	1.3(<i>S,S</i>)	2.0(<i>S</i>)	1.3(<i>S</i>)	2.0(<i>R</i>)	1.3(<i>R</i>)	
5.1.9	1.5(<i>S,S</i>)	2.9(<i>S</i>)	3.5(<i>S</i>)	3.5(<i>R</i>)	1.7(<i>R</i>)	
5.1.10^c	—	2.2(<i>S</i>)	2.8(<i>S</i>)	3.0(<i>R</i>)	1.4(<i>R</i>)	
<i>d</i>	1.4(<i>S,S</i>)	—	—	—	—	
<i>e</i>	3.2(<i>S,S</i>)	—	—	—	—	
5.1.12	(<i>S,S</i>)	(<i>S</i>)	—	—	—	

^a Catalysts concentration *ca.* 0.40 mol dm^{-3} . ^b More reactive enantiomer shown in parentheses. ^c A mixture of both isomers of **5.1.10** used for resolutions. ^d First eluting isomer by HPLC (Chiralcel OD) used for resolution. ^e Second eluting isomer by HPLC (Chiralcel OD) used for resolution.

becomes the medium-sized group at C_α and the steric chirality of the (*R*)-enantiomer is ρ . For **5.2.5** and **5.2.6** the R_3SiO moiety is the small group and the steric chirality of the (*R*)-enantiomer is σ .

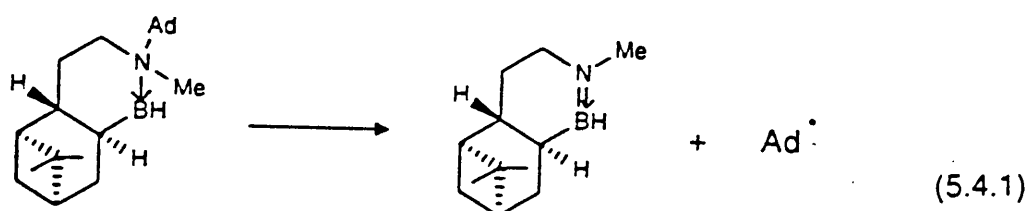
It was hoped, that an increase ⁱⁿ the effective size of the alkyl substituents at silicon would lead to an increase in enantioselectivity and, *s*-values were expected to be largest when the *O*-triisopropylsilylpantolactone derivative **5.2.8** was used as a substrate. However, enantioselectivities remained disappointingly small, presumably for the following reasons. In a first instance, as the size of the alkyl groups increased in the following order $Me_3 < Me_2Bu^t < Et_3 < ^iPr_3$ the hydrogen at C_α became more hindered and, as a result, reactivity towards hydrogen-atom abstraction decreased. This meant that longer irradiation times were required for reasonable consumptions to be achieved, making side reactions more likely. Secondly, a switch in the direction of the enantioselectivities is observed as the methyl groups on silicon are replaced by the larger ethyl and isopropyl groups, the value of *s* must go through a minimum.

The enantioselectivities achieved with the catalysts **5.1.7** and **5.1.8** were similar in magnitude and replacing the pyrrolidine ring by a piperidine ring did not have a major effect on the environment at the boron-centre in the transition state. In general, the largest enantioselectivities were achieved with **5.1.9** presumably because the addition of two equatorial methyl groups on the

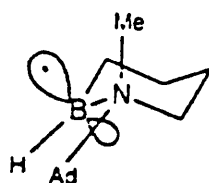
piperidine ring accentuated the asymmetry about the boron-atom in the transition state. The catalyst **5.1.10** was used as the mixture of the two isomers with the substrates **5.2.5-5.2.8**, the values of s obtained were close to those achieved with **5.1.9** as catalyst. In kinetic resolution of **5.2.1** with **5.1.10**, the individual isomers were used and, very different enantioselectivity-factors were obtained in each case, although the direction of the selectivity was the same. If the steric strain model holds for this example, then the larger s -value obtained with the second eluting isomer of the catalyst should arise from the isomer having the *n*-butyl group in the equatorial position, as this would create the greater asymmetry about the boron-centre in the TS. The lower s -value should be associated with the catalyst isomer having the methyl group in the equatorial position. Since both isomers gave different values of s , the s -values observed with the substrates **5.2.5-5.2.8** (which were obtained using the isomer mixture) could in principle be improved by using only the isomer having the *n*-butyl group equatorial. Examination of molecular models confirms that the bulkier of the groups attached to the nitrogen atom in the polycyclic amine-boranes should be in the equatorial position to create the greatest asymmetry about the boron-atom in the TS.

The catalyst **5.1.12** was included for the kinetic resolutions of **5.2.1** and **5.2.5** (see Table 5.4.2). This catalyst was designed in the hope that the large difference in size between the adamantyl and the methyl group at nitrogen would bring about large enantiomeric excesses by maximising the asymmetry

about the boron-centre in the TS. The adamantyl group (Ad) was chosen as the bulky alkyl group, in preference to groups like t-butyl, because amine-boryl radicals of the type $R^1-N\rightarrow\dot{B}H_2$ (where R^1 is a tertiary alkyl group) have a strong tendency to lose $R^1\cdot$ and give $>N=BH_2$. The radical derived by hydrogen-atom abstraction from 5.1.12 is shown in 5.4.4. If 5.4.4 was to undergo β -scission to some extent [eqn. (5.4.1)], the 1-adamantyl radical (1-Ad \cdot) would be produced, which would then go on to give adamantane. GLC analyses of the reaction mixture after photolysis showed no trace of adamantane. The 1-adamantyl radical is an unstable tertiary radical because of enforced pyramidal geometry at the radical centre and, moreover, β -scission is less likely for 5.4.4 than for an acyclic analogue because of stereoelectronic effects. Thus, because the adamantyl group in 5.4.4 assumes an equatorial position, the dihedral angle θ formed between the N-Ad bond and the axis of the SOMO on boron is very small (see 5.4.5) and consequently β -scission will be slow. It is therefore safe to conclude that none of the amine-boryl radical 5.4.4 is destroyed by β -scission.



5.4.4



5.4.5

The enantioselectivity achieved with the isopropylidene tartrate **5.2.1** as a substrate and **5.1.12** as a catalyst, was indeed greater than those obtained with other polycyclic amine-boranes, but of the same order of magnitude as that obtained with the second eluting isomer of **5.1.10**, and still not as large as the value obtained with the lpcT catalysts. With the substrate **5.2.5**, the *s*-value obtained is very small, smaller than with the other polycyclic amine-boranes. The amine-borane **5.1.12** is a relatively hindered catalyst and as such its reactivity towards hydrogen-atom abstraction is greatly reduced, longer reaction times were required to achieve reasonable consumption of substrates. For example, after 360 min of photolysis using **5.2.5** as the substrate and **5.1.12** as a catalyst, only 32% of the substrate had reacted, compared with 53% consumption obtained after 120 min of photolysis when **5.2.10** was used as catalyst. An unreactive catalyst increases the risk from direct hydrogen-atom abstraction from the substrate by the *t*-butoxyl radical.

5.5. Relationships Between Structure, Reactivity and Enantioselectivity for Hydrogen-Atom Abstraction by Chiral Amine-Boryl Radicals

The amine-boryl radical derived from lpcT is appreciably more enantioselective in hydrogen-atom abstraction from the isopropylidene tartrate **5.2.1** than is the corresponding radical derived from the DABCO complex lpcD.

This suggests that the steric asymmetry* around boron in the transition state for abstraction by the former radical may be greater than that for abstraction by the latter. Alternatively, the second chiral borane residue in the amine-boryl radical from *lpcT* could interact in the transition state to increase enantioselectivity in a manner not possible for the more rigid DABCO complex. The single-crystal X-ray structure of ^d*lpcT* has been determined previously.¹² Although crystals suitable for X-ray diffraction could not be grown for *lpcD*, they could be obtained for the related monoborane complex *lpcQ*. The steric environment about boron in the transition states for abstraction by the amine-boryl radicals from *lpcD* and *lpcQ* should be very similar and, indeed, the same enantioselectivity is shown by both these radicals when they abstract from racemic **5.2.1** (see Table 5.4.1).

The crystal structure determined for *lpcQ* is shown in Figure 5.5.1. In Figure 5.5.2a the mirror image of this (\equiv ^d*lpcQ*) is drawn for comparison with the structure of ^d*lpcT* (Figure 5.5.2b) determined previously.¹² The geometry of the *lpcBH*₂ group is very similar in both complexes and is probably also similar in *lpcD*. Provided that the structures of these complexes in the solid state are close to those of the developing amine-boranes in the corresponding transition states **5.5.1** for H-atom transfer, molecular models indicate that the

* The size difference between substituents of large, medium and small bulk.²⁶

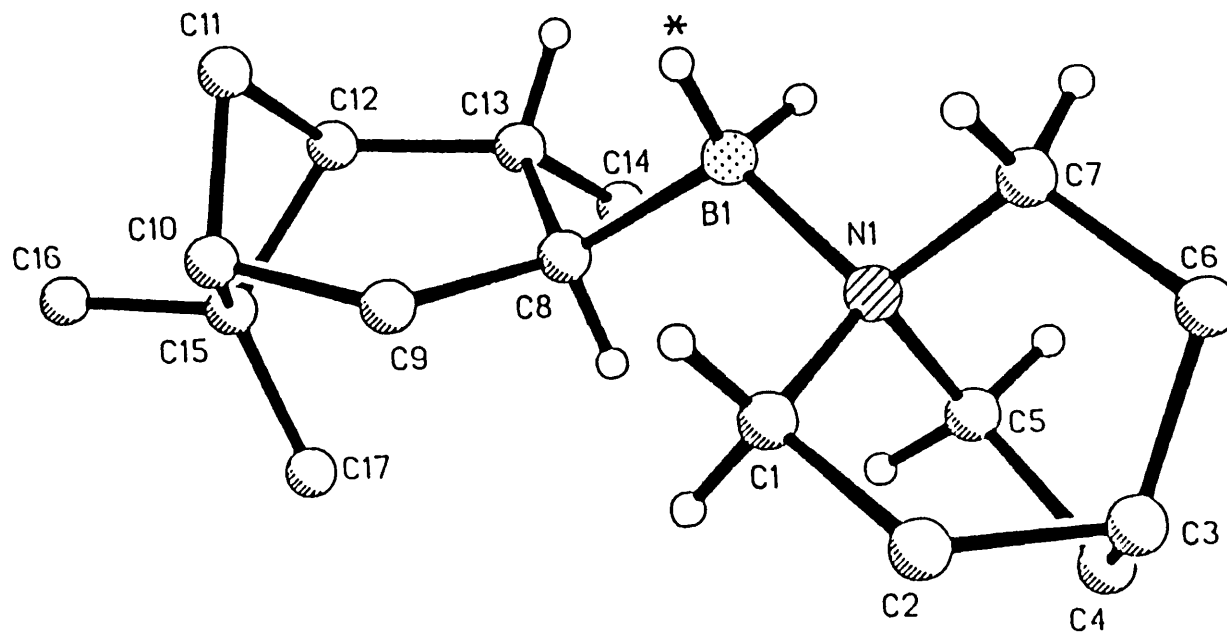


Figure 5.5.1: Crystal structure of 'lpcQ 5.1.6; only key hydrogen atoms are shown. The hydrogen atom attached to boron and marked with an asterisk is that thought to be involved in H-atom transfer reactions (see text). The BN and BC bond lengths are 1.636(6) and 1.620(7) Å, respectively, and the CBN angle is 115.9(4)°.

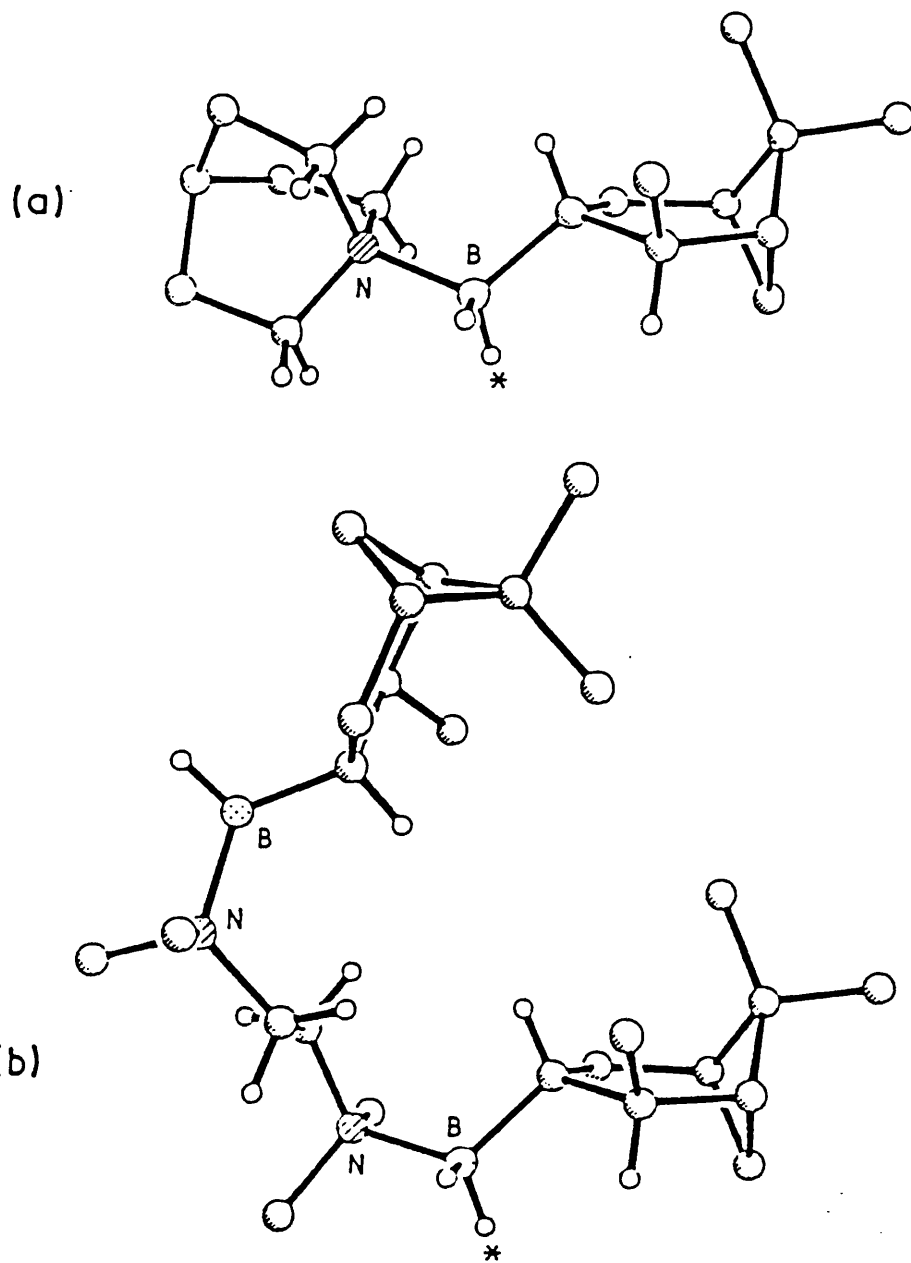


Figure 5.5.2: (a) Mirror image of the crystal structure of ${}^1\text{lpcQ}$ ($= {}^0\text{lpcQ}$). (b) Crystal structure of ${}^0\text{lpcT}$ 5.1.1, drawn from the coordinates given by Soderquist *et al.* (ref. 12).

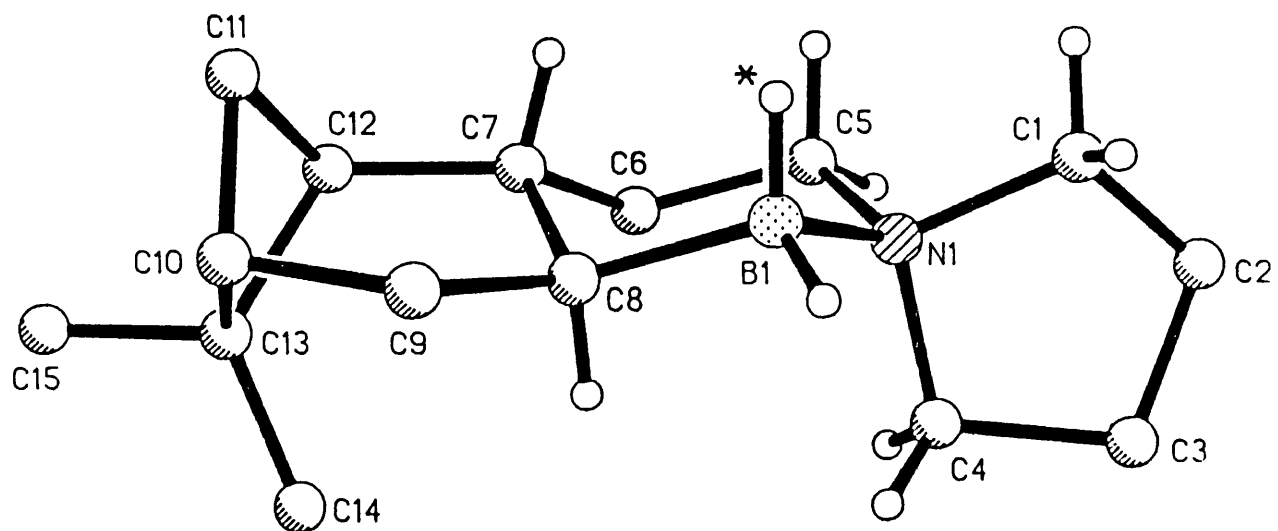
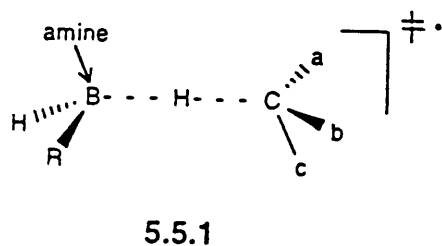
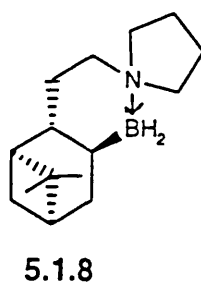
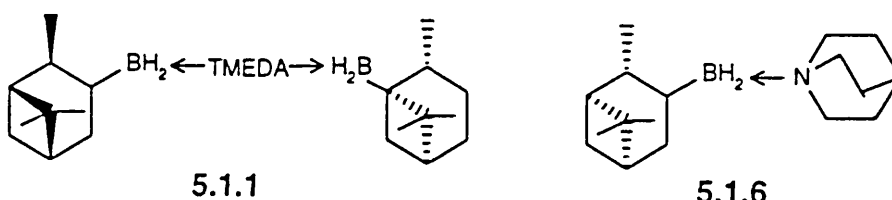


Figure 5.5.3: Crystal structure of the polycyclic amine-borane 5.1.7; only key hydrogen atoms are shown. The hydrogen atom attached to boron and marked with an asterisk is that thought to be involved in H-atom transfer reactions (see text). The BN and BC bond lengths are 1.643(3) and 1.615(4) Å, respectively, and the CBN angle is 107.3(2)°

steric asymmetry around boron is greater for lpcT than for lpcD or lpcQ, suggesting that this is the likely reason for the greater chiral discrimination obtained with the TMEDA complex.

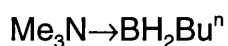


The X-ray crystal structure of 5.1.7 is shown in Figure 5.5.3 and this confirms the assumptions made previously in Section 5.1.²⁵ The relatively rigid structure of 5.1.7 makes this amine-borane and, the related complexes 5.1.8-5.1.12 with other *N*-alkyl groups, particularly suitable for probing the origins of the chiral discrimination shown by the derived amine-boryl radicals. Of the two hydrogen atoms attached to boron in each of the complexes 5.1.1, 5.1.3 and 5.1.7, that which is the less sterically protected is indicated with an asterisk in Figures 5.5.1-5.5.3. The hydrogen atom being transferred between carbon and

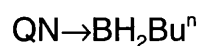
boron in the preferred transition state of the type **5.5.1** will probably occupy a position similar to that of H*.

Electron Spin Resonance Studies

In order to probe the steric demands of the amine-boryl radicals derived from **5.1.1-5.1.13**, the relative rates of α -hydrogen-atom abstraction from diethyl malonate **5.5.2** and diethyl methylmalonate **5.5.3** were measured using ESR spectroscopy under conditions of polarity reversal catalysis.^{26,27} Photolysis of di-t-butyl peroxide (DTBP) produces the electrophilic t-butoxyl radical which rapidly abstracts electron-rich hydrogen from boron in an amine-borane complex to give a nucleophilic amine-boryl radical, which in turn rapidly abstracts an electron-deficient α -hydrogen atom from the malonate [eqns. (5.5.1-5.5.3)]. The achiral amine-boranes **5.5.4-5.5.7** were included for comparative purposes and the relative reactivities of these malonates towards the amine-boryl radical from trimethylamine-thexylborane* **5.5.8** has been determined previously in cyclopropane solvent.¹⁵

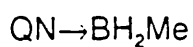


5.5.4



5.5.5

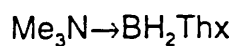
* The 1,1,2-trimethylpropyl group is known as the thexyl group (Thx).



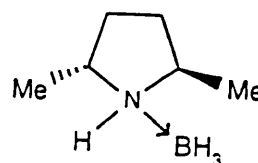
5.5.6



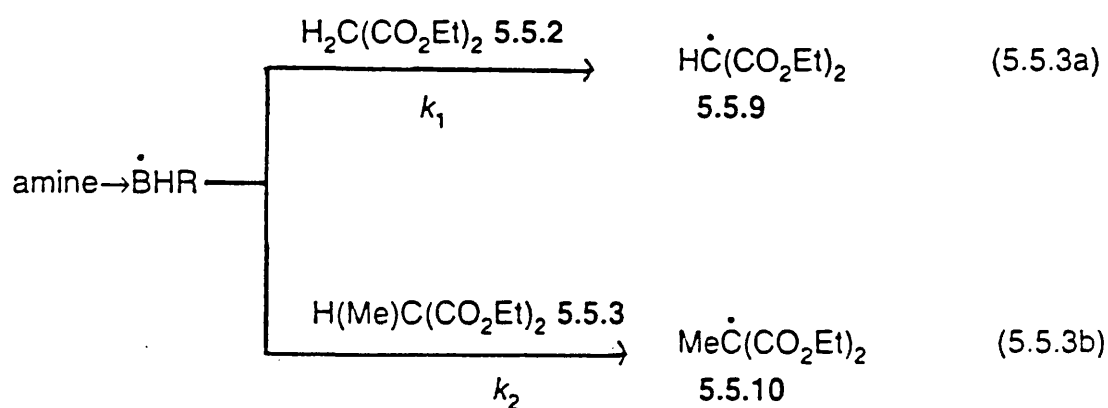
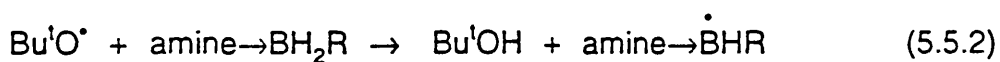
5.5.7



5.5.8



5.5.11



UV irradiation of an oxirane solution containing the amine-borane (0.15-0.30 mol dm⁻³), the two malonates (each 0.2-1.0 mol dm⁻³) and DTBP (15% v/v) afforded overlapping ESR spectra of the two radicals 5.5.9 and

5.5.10, as described previously (section 2.1).^{27*} The relative concentrations of **5.5.9** and **5.5.10** under steady-state conditions during continuous UV photolysis will be given by equation (5.5.4), provided that these two radicals are removed by self- and cross-reactions which have equal (diffusion-controlled) rate constants.^{26,27} Values of k_1/k_2 at -84 °C were determined by double integration

$$k_1/k_2 = [\mathbf{5.5.9}][\mathbf{5.5.3}]/[\mathbf{5.5.2}][\mathbf{5.5.10}] \quad (5.5.4)$$

of appropriate non-overlapping lines in the ESR spectrum, usually for two different malonate concentration ratios $[\mathbf{5.5.2}]:[\mathbf{5.5.3}]$. Radical concentration ratios were confirmed by computer simulation of the spectra and the results are summarised in Table 5.5.1.

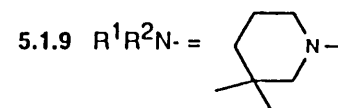
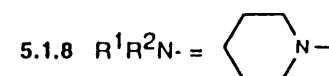
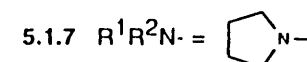
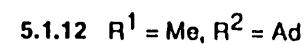
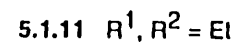
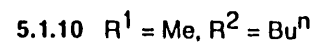
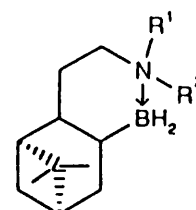
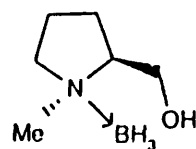
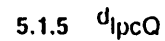
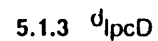
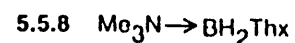
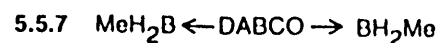
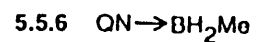
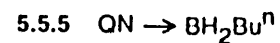
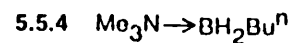
Only weak spectra of the radicals **5.5.9** and **5.5.10** were obtained when the secondary amine-borane **5.5.11**²⁵ was used as polarity reversal catalyst. We attribute this to the occurrence of a competitive reaction between the amine-boryl radical and its parent **5.5.11** to yield an electrophilic aminyl-borane radical incapable of abstracting hydrogen from the malonates.^{28,29} The ESR spectrum of the aminyl-borane radical would consist of many lines and this

* The ESR parameters under these reactions are: for **5.5.9**, $a(\text{H}_\alpha)$ 20.30, $a(4\text{H}_\delta)$ 1.40 G and g 2.0040, and **5.5.10**, $a(3\text{H}_\beta)$ 23.92, $a(4\text{H}_\delta)$ 1.10 G and g 2.0037.

Table 5.5.1: Relative rate constants for hydrogen-atom abstraction by amine-boryl radicals from $\text{H}_2\text{C}(\text{CO}_2\text{Et})_2$ and $\text{MeCH}(\text{CO}_2\text{Et})_2$ in oxirane at $-84\text{ }^\circ\text{C}$ under conditions of polarity-reversal catalysis.

Amine-borane catalyst															
k_1/k_2^a	5.5.4	5.5.5	5.5.6	5.1.7	5.1.13	5.5.7	5.1.11	5.1.12	5.1.8	5.1.10	5.1.9	5.1.5	5.1.3	5.1.1	5.5.8
	0.88	0.88	0.89	1.6	1.7	2.0	2.0	2.3	2.6	3.2	4.5	8.9	9.6	19	21

^a Estimated error $\pm 5\%$. ^b In cyclopropane solvent; data from ref. 15.



radical would be difficult to detect in low concentration. When a solution of DTBP and **5.5.11** in t-butyl alcohol-t-pentyl alcohol (4 : 1 v/v) was UV irradiated at -6 °C, a complex spectrum which we assign to the expected aminyl-borane radical $\text{MeCH}(\text{CH}_2)_2\text{CH}(\text{Me})\dot{\text{N}}\rightarrow\text{BH}_3$ was observed [$a(3\text{H}_\beta)$ 48.2, $a(2\text{H}_\beta)$ 34.1, $a(\text{N})$ 17.2, $a(^{11}\text{B})$ 11.2 and $a(^{10}\text{B})$ 3.7(5) G].

For competitive hydrogen-atom abstraction by a series of amine-boryl radicals, polar effects in the transition states should be similar and the value of k_1/k_2 would be expected to increase with increasing steric congestion about the boron-centre. The amine-boryl radicals from the complexes **5.5.4-5.5.7** of methyl- and butyl-boranes should be amongst the least sterically-hindered and indeed give rise to the smallest values of k_1/k_2 . The relatively large value of k_1/k_2 for abstraction catalysed by the DABCO complex of methylborane **5.5.7** is somewhat surprising. Similar selectivities are found for abstraction by the amine-boryl radicals derived from **5.1.7**, **5.1.11** and **5.1.13**, with diethyl malonate being about twice as reactive as diethyl methylmalonate. The isopinocampheylborane complexes are associated with much larger values of k_1/k_2 , indicating increased steric hindrance around the boron centres in the derived amine-boryl radicals. Similar values of k_1/k_2 (9-10) are shown by the amine-boryl radicals from the quinuclidine and DABCO complexes of IpcBH_2 **5.1.5** and **5.1.3**, respectively, but an appreciably larger value (19) was obtained with the TMEDA complex as catalyst. This high chemoselectivity, which is presumably steric in origin, is probably related to the higher enantioselectivities

obtained with IpcT in comparison with IpcD and IpcQ (see Table 5.4.1). The selectivity obtained with IpcT is similar to those found previously¹⁵ with $\text{Me}_3\text{N}\rightarrow\text{BH}_2\text{Thx}$, when a bulky tertiary alkyl group is attached to the boron centre in the amine-boryl radical which brings about hydrogen abstraction.

5.6. Conclusion

The enantioselectivities achieved for hydrogen-atom abstraction by chiral amine-boryl radicals are not large. The more reactive substrate enantiomer can generally be predicted by consideration of the steric interactions between the substituents attached to the boron atom and to the α -carbon atom in the diastereoisomeric transition states of the general type 5.5.1. However, hydrogen bonding and dipole-dipole interactions, together with stereoelectronic effects, may also play a part in determining enantioselectivity particularly when there is not marked asymmetry around the reacting centres. Larger enantioselectivities might be obtained with amine-boranes in which there is a relatively rigid and more sterically asymmetric environment around the boron atom,³⁰ without compromising too much on the reactivity of the hydrogens at the boron centre.

5.7. References to Chapter 5

- 1 P.L.H. Mok, B.P. Roberts and P.T. McKetty, *J. Chem. Soc., Perkin Trans. 2*, 1993, 665.
- 2 H.C. Brown, J.R. Schwier and B. Singaram, *J. Org. Chem.*, 1978, **43**, 4395.
- 3 B. Singaram and J.R. Schwier, *J. Organomet. Chem.*, 1978, **156**, C1.
- 4 H.C. Brown, B. Singaram and J.R. Schwier, *Inorg. Chem.*, 1979, **18**, 51.
- 5 A.K. Mandal, P.K. Jadhav and H.C. Brown, *J. Org. Chem.*, 1980, **45**, 3543.
- 6 P.K. Jadhav and M.C. Desai, *Heterocycles*, 1982, **18**, 233.
- 7 H.C. Brown, R.S. Randad, K.S. Bhat, M. Zaidlewicz, S.A. Weissman, P.K. Jadhav and P.T. Perumal, *J. Org. Chem.*, 1988, **53**, 5513.
- 8 H.C. Brown, P.V. Ramachandran, S.A. Weissman and S. Swaminathan, *J. Org. Chem.*, 1990, **55**, 6328.
- 9 H.C. Brown and P.V. Ramachandran, *J. Org. Chem.*, 1989, **54**, 4504.
- 10 N.N. Joshi, M. Srebnik and H.C. Brown, *J. Am. Chem. Soc.*, 1988, **110**, 6246.
- 11 H.C. Brown and B. Singaram, *Adv. Chem. Res.*, 1992, **25**, 16.
- 12 J.A Soderquist, S.-J. Hwang-Lee and C.L. Barnes, *Tetrahedron Lett.*, 1988, **29**, 3385.
- 13 V. Paul and B.P. Roberts, *J. Chem. Soc., Chem. Commun.*, 1987, 1322.
- 14 V. Paul and B.P. Roberts, *J. Chem. Soc., Perkin Trans. 2*, 1988, 1895.

- 15 V. Paul and B.P. Roberts , *J. Chem. Soc., Perkin Trans. 2*, 1988, 1183.
- 16 P. Kaushal, P.L.H. Mok and B.P. Roberts, *J. Chem. Soc., Perkin Trans. 2*, 1990, 1663.
- 17 P.L.H. Mok and B.P. Roberts, *J. Chem. Soc., Chem. Commun.*, 1991, 150.
- 18 P.L.H. Mok and B.P. Roberts, *Tetrahedron Lett.*, 1992, **33**, 7249.
- 19 C.T. Ng, X. Wang and T.-Y. Luh, *J. Org. Chem.*, 1988, **53**, 2536.
- 20 V.S. Martin, S.S. Woodard, T. Katsuki, Y. Yamada, M. Ikeda and K.B. Sharpless, *J. Am. Chem. Soc.*, 1981, **103**, 6237.
- 21 H.B. Kagan and J.C. Fiaud, in *Topics in Stereochem.*, 1988, **18**, 249.
- 22 A.L.J. Beckwith, S. Brumby and C.L.L. Chai, *J. Chem. Soc., Perkin Trans. 2*, 1992, 2117.
- 23 R.S. Cahn, C.K. Ingold and V. Prelog, *Angew. Chem., Int. Ed. Engl.*, 1966, **5**, 385.
- 24 A.L.J. Beckwith, R. Hesperger and J.M. White, *J. Chem. Soc., Chem. Commun.*, 1991, 1151.
- 25 H.-S. Dang, V. Diart and B.P. Roberts, *J. Chem. Soc., Perkin Trans. 1*, 1994, 1033. (See Chapter 5).
- 26 A.G. Davies, D. Griller and B.P. Roberts, *J. Chem. Soc. B*, 1971, 1823.
- 28 V. Diart and B.P. Roberts, *J. Chem. Soc., Perkin Trans 2*, 1992, 1761 (see Chapter 2).
- 28 I.G. Green and B.P. Roberts, *J. Chem. Soc., Perkin Trans. 2*, 1986, 1597.

- 29 J.N. Kirwan and B.P. Roberts, *J. Chem. Soc., Perkin Trans. 2*, 1989, 539.
- 30 S. Masamune, B.-M Kim, J.S. Petersen, T. Sato, S.J. Veenstra and T. Imai, *J. Am. Chem. Soc.*, 1985, **107**, 4549.

Chapter 6: EXPERIMENTAL

6.1. NMR Spectroscopy

NMR spectra were recorded using a Varian VXR-400 instrument (400 MHz for ^1H). The solvent was CDCl_3 and chemical shifts are reported relative to Me_4Si (^1H and ^{13}C) and to external $\text{BF}_3\cdot\text{OEt}_2$ (^{11}B); J -values are quoted in Hz. The optically active shift reagents $\text{Eu}(\text{hfc})_3$ and $\text{Eu}(\text{tfc})_3$ (Aldrich) and DNPB (Fluka) were used as supplied.*

6.2. ESR Spectroscopy

ESR spectra were recorded during continuous UV irradiation of samples positioned in a standard variable temperature insert in the microwave cavity of a Varian E-109 or Bruker ESP-300 spectrometer operating at 9.1-9.4 GHz. The light source was a 500 W mercury discharge lamp (Osram HBO 500 W/2) and the optical system has been described previously (Section 3.1). Samples were prepared using a vacuum line and were sealed in evacuated Suprasil quartz

* The shift reagents used were tris[3-(heptafluoropropylhydroxymethylene)-(+)-camphorato]europium(III) [$\text{Eu}(\text{hfc})_3$], tris[3-(trifluoromethylhydroxymethylene)-(+)-camphorato]europium(III) [$\text{Eu}(\text{tfc})_3$] and (S)-(+)-3,5-dinitro-*N*-(1-phenylethyl)benzamide (DNPB).

tubes (2 mm i.d., 0.5 mm wall), for oxirane solvent. Stock mixtures of diethyl malonate and diethyl methylmalonate (both distilled before use) were made up by weight and portions of these were used for sample preparation. The experimental methods for determination of relative rate constants using the ESR method have been described in detail previously (Section 3.1).

6.3. Gas Liquid Chromatography (GLC)

GLC analyses were carried out using a Pye-Unicam 204 chromatograph equipped with a flame-ionisation detector and a Hewlett-Packard model 3392A integrator. A glass column (2 m x 4 mm) packed with 10% OV-101 on Chromosorb WHP 80-100 mesh was used with nitrogen carrier gas.

6.4. High-Performance Liquid Chromatography (HPLC)

HPLC was carried out using a Gilson 305 instrument in conjunction with UV or refractive index detectors; a 250 mm x 4 mm column containing Chiralcel OD (Daicel Chemical Industries) was used to effect analytical separation of enantiomers (hexane-isopropyl alcohol mobile phase), a 250 mm x 4.6 mm column containing Nucleosil 100 5 μm , silica gel was used for analytical separation of isomers, and preparative separations were effected using a 250 mm x 10 mm, Nucleosil 100 5 μm , silica gel column (hexane-ethyl acetate, 98 : 2).

6.5. Column Chromatography and Thin Layer Chromatography (TLC)

Column chromatography and TLC were carried out using Merck Kieselgel 60 (230-400 mesh) and Kieselgel 60 F₂₅₄ aluminium-backed pre-coated plates, respectively.

6.6. Optical Rotations

Optical rotations were determined at 589 nm (sodium D line) with an Optical Activity AA-10 automatic digital polarimeter, using a 1 dm pathlength cell.

6.7. Materials

All preparations and handling of boron-containing compounds were carried out under an atmosphere of dry argon. All solvents were dried by conventional methods and were stored under argon. (*R*)-(+)- and (*S*)-(-)- α -pinenes (Aldrich) were distilled from CaH₂; they showed $[\alpha]_D^{20}$ +50.1° and -50.1° (neat), respectively, corresponding¹ to an e.e. of >99%. Nopol **5.1.16** (Aldrich) was distilled before use and showed $[\alpha]_D^{20}$ -36.4° (neat) corresponding² to an e.e. of 91%. *t*-Butylbenzene and TMEDA were distilled from CaH₂ and 1,4-di-*t*-butylbenzene was recrystallised from diethyl ether. Di-*t*-butyl peroxide (98%, Aldrich) was passed down a column of basic alumina (activity 1) and then

distilled (b.p. 46-47 °C at 76 Torr). Quinuclidine, DABCO and BMS (10 mol dm⁻³ solution in excess Me₂S) (all Aldrich) and oxirane (Fluka) were used as received.

Amine-Borane Catalysts

The amine-boranes ^dlpcT **5.1.1**^{1,4-7} (m.p. 120-145 °C dec., lit.⁴⁻⁷ m.p. 140-141 °C) and ^dlpcD **5.1.3**⁸ (m.p. 124-147 °C dec., lit.⁸ m.p. 160-161 °C) were prepared as described in the literature. The complexes ^llpcT and ^llpcD were prepared from (1*S*)-(-)- α -pinene in the same way as their antipodes.

The quinuclidine complex ^dlpcQ **5.1.5** and its antipode were prepared in a similar way to ^dlpcT by treatment of ^dlpc₂BH with one molar equivalent of quinuclidine. Recrystallisation from diethyl ether-hexane (6:4 v/v) gave ^dlpcQ, m.p. 74-76 °C. (Found: C, 78.1; H, 12.6; N, 5.2. C₁₇H₃₂BN requires C, 78.2; H, 12.4; N, 5.4%). δ_{H} 0.63 (m, 1H), 0.76 (d, 1H, *J* 8.71), 0.94 (d, 3H, *J* 7.05), 1.07 (s, 3H), 1.12 (s, 3H), 1.52 (m, 2H), 1.72 (m, 7H), 1.77 (m, 2H), 1.98 (m, 2H), 2.16 (m, 2H) and 2.98 (m, 6H) ; δ_{C} 20.67, 22.44, 22.84, 25.01, 28.45, 34.13 (2 peaks), 38.33, 38.95, 42.62, 43.08, 48.61 and 51.83; δ_{B} 1.46 (br.s).

N-Methyl-(S)-(-)-2-hydroxymethylpyrrolidine. - This was prepared from (S)-(-)-proline by the published method,⁹ b.p. 45 °C at 0.5 Torr (lit.⁹ b.p. 71-74 °C at 21 Torr), $[\alpha]_{\text{D}}^{22}$ -7.2° (c 5.0, CHCl₃), -59.0° (c 3.9, MeOH) [lit.⁹ $[\alpha]_{\text{D}}^{25}$

-5.036° (l 0.1, neat)]. δ_{H} 1.70 (m, 4H) 2.25 (m, 2H), 2.30 (s, 3H, *N*-Me), 2.92 (br.s., 1H, OH), 3.05 (m, 1H), 3.39 (m, 1H) and 3.60 (m, 1H); δ_{C} 23.18, 27.50, 40.53, 57.50, 61.60 and 66.05.

(*S*)-*N*-Methyl-2-hydroxymethylpyrrolidine-borane **5.1.13**. - BMS (1.70 cm³, 0.017 mol) in diethyl ether (5 cm³) was added dropwise to a stirred solution of the amine (2.00 g, 0.0174 mol) in ether (10 cm³) cooled in a bath at *ca.* -40 °C. After the addition, the mixture was stirred at -40 °C for 15 min and then allowed to warm to room temperature. The solvent and Me₂S were removed by evaporation under reduced pressure and the residual solid was recrystallised from hexane-diethyl ether, m.p. 55-57 °C, $[\alpha]_{\text{D}}^{22}$ -9.6° (*c* 3.8, CHCl₃). δ_{H} 1.80-2.20 (m, 4H), 1.50 (br.q, 3H, J_{BH} 97, BH₃) 2.70 (s, 3H, *N*-Me), 2.75-2.95 (m, 3H), 3.30 (m, 1H), 3.86 (m, 2H); δ_{C} 20.71, 24.74, 52.50, 60.68, 65.38 and 72.69; δ_{B} -14.9 (q, J_{BH} 97). (Found: C, 55.7; H, 12.5; N, 10.7. C₁₆H₁₆BNO requires C, 55.9; H, 12.5; N, 10.9%). A much larger NOE was observed for the *N*-methyl protons (δ 2.70) when H-2 (δ 3.30) was irradiated than when the methylene protons of the CH₂OH group (δ 3.86) were irradiated. However, when the *N*-methyl protons were irradiated, a much larger NOE was observed for H-2 than for the methylene protons of the CH₂OH group. This indicates that the *N*-methyl group and the CH₂OH group are probably on opposite sides of the ring in the single isomer obtained, which thus has the (*E*)-configuration.

The nopylamines **5.1.17**. - Nopyl tosylate^{10,11} **5.1.16** was prepared from

(1*R*)-(-)-nopol (91% e.e.) according to the published method.¹⁰ The crude tosylate, which was essentially pure by NMR spectroscopy, showed $[\alpha]_D^{22}$ -26.2° (*c* 7.5, CHCl₃) and, since no enantiomeric fractionation should have taken place prior to the measurement, the e.e. of this material will be 91%. Recrystallisation from pentane gave analytically pure tosylate, m.p. 51-52 °C (lit.¹¹ m.p. 51.0-51.8 °C), $[\alpha]_D^{22}$ -26.9° (*c* 6.2, CHCl₃) and we assume the e.e. to be still 91%. This tosylate (0.1 mol) and the appropriate amine (0.4 mol) in tetrahydrofuran (THF, 150 cm³) were heated under reflux for 14 h (pyrrolidine, piperidine, 3,3-dimethylpiperidine, *N,N*-butylmethylamine and diethylamine). After work-up as described for similar compounds¹³ the nopylamines were purified by distillation; each is assumed to contain a 91% excess of the (1*R*)-enantiomer.

N-(1*R*)-*Nopylpyrrolidine*. - Yield 95%, b.p. 70-72 °C at 0.05 Torr (lit.¹⁰ b.p. 82-83 °C at 0.3 Torr), $[\alpha]_D^{23}$ -34.0° (*c* 5.8, CHCl₃). δ_H 0.79 (s, 3H), 1.11 (d, 1H, *J* 8.0), 1.24 (s, 3H), 1.76 (m, 4H), 2.01 (m, 2H), 2.17 (m, 4H), 2.32 (m, 1H), 2.43 (m, 2H), 2.50 (m, 4H) and 5.2 (s, 1H); δ_C 21.22, 23.41, 26.31, 31.29, 31.66, 36.56, 37.98, 40.76, 45.99, 54.15, 54.66, 116.82 and 146.60.

N-(1*R*)-*Nopylpiperidine*. - Yield 85%, b.p. 90-92 °C at 0.05 Torr, (lit.¹⁴ 93-95 °C at 0.3 Torr), $[\alpha]_D^{19}$ -31.8° (*c* 13.2, CHCl₃) [lit.¹⁴ -18.8 (neat)]. δ_H 0.77 (s, 3H), 1.09 (d, 1H, *J* 8.42), 1.22 (s, 3H), 1.38 (m, 2H), 1.55 (q, 4H, *J* 5.63), 2.02 (m, 2H), 2.12 (m, 4H), 2.29 (m, 7H), 5.17 (s, 1H); δ_C 21.20, 24.45, 36.01,

26.27, 31.26, 31.62, 34.41, 40.70, 45.95, 54.49, 57.57, 76.67, 116.71, 146.62.

N-(1*R*)-*Nopyl*-*N*-(*butyl*)*methylamine*. - Yield 90%, b.p. 90-94 °C at 0.03 Torr, $[\alpha]_D^{19}$ -29.3° (c 11.3, CHCl₃). δ_H 0.78 (s, 3H), 0.88 (t, 3H, *J* 7.29), 1.10 (d, 1H, *J* 8.42), 1.23 (s, 3H), 1.28 (sextet, 2H, *J* 7.50), 1.40 (m, 2H), 1.98 (m, 1H), 2.03 (m, 1H), 2.08 (m, 2H), 2.15 (m, 1H), 2.18 (s, 4H), 2.30 (m, 5H), 5.18 (m, 1H); δ_C 14.06, 20.72, 21.19, 26.28, 29.57, 31.25, 31.62, 34.65, 37.92, 40.71, 42.17, 45.55, 47.43, 55.99, 116.71, 146.59. (Found C, 81.4; H, 12.2; N, 6.1. C₁₆H₂₉N requires C, 81.6; H, 12.4; N, 5.9%).

N-(1*R*)-*Nopyl*-3,3-*dimethylpiperidine*. - Yield 81%, b.p. 110-112 °C at 0.05 Torr, $[\alpha]_D^{20}$ -38.8° (c 7.4, CHCl₃). δ_H 0.80 (s, 3H), 0.89 (s, 6H), 1.10 (d, 1H, *J* 8.42), 1.17 (m, 2H), 1.23 (s, 3H), 1.55 (quintet, 2H, *J* 6.04), 1.90-2.35 (complex m, 13H), 5.18 (s, 1H); δ_C 21.45, 23.00, 26.35, 30.70, 31.32, 31.67, 34.32, 37.65, 37.94, 40.80, 45.95, 46.00, 54.94, 57.34, 66.07, 116.66, 146.86. (Found C, 82.5; H, 11.9; N, 5.4. C₁₈H₃₂N requires C, 82.7, H, 12.0, N, 5.4%).

N-(1*R*)-*Nopyl*-*N,N*-*diethylamine*. - Yield 91%, b.p. 68-70 °C at 0.05 Torr, $[\alpha]_D^{22}$ -32.6° (c 6.5, CHCl₃). δ_H 0.80 (s, 3H), 1.00 (t, 6H, *J* 7.15), 1.12 (d, 1H, *J* 8.58), 1.24 (s, 3H), 1.95-2.45 (complex m, 8H), 2.46 (m, 6H), 5.19 (m, 1H); δ_C 11.87, 21.24, 26.33, 31.30, 31.68, 34.04, 37.97, 40.78, 46.08, 51.00, 116.70 and 146.79. (Found C, 81.2; H, 12.1; N, 6.4. C₁₅H₂₇N requires C, 81.4; H, 12.3; N, 6.3%).

The nopylamine-boranes 5.1.18. - BMS (2.00 cm³, 0.020 mol) in diethyl ether (5 cm³) was added dropwise to a stirred solution of the nopylamine (0.020 mol) in ether (20 cm³) cooled in a bath at -20 °C. After the addition, the mixture was stirred at -20 °C for 30 min, allowed to warm to room temperature and stirred for a further 30 min. The solvent and Me₂S were removed by evaporation under reduced pressure and the residue was kept under vacuum (0.05 Torr) for 2 h to give a near-quantitative yield of essentially-pure amine-borane.

N-(1R)-Nopylpyrrolidine-borane. - This showed m.p. 49-50 °C after recrystallisation from hexane. Unrecrystallised amine-borane of presumed e.e. 91% was used in the next stage to give **5.1.7**, [α]_D²² -33.2° (c 5.6, CHCl₃). δ_{H} 0.78 (s, 3H), 1.09 (d, 1H, *J* 8.6), 1.24 (s, 3H), 1.84 (m, 2H), 2.02 (m, 2H), 2.16 (m, 4H), 2.34 (m, 1H), 2.44 (m, 2H), 2.70 (m, 4H), 3.16 (m, 2H) and 5.24 (m, 1H) (the BH₃ resonance was obscured); δ_{C} 21.15, 22.79, 26.18, 31.25, 31.63, 32.74, 37.96, 40.62, 45.81, 61.36, 62.18, 118.20 and 144.70 ; δ_{B} -12.8 (q, *J*_{BH} 93). (Found C, 77.5; H, 12.3; N, 5.8. C₁₅H₂₈BN requires C, 77.3; H, 12.1; N, 6.0%).

N-(1R)-Nopylpiperidine-borane. - Viscous oil, δ_{H} 0.78 (s, 3H), 1.09 (d, 1H, *J* 8.64), 1.24 (s, 3H), 1.55(m, 4H), 1.62 (m, 2H), 2.04 (m, 2H), 2.16 (m, 2H), 2.36 (m, 4H), 2.70 (m, 3H), 2.92 (m, 2H), 5.25 (m, 1H) (the BH₃ resonance was obscured); δ_{C} 20.36, 21.16, 22.73, 25.99, 26.16, 30.64, 31.24, 31.64, 40.57,

45.75, 54.46, 58.25, 58.11, 118.29, 144.74; δ_B 0.34 (unresolved). (Found: C, 77.4; H, 11.9; N, 5.8. $C_{16}H_{30}BN$ requires C, 77.7; H, 12.2; N, 5.7%).

N-(1*R*)-*Nopyl*-*N*-(*butyl*)*methylamine-borane*. - Viscous oil, δ_H 0.78 (s, 3H), 0.92 (t, 3H, *J* 8.04), 1.09 (d, 1H, *J* 8.48), 1.24 (s, 3H), 1.28 (m, 2H), 1.60 (m, 2H), 1.97 (m, 1H), 2.04 (m, 1H), 2.16-2.36 (complex m, 5H), 2.48 (s, 3H), 2.67 (m, 4H), 5.24 (s, 1H); δ_C 13.82, 20.44, 21.13, 25.30, 26.14, 31.24, 37.96, 40.53, 43.78, 49.27, 59.27, 61.04, 61.16, 118.48, 144.28; δ_B -11.25 (q, J_{BH} 95). (Found C, 76.8; H, 12.7; N, 5.8. $C_{16}H_{32}BN$ requires C, 77.1; H, 12.9; N, 5.6%).

N-(1*R*)-*Nopyl*-3,3-*dimethylpiperidine-borane*. - Viscous oil. δ_H 0.78 (s, 3H), 0.99 (s, 3H), 1.04 (s, 3H), 1.11 (d, 1H, *J* 8.36), 1.25 (s, 3H), 1.35 (m, 1H), 1.73 (m, 4H), 2.03 (m, 2H), 2.19 (m, 2H), 2.34 (m, 2H), 2.52-2.95 (complex, 8H), 5.24 (s, 1H); δ_C 17.94, 21.29, 26.22, 27.92, 30.77, 30.83, 31.31, 31.49, 31.70, 36.54, 40.63, 45.83, 59.09, 59.24, 66.47, 118.34, 144.85; δ_B -10.06 (q, J_{BH} 90). (Found C, 78.1; H, 12.7; N, 5.1. $C_{18}H_{34}BN$ requires C, 78.5; H, 12.4; N, 5.1%).

N-(1*R*)-*Nopyl*-*N,N*-*diethylamine-borane*. - Viscous oil. δ_H 0.80 (s, 3H), 1.11 (d, 1H, *J* 8.70), 1.17 (t, 6H, *J* 7.30), 1.25 (s, 3H), 1.41 (br.q, 3H, J_{BH} 91, BH_3), 1.95-2.40 (complex, 8H), 2.65 (m, 2H), 2.77 (q, 4H, *J* 7.30) and 5.26 (m, 1H); δ_B -13.4 (q, J_{BH} 91).

The polycyclic amine-boranes **5.1.7-5.1.11**. - The essentially-pure nopylamine-borane (ca. 0.020 mol) was dissolved in toluene (25 cm³) and heated under reflux for 14 h [$R^1R^2N = (CH_2)_4N$], [$R^1R^2N = (CH_2)_5N$], [$R^1R^2N = MeBu^nN$], [$R^1R^2N = (Me)_2C(CH_2)_4N$], and 16 h for ($R^1R^2N = Et_2N$). The solvent was removed under reduced pressure and the residue was purified by distillation to give 85-95% yields of **5.1.7-5.1.11**, which crystallised on standing. For each of **5.1.7-5.1.11** the e.e. should be ca. 91%.

Compound 5.1.7. - B.p. 134-136 °C at 0.03 Torr, m.p. 53-55 °C, $[\alpha]_D^{20}$ -7.1° (c 5.9, CHCl₃). δ_H 0.77 (d, 1H, J 9.00), 1.18 (s, 3H), 1.23 (s, 3H), 1.46 (m, 2H), 1.58-2.07 (complex m, 12H), 2.46 (m, 1H), 2.78 (m, 4H) and 3.25 (m, 2H) (the broad BH₂ resonance was obscured); δ_C 22.28, 23.01, 23.43, 30.49, 32.20, 33.89, 40.03, 44.05, 48.99, 52.50, 57.35, 62.77, 64.55; δ_B -1.47 (br.t, J_{BH} ca. 74). (Found C, 77.5; H, 11.9; N, 5.9. C₁₅H₂₈BN requires C, 77.3; H, 12.1; N, 6.0%).

Compound 5.1.8. - B.p. 126-128 °C at 0.03 Torr, m.p. 83-85 °C, $[\alpha]_D^{20}$ -17.6° (c 2.0, CHCl₃); δ_H 0.72 (d, 1H, J 8.98), 1.16 (s, 3H), 1.20 (s, 3H), 1.52 (m, 8H), 1.76 (m, 1H), 1.82 (m, 4H), 1.98 (m, 1H), 2.42 (m, 1H), 2.66 (m, 2H), 2.88 (m, 1H), 2.97 (m, 1H), 3.08 (m, 2H), the broad BH₂ resonance is obscured; δ_C 20.02, 20.13, 21.43, 23.52, 30.50, 31.64, 32.14, 39.24, 40.13, 44.03, 48.33, 53.30, 53.87, 60.11, 62.62; δ_B -1.6 (unresolved). (Found C, 77.8; H, 12.0; N, 5.5. C₁₆H₃₁BN requires C, 77.7; H, 12.2; N, 5.7%).

Compound 5.1.9. - This material was mixed with diethyl ether, heated under reflux for *ca.* 5 min, and filtered whilst hot, in order to dissolve any impurities, m.p. 112-125 °C (decomp.), $[\alpha]_D^{20}$ -20.87° (*c* 2.7, CHCl₃); δ_H 0.72 (d, 1H, *J* 8.71), 0.97 (s, 3H), 1.05 (s, 3H), 1.16 (s, 3H), 1.20 (s, 3H), 1.39 (m, 4H), 1.70 (m, 7H), 1.94 (m, 1H), 2.42 (m, 1H), 2.58 (m, 2H), 2.79 (m, 2H), 3.18 (m, 1H), 3.35 (m, 1H); δ_C 17.65, 23.55, 28.46, 30.55, 30.79, 31.50, 32.10, 32.51, 36.99, 39.35, 40.11, 44.07, 48.73, 52.59, 53.44, 59.57, 72.48; δ_B 1.14 (t, *J*_{BH} 93). (Found C, 78.8; H, 12.3; N, 5.0. C₁₈H₃₄BN requires C, 78.5; H, 12.4; N, 5.1%).

Compound 5.1.10. - This was obtained as a 1 : 1 mixture of isomers, b.p. 116-128 °C at 0.03 Torr, $[\alpha]_D^{20}$ -13.33° (*c* 7.5, CHCl₃). The two isomers were separated by HPLC using a 250 mm x 10 mm, Nucleosil 100 5 μm, silica gel column and eluting with a 99:1 mixture of hexane and ethyl acetate (refractive index detector). The first eluting isomer showed δ_H 0.73 (d, 1H, *J* 8.92), 0.94 (t, 3H, *J* 7.20), 1.16 (s, 3H), 1.21 (s, 3H), 1.29 (q, 2H, *J* 7.30), 1.32-1.83 (complex m, 8H), 1.95 (m, 1H), 2.43 (m, 1H), 2.48 (s, 3H), 2.66 (m, 1H), 2.69 (m, 2H), 2.85 (m, 1H); δ_C 13.87, 20.66, 23.48, 24.57, 30.49, 32.09, 32.49, 39.28, 40.04, 44.02, 44.90, 48.90, 52.75, 62.97, 66.90 The second eluting isomer showed δ_H 0.72 (d, 1H, *J* 8.93), 0.92 (t, 3H, *J* 7.30), 1.17 (s, 3H), 1.20 (s, 3H), 1.27 (q, 2H, *J* 7.41), 1.40 (m, 1H), 1.48-1.86 (complex m, 8H), 1.95 (m, 1H), 2.42 (m, 1H), 2.52 (s, 3H), 2.66 (m, 1H), 2.73 (m, 2H), 2.78 (m, 1H); δ_C 13.85, 20.54, 23.51, 25.23, 30.53, 31.95, 32.08, 39.22, 40.20, 44.02,

48.86, 50.84, 52.43, 57.04, 60.89. (Found C, 81.4; H, 12.3; N, 6.1. $C_{16}H_{29}BN$ requires C, 81.6; H, 12.4; N, 6.0%).

Compound 5.1.11. - B.p. 98-100 °C at 0.05 Torr, m.p. 55 °C, $[\alpha]_D^{20}$ -21.1° (c 5.3, $CHCl_3$). δ_H 0.73 (d, 1H, J 8.92), 1.04 (t, 3H, J 7.33), 1.17 (s, 3H), 1.18 (t, 3H, J 7.30), 1.21 (s, 3H), 1.38-2.04 (complex m, 10 H), 2.40-3.10 (complex m, 7H) (the broad BH_2 resonance was obscured); δ_C 11.87, 21.24, 26.33, 31.30, 31.68, 34.04, 37.97, 40.78, 46.08, 51.00, 116.70, 146.70; δ_B -2.25 (br. t, J_{BH} ca. 73). (Found C, 76.9; H, 13.1; N, 5.9. $C_{15}H_{30}BN$ requires C, 76.6; H, 12.9; N, 6.0%).

*N-Adamantylmethylamine 5.1.21.*¹⁵ - Bromoadamantane (24.93 g, 0.11 mol) was placed in the autoclave vessel along with a magnetic stirrer. Methylamine (26 cm³, 0.55 mol) was condensed in a measuring cylinder and added to bromoadamantane. The autoclave was then sealed carefully and the mixture was heated to 215 °C at 70-80 bar for 8 h. The apparatus was allowed to cool down overnight before opening. The contents were recovered using HCl (250 cm³, 2 mol dm⁻³). This mixture was then shaken with ether, the ether layer was discarded and the water layer was rendered strongly basic with NaOH (200 cm³, 5 mol dm⁻³). This was then extracted with ether (4 x 100 cm³) and the combined ether extracts were dried ($K_2CO_3/MgSO_4$). Ether was removed under reduced pressure. The crude *N*-adamantylmethylamine was purified by sublimation at 0.1 Torr with a bath temperature of ca. 90 °C. Yield (14.81g,

0.10 mol), 82%. M.p. 46 °C (Lit¹⁵ 46 °C).

N-(1R)-Nopyl-N-(adamantyl)methylamine 5.1.22. - N-Adamantylmethylamine (14.30 g, 0.09 mol) and (1R)-nopyl tosylate (28.7 g, 0.09 mol) were dissolved in dioxan (150 cm³) and the mixture was heated under reflux under a slow flow of argon for 48 h. Dioxan was then removed under reduced pressure and the residue was redissolved in diethyl ether (100 cm³) and p-toluenesulfonic acid (*ca.* 1.0 g) was added in order to fully precipitate the amine toluenesulfonate salt. This salt was isolated by filtration, dissolved in water (250 cm³) and aqueous sodium hydroxide solution (5 mol dm⁻³) was added until the mixture was strongly basic. After stirring for 1 h at room temperature, the two-phased mixture was extracted with diethyl ether (4 x 100 cm³) and the combined ether extracts were dried (MgSO₄). Ether was then removed under reduced pressure, and the residue was passed through a silica gel column eluting with 100% methanol. The amine was purified by recrystallisation from a 7 : 1 mixture of diethyl ether and petroleum (b.p. 60-80 °C) to give the product (11.32 g, 0.38 mol) 42%, m.p. 62 °C; $[\alpha]_D^{22}$ -24.5° (*c* 5.8, CHCl₃). δ_H 0.80 (s, 3H), 1.08 (d, 1H, *J* 8.49), 1.24 (s, 3H), 1.57 (m, 15H), 2.03 (m, 5H), 2.11 (m, 2H), 2.18 (m, 2H), 2.33 (m, 1H), 2.57 (m, 2H), 5.26 (m, 1H); δ_C 21.29, 26.30, 29.56, 31.30, 31.85, 36.76, 37.42, 37.91, 40.77, 45.36, 50.22, 117.82, 146.28. (Found C, 84.5; H, 11.0; N, 4.7. C₂₂H₃₅N requires C, 84.3; H, 11.3; N, 4.5%).

(1R)-N-Nopyl-N-(adamantyl)methylamine-borane **5.1.23**. - This amine-borane was prepared by hydroboration of **5.1.22** at -20 °C, as described previously for **5.1.18**, and purified by recrystallisation from diethyl ether; yield 96%. The reaction gave a mixture of two diastereomers in the ratio 3 : 1; m.p. 106-112 °C (decomp.); $[\alpha]_D^{22}$ -24.6° (*c* 2.3, CHCl₃). The major isomer showed δ_H 0.82 (s, 3H), 1.06 (d, 1H, *J* 8.64), 1.26 (s, 3H), 1.61 (m, 15H), 1.90-2.68 (complex m, 12H), 2.97 (m, 1H), 5.44 (s, 1H); δ_C 20.98, 26.24, 29.46, 31.48, 31.96, 36.08, 38.75, 40.56, 45.03, 45.35, 58.56, 121.39, 143.75. The minor isomer showed δ_H 0.81 (s, 3H), 1.17 (d, 1H, *J* 8.64), 1.26 (s, 3H), 1.84 (m, 15H), 1.90-2.68 (complex m, 12H), 2.97 (m, 1H), 5.31 (s, 1H); δ_C 21.31, 26.19, 29.46, 31.34, 31.78, 35.52, 36.31, 38.87, 45.75, 46.77, 54.89, 119.35, 144.68; only one boron resonance was detected, δ_B 0.3 (unresolved). (Found C, 80.0; H, 11.9; N, 4.3. C₂₂H₃₈BN requires C, 80.7; H, 11.7; N, 4.3%).

Compound 5.1.12. - This was prepared by heating **5.1.23** (5.51g, 0.018 mol) in dioxan (80 cm³), under a slow flow of argon, for 3 h. The dioxan was removed under reduced pressure and the residue was purified by column chromatography on silica gel (petroleum spirit b.p. 60-80 °C-ethyl acetate, 90:10), yield (3.93 g, 0.013 mol) 70%; m.p. 134-135 °C, $[\alpha]_D^{23}$ -25.2° (*c* 2.3, CHCl₃). δ_H 0.73 (d, 1H, *J* 8.70), 0.99 (m, 1H), 1.12 (s, 3H), 1.19 (s, 3H), 1.48 (m, 2H), 1.63 (m, 7H), 1.76 (m, 4H), 1.94 (m, 7H), 2.13 (s, 3H), 2.41 (m, 3H), 2.60 (m, 1H), 3.28 (m, 1H); δ_C 23.33, 29.50, 29.72, 30.43, 32.79, 36.20, 36.56, 38.90, 39.25, 39.60, 39.85, 43.83, 46.72, 48.60, 51.99, 58.21; δ_B -9.35 (br. t,

J_{BH} 108). (Found C, 80.6; H, 11.6; N, 4.3. $\text{C}_{22}\text{H}_{38}\text{BN}$ requires C, 80.7; H, 11.7; N, 4.3%).

Quinuclidine-butylborane 5.5.5. - A solution of trimethylamine-butylborane (2.36 g, 0.018 mol) and quinuclidine (1.89 g, 0.017 mol) in benzene (10 cm³) was heated under reflux for 4 h under argon. The solvent was removed by evaporation under reduced pressure and the residual oil was distilled to give **5.5.5** (2.77 g, 90%), b.p. 97-100 °C at 0.03 Torr. (Found: C, 73.0; H, 13.2; N, 7.8. $\text{C}_{11}\text{H}_{24}\text{BN}$ requires C, 72.9; H, 13.4; N, 7.7%). δ_{H} 0.31 (m, 2H), 0.88 (t, 3H, J 7.27), 1.18 (m, 2H), 1.29 (m, 2H), 1.73 (m, 6H), 1.99 (septet, 1H, J 3.23) and 2.96 (m, 6H) (the BH_2 resonance was obscured); δ_{C} 14.33, 20.98, 25.30, 26.80, 31.70, 51.90 and 52.10 (the peak from the carbon attached to boron was too broad to detect); δ_{B} -1.69 (br.t, J_{BH} 89).

Quinuclidine-methylborane 5.5.6. - This was prepared in the same way as **5.5.5** from trimethylamine-methylborane,¹ b.p. 66-68 °C at 0.03 Torr. (Found: C, 69.1; H, 13.2; N, 10.2. $\text{C}_8\text{H}_{18}\text{BN}$ requires C, 69.1; H, 13.1; N, 10.1%). δ_{H} -0.23 (t, 3H, J 5.79), 1.59 (br.q, 2H, J ca.93), 1.67 (m, 6H), 1.97 (septet, 1H, J 3.23) and 2.87 (m, 6H); δ_{C} 20.69, 24.90 and 51.18 (the peak from the carbon attached to boron was too broad to detect); δ_{B} -8.33 (br.t, J_{BH} ca. 93).

DABCO-bis(methylborane) 5.5.7. - This was prepared in a similar way

to **5.5.4** from trimethylamine-methylborane (1.83 g, 0.021 mol) and DABCO (1.07 g, 0.0095 mol) in benzene (10 cm³). After heating under reflux for 4 h the solution was allowed to cool to room temperature when some of the product crystallised. Hexane (5 cm³) was added and the mixture was kept at 5 °C overnight. The amine-borane was removed by filtration and dried under reduced pressure (0.05 Torr) for 4 h at room temperature to give **5.5.7** (1.46 g, 92%), m.p. 167-178 °C (dec.). (Found: C, 57.5; H, 13.2; N, 16.7. C₈H₂₂B₂N₂ requires C, 57.2; H, 13.2; N, 16.7%). δ_{H} -0.20 (t, 6H, *J* 5.86), 1.81 (br.q, 4H, *J* ca. 98) and 3.30 (s, 12H); δ_{C} 49.16 (the peak from the carbon attached to boron was too broad to detect); δ_{B} -7.10 (br.t, *J*_{BH} ca. 99).

No changes were observed in the NMR spectra of the complexes **5.5.4-5.5.6** after they had been kept exposed to the atmosphere for 1 week. The complex **5.5.4** QN→BHBuⁿ shows particular promise as a readily prepared and easily handled amine-alkylborane for the generation of alkyl radicals from chloroalkanes at low temperatures for ESR studies¹⁶ and as an achiral polarity-reversal catalyst.¹⁶⁻²⁰

Substrates

Racemic methyl (phenylsulfinyl)acetate **5.2.4** was obtained from Aldrich.

Racemic dimethyl 2,2-dimethyl-1,3-dioxolane-trans-4,5-dicarboxylate

5.2.1 was prepared from racemic dimethyl tartrate²¹ and 2,2-dimethoxypropane by the method of Carmack and Kelley²²; b.p. 84-86 °C at 0.13 Torr (lit.²² b.p. 82-90 °C at 0.2 Torr). δ_{H} 1.50 (s, 6H), 3.83 (s, 6H) and 4.82 (s, 2H). The (*4R,5R*)- and (*4S,5S*)-enantiomers were obtained from Fluka. The e.e. was determined in the presence of Eu(hfc)₃ when the methoxy protons (δ 3.83) of the (*R,R*)-enantiomer are shifted to lower field than those of the (*S,S*)-enantiomer.

Racemic 2-t-butyl-1,3-dioxolane-4-one **5.2.2** was prepared by condensation of trimethylacetaldehyde with glycolic acid. Powdered glycolic acid (2.03 g, 0.027 mol), trimethylacetaldehyde (4.56 g, 0.053 mol), *p*-toluenesulfonic acid (0.2 g) and 1 drop of concentrated sulfuric acid in dichloromethane (60 cm³) were heated under reflux for 6 h with azeotropic removal of water using a Dean and Stark apparatus. The residual solution was washed with water (30 cm³) and the organic layer was dried (MgSO₄). The solvent was removed under reduced pressure and the residual oil was distilled to give **5.2.2** (2.76 g, 72%), b.p. 82-84 °C at 20 Torr (lit.²³ b.p. 60 °C at 200 Torr, which appears to be in error). δ_{H} 0.95 (s, 9H), 4.29 (AB q, 2H) and 5.23 (s, 1H); δ_{C} 23.24, 35.50, 64.45, 111.86 and 171.85. The enantiomers could be resolved by HPLC using a Chiralcel OD column (hexane eluent, UV detection at 230 nm).

The racemic methyl ester of *N*-(*t*-butoxycarbonyl)proline **5.2.3** was

prepared from (\pm)-proline by *N*-t-butoxycarbonylation²⁴ followed by methyl esterification using methyl chloroformate in the presence of triethylamine and 4-dimethylaminopyridine,²⁵ b.p. 80-83 °C at 0.2 Torr; smaller quantities were purified by chromatography on silica gel (pentane-diethyl ether 7 : 3 v/v eluent). Two amide rotamers were detected by NMR spectroscopy in the ratio ca. 2 : 1 at 25 °C. Major rotamer: δ_{H} 1.36 (s, 9H), 1.81 (m, 1H), 1.87 (m, 2H), 2.15 (m, 1H), 3.45 (m, 2H), 3.67 (s, 3H) and 4.16 (dd, 1H, *J* 8.71 and 4.28); δ_{C} 23.58, 28.17, 30.76, 46.19, 51.83, 58.98, 79.68, 153.66 and 173.66. Minor rotamer: δ_{H} 1.41 (s, 9H), 1.81 (m, 1H), 1.87 (m, 2H), 2.13 (m, 1H), 3.31 (m, 2H), 3.67 (s, 3H) and 4.25 (dd, 1H, *J* 8.49 and 2.30); δ_{C} 24.23, 28.31, 29.81, 46.44, 51.99, 58.59, 80.49, 150.30 and 173.40. The (*S*)-enantiomer was obtained in the same way from (*S*)-(-)-proline and purified by chromatography on silica gel. For the (*S*)-enantiomer in the presence of $\text{Eu}(\text{tfc})_3$, the single peak from the methoxy protons (originally at δ 3.67) resolved into two peaks, with that arising from the major rotamer shifted to lower field than that from the minor rotamer. The racemic material showed four peaks in this region; the peaks from the (*R*)-enantiomer appeared inside those from the (*S*). The e.e. of a partially resolved sample was estimated by comparison with the spectrum obtained from the racemic compound.

A sample of methyl (phenylsulfinyl)acetate **5.2.4** enriched in the (*R*)-(+)-enantiomer was prepared by a modified Sharpless oxidation of methyl (phenylthio)acetate using (+)-diethyl (2*R*,3*R*)-tartrate as the source of chirality.²⁶

The sample showed $[\alpha]_D^{20} +53.0^\circ$ (c 1.20, acetone); by HPLC on Chiralcel OD (hexane-PrⁱOH 9:1 v/v eluent) the e.e. was found to be 37% and using (*S*)-(+)-DNPB shift reagent it was found to be 38%. For an e.e. of 64% Duñach and Kagan²⁷ found $[\alpha]_D^{20} +98^\circ$ (c 1, acetone), equivalent to $+58^\circ$ for an e.e. of 38%.

Racemic dihydro-3-trialkylsiloxy-4,4-dimethylfuran-2(3H)-one.²⁸ - In a dry flask, a mixture of (\pm)-pantolactone (1.80 g, 0.014 mol), the trialkylsilyl chloride (0.051 mol) and imidazole (0.060 mol) were dissolved in dichloromethane (15 cm³) and stirred for 24-48 h, depending on the nature of the trialkylsilyl chloride. The mixture was then diluted with dichloromethane, washed with water and dried (MgSO₄). The solvent was removed by evaporation under reduced pressure and the residue was purified by chromatography on silica gel (pentane-diethyl ether 10:1 v/v eluent) to give the product in *ca.* 70% yield. The (*R*)-enantiomers were prepared in the same way as the racemic compounds, but starting from the (*R*)-(-)-pantolactone

Racemic dihydro-3-trimethylsiloxy-4,4-dimethyl-2-(3H)-furanone 5.2.5. - A clear oil which solidified on storage at 5 °C. δ_H 0.17 (s, 9H), 1.00 (s, 3H), 1.09 (s, 3H), 3.86 (d, 1H, J 8.43), 3.95 (s, 1H) and 3.96 (d, 1H, J 8.43); δ_C -0.01, 18.98, 22.88, 40.67, 75.78, 76.40 and 175.87. The (*R*)-(+)-enantiomer prepared from (*R*)-(-)-pantolactone, m.p. 41 °C, $[\alpha]_D^{25} + 34.5^\circ$ (c 3.6, CHCl₃). (Found: C, 53.6; H, 9.1. C₉H₁₈O₃Si requires C, 53.4; H, 9.0%). Enantiomeric ratios were determined using either Eu(hfc)₃ or Eu(tfc)₃ when the Me₃Si

resonance (δ 0.17) shifts further downfield for the (*S*)-enantiomer than for its antipode.

Racemic dihydro-3-t-butyl-dimethylsiloxy-4,4-dimethylfuran-2(3H)-one 5.2.6. - A white crystalline solid, m.p. 65-66 °C. δ_{H} 0.20 (s, 3H), 0.17 (s, 3H), 0.91 (s, 9H), 1.02 (s, 3H), 1.11(s, 3H), 3.87 (d, 1H, *J* 8.74), 3.97 (s, 1H), 3.97(d, 1H, *J* 8.74); δ_{C} 18.70, 19.01, 19.12, 23.04, 25.63, 33.80, 41.60, 75.74, 76.62, 176.20. (Found C, 58.6; H, 9.8. $\text{C}_{12}\text{H}_{24}\text{O}_2\text{Si}$ requires C, 59.0; H, 9.8%). Enantiomeric ratios were determined by chiral stationary phase HPLC (hexane-isopropanol, 99:1 v/v eluent, UV detection 225 nm). The (*R*)-enantiomer is the second to elute.

Racemic dihydro-3-triethylsiloxy-4,4-dimethylfuran-2(3H)-one 5.2.7. - A colourless oil, b.p. 84 °C at 0.03 Torr. δ_{H} 0.62 (q, 6H, *J* 7.83), 0.96 (t, 9H, *J* 7.80), 1.11 (s, 3H), 1.62 (s, 3H), 3.83 (d, 1H, *J* 8.83), 3.96 (d, 1H, *J* 8.83), 3.97 (s, 1H); δ_{C} 4.75, 6.64, 18.98, 23.00, 40.96, 75.78, 76.54, 175.88. (Found C, 58.6; H, 9.8. $\text{C}_{12}\text{H}_{23}\text{O}_2\text{Si}$ requires C, 59.0; H, 9.9%). The enantiomeric ratios were determined by chiral stationary phase HPLC (hexane-isopropanol, 99:1 v/v eluent, UV detection 225 nm), the (*R*)-enantiomer is the first to elute.

Racemic dihydro-3-triisopropylsiloxy-4,4-dimethylfuran-2(3H)-one 5.2.8. - A colourless oil, b.p. 92-94 °C at 0.03 Torr. δ_{H} 1.03 (s, 3H), 1.07 (s, 3H), 1.08 (d, 18H, *J* 7.60), 1.17 (septet, 3H, *J* 7.20), 3.85 (d, 1H, *J* 8.98), 3.96 (d, 1H, *J*

8.98), 4.15 (s, 1H); δ_{C} 12.53, 17.68, 17.94, 19.12, 23.18, 41.46, 75.60, 175.71; (Found C, 63.8; H, 10.7. $\text{C}_{15}\text{H}_{29}\text{O}_2\text{Si}$ requires C, 63.9; H, 10.5%). The enantiomeric ratios were determined by chiral stationary phase HPLC (hexane-isopropanol, 99:1 v/v eluent, UV detection 235 nm), the (*R*)-enantiomer is the first to elute.

6.8. Kinetic Resolutions²⁹

The amine-borane complex (*ca.* 0.2 mol dm⁻³ for **5.1.1** and **5.1.2** and *ca.* 0.4 mol dm⁻³ for **5.1.3-5.1.13**) was transferred to a dry, argon-filled quartz sample tube (9 mm o.d., 1 mm wall). A mixture of racemic substrate (*ca.* 1.0 mol dm⁻³), DTBP (560 mm³) and *t*-butylbenzene (*ca.* 0.15-0.20 mol dm⁻³) was prepared and a portion of this (490 mm³) was transferred to the sample tube, which was then attached to the vacuum line and the contents were frozen in liquid nitrogen. The tube was evacuated and oxirane (600 mm³) was condensed onto the frozen reagents before the tube was flame-sealed under vacuum. The sample was transferred to a solid CO₂-ethanol bath and the contents were mixed by repeated inversion of the tube. The sample was then UV irradiated at -77 °C with the light from a 160 W medium-pressure mercury discharge lamp (Heraeus). The tube was removed from the dewar insert every 15-20 min and the contents were mixed by shaking. The sample tube was then cooled in a solid CO₂-ethanol bath and cracked open at the neck. Toluene (2 cm³) was added and the contents were transferred to a small round bottom

flask which was kept in the freezer. The substrate consumption was determined by GLC analysis of this solution, using the t-butylbenzene as internal standard, by comparison with the chromatogram obtained from the stock mixture before photolysis. Volatiles were removed under reduced pressure and the residual substrate was purified by column chromatography. The substrate was then examined by chiral stationary phase HPLC or ^1H NMR spectroscopy in the presence of chiral shift reagents in order to determine the e.e.

6.9. X-Ray Crystallography

Data were collected on a Nicolet R3mV diffractometer at 20 °C using graphite monochromated Mo-K α radiation. Three standard reflections monitored throughout the data collection showed no loss in intensity with time. The data were corrected for Lorentz and polarisation effects. The structures were solved by direct methods and developed using alternating cycles of least squares refinement and difference-fourier synthesis. Non-hydrogen atoms were refined anisotropically while hydrogens were placed in idealised positions and assigned a common isotropic thermal parameter ($U = 0.08 \text{ \AA}^2$). All calculations were performed with the SHELXTL PLUS program package³⁰ on a MicroVax II computer.

Crystal data for $^1\text{IpcQ}$ 5.1.6. - $\text{C}_{17}\text{H}_{32}\text{B}_1\text{N}_1$, $M = 261.3$, Orthorhombic,

space group $P2_12_12_1$, $a = 9.279(3)$, $b = 9.596(3)$, $c = 19.250(5)$, $U = 1714 \text{ \AA}^3$ (by least-squares refinement of diffractometer angles for 35 reflections in the range $12^\circ \leq 2\theta \leq 22^\circ$, $\lambda = 0.71073 \text{ \AA}$), $Z = 4$, $F(000) = 584$, $D_c = 1.01 \text{ g cm}^{-3}$, $\mu(\text{Mo-K}\alpha) = 0.53 \text{ cm}^{-1}$. Colourless block $0.65 \times 0.60 \times 0.45 \text{ mm}$. Full-matrix least-squares refinement of 172 parameters gave $R = 0.0605$ ($R_w = 0.0639$) for 1425 independent reflections [$I \geq 3\sigma(I)$] in the range $5^\circ \leq 2\theta \leq 55^\circ$. The final electron difference map was featureless with the largest peak 0.21 e \AA^{-3} .

Crystal data for the amine-borane complex 5.1.7. - $\text{C}_{15}\text{H}_{28}\text{B}_1\text{N}_1$, $M = 233.25$, Orthorhombic, space group $P2_12_12_1$, $a = 7.006(3)$, $b = 7.876(3)$, $c = 26.811(11)$, $U = 1479 \text{ \AA}^3$ (by least-squares refinement of diffractometer angles for 30 reflections in the range $15^\circ \leq 2\theta \leq 27^\circ$, $\lambda = 0.71073 \text{ \AA}$), $Z = 4$, $F(000) = 520$, $D_c = 1.05 \text{ g cm}^{-3}$, $\mu(\text{Mo-K}\alpha) = 0.55 \text{ cm}^{-1}$. Colourless block $0.75 \times 0.35 \times 0.30 \text{ mm}$, prepared by slow sublimation in an evacuated sealed tube. Full-matrix least-squares refinement of 154 parameters gave $R = 0.0559$ ($R_w = 0.0637$) for 1985 independent reflections [$I \geq 3\sigma(I)$] in the range $5^\circ \leq 2\theta \leq 50^\circ$. The final electron difference map was featureless with the largest peak 0.28 e \AA^{-3} .

I am grateful to Dr. D.A. Tocher for carrying out the X-ray structure determinations.

6.10 References to chapter 6

- 1 H.-S. Dang, V. Diart, B.P. Roberts and D.A. Tocher, *J. Chem. Soc., Perkin Trans. 2*, 1994, 1039. (See Chapter 5).
- 2 F.H. Thurber and R.C. Thieke, *J. Am. Chem. Soc.*, 1931, **53**, 1030.
- 3 M.M. Midland and H. Kazubski, *J. Org. Chem.*, 1982, **47**, 2814.
- 4 H.C. Brown, J.R. Schwier and B. Singaram, *J. Org. Chem.*, 1978, **43**, 4395.
- 5 B. Singaram and J.R. Schwier, *J. Organomet. Chem.*, 1978, **156**, C1.
- 6 H.C. Brown, B. Singaram and J.R. Schwier, *Inorg. Chem.*, 1979, **18**, 51.
- 7 A.K. Mandal, P.K. Jadhav and H.C. Brown, *J. Org. Chem.*, 1980, **45**, 3543.
- 8 P.K. Jadhav and M.C. Desai, *Heterocycles*, 1982, **18**, 233.
- 9 R.P. Short, R.M. Kennedy and S. Masamune, *J. Org. Chem.*, 1989, **54**, 1755.
- 10 G.F. Hennion, C.C. Price and V.C. Wolff, jr., *J. Am. Chem. Soc.*, 1955, **77**, 4633.
- 11 L.A. Paquette and M.L. McLaughlin, *Org. Synth.*, 1990, **68**, 220.
- 12 H.C. Brown, R.S. Randad, K.S. Bhat, M. Zaidlewicz, S.A. Weissman, P.K. Jadhav and P.T. Perumal, *J. Org. Chem.*, 1988, **53**, 5513.
- 13 M.M. Midland and H. Kazubski, *J. Org. Chem.*, 1992, **57**, 2953.
- 14 G.F. Hennion, C.C. Price, C. Vernon and V.C. Wolff, jr., *J. Am. Chem. Soc.*, 1957, **77**, 4633.

- 15 P.E. Aldrich, E.C. Hermann, W.E. Meier, M. Paulshock, W.W. Prichard, J.A. Snyder and J.C. Watts, *J. Med. Chem.*, 1971, **14**, 535.
- 16 P. Kaushal, P.L.H. Mok and B.P. Roberts, *J. Chem. Soc., Perkin Trans. 2.*, 1990, 1663.
- 17 V. Paul and B.P. Roberts, *J. Chem. Soc., Perkin Trans. 2*, 1988, 1183.
- 18 V. Paul, B.P. Roberts and C.R. Willis, *J. Chem. Soc., Perkin Trans. 2*, 1989, 1953.
- 19 H.-S. Dang and B.P. Roberts, *Tetrahedron Lett.*, 1992, **33**, 4621 (corrigendum p.7070) and 6169.
- 20 H.-S. Dang and B.P. Roberts, *J. Chem. Soc., Perkin Trans. 1*, 1993, 891.
- 21 P. Kocienski and S.D.A. Street, *Synth. Commun.*, 1984, **14**, 1087.
- 22 M. Carmack and C.J. Kelley, *J. Org. Chem.*, 1968, **33**, 2171.
- 23 A.L.J. Beckwith, S. Brumby and C.L.L. Chai, *J. Chem. Soc., Perkin Trans. 2*, 1992, 2117.
- 24 S. Hoppe and Z. Seyter, *Physiol. Chem.*, 1976, **357**, 1651.
- 25 S. Kim, J.I. Lee and Y.C. Kim, *J. Org. Chem.*, 1985, **50**, 560.
- 26 P. Pitchen, E. Duñach, M.N. Deshmukh and H.B. Kagan, *J. Am. Chem. Soc.*, 1984, **106**, 8188.
- 27 E. Duñach and H.B. Kagan, *New. J. Chem.*, 1985, **9**, 1.9.
- 28 L.P. Vakhrushev, I.S. Akchurina, V.T. Panyushkin and A.A. Karepov, *Zhurnal Obshchei Khimii*, 1975, **45**, 710.
- 29 P.L.H. Mok, B.P. Roberts and P.T. McKetty, *J. Chem. Soc., Perkin*

Trans. 2, 1993, 665.

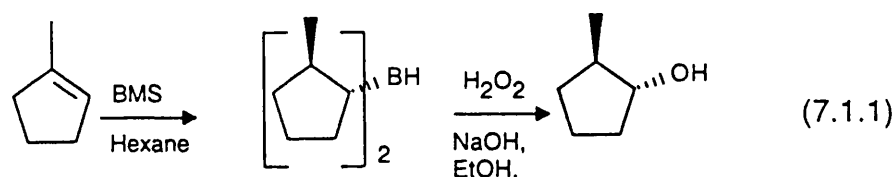
- 30 G.M. Sheldrick, SHELXTL PLUS, an integrated system for refining and displaying crystal structures from diffraction data, University of Gottingen. 1986.

**SECTION C: HYDROBORATION OF 1-METHYLCYCLOHEXENE AND
REDUCTION OF PHENYLACETONE USING THE POLYCYCLIC AMINE-
BORANE FORMED BY CYCLISATION OF *N*-NOPYLPYPERIDINE-BORANE**

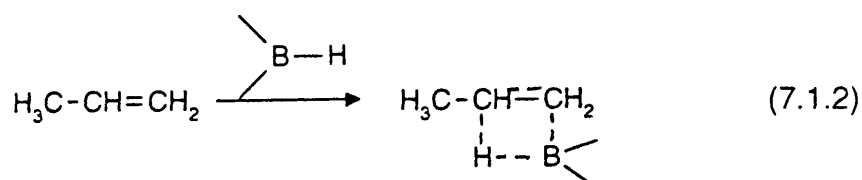
Chapter 7: INTRODUCTION

7.1. Hydroboration of Alkenes

Hydroboration is the addition of a B-H bond across the carbon-carbon multiple bond of an unsaturated organic compound, to give an organoborane.¹⁻³ Hydroboration of alkenes and alkynes is highly stereoselective and takes place by *syn*-addition of B and H, with the boron atom adding to the less alkylated end of and to the less hindered side of the multiple bond [eqn. (7.1.1)].



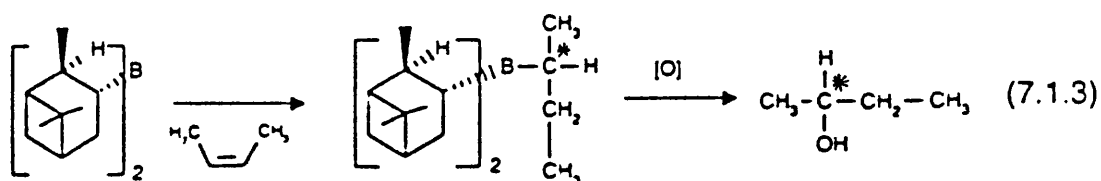
Available evidence suggests that hydroboration is a concerted process which takes place through a 4-membered cyclic TS and, the direction of the addition is controlled primarily by the polarization of the $B^{\delta+}-H^{\delta-}$ bond [eqn. (7.1.2)].¹⁻³



Hydroboration of simple unhindered alkenes with B_2H_6 , BMS or $BH_3 \cdot THF$, proceeds rapidly past the monoalkylborane (RBH_2) stage, through the dialkylborane (R_2BH) stage, to the trialkylborane (R_3B) stage.¹⁻³ However, with hindered alkenes the reaction proceeds rapidly only to the monoalkylborane or

the dialkylborane stages. The boron atom in organoboranes can be readily converted into a variety of organic groups under relatively mild conditions.¹⁻³ For example, oxidation of organoboranes with alkaline hydrogen peroxide is used to form alcohols. This reaction places the OH group at the least substituted end of the original double bond (anti-Markovnikoff hydration), which follows from the fact that the boron atom adds to the least substituted end of the multiple bond [eqn. (7.1.1)].

A chiral hydroborating agent can approach a prochiral alkene from either of the two enantiopic faces to form two diastereoisomeric transition states. The preferred TS is the one where steric interactions are at a minimum, leading to the formation of the diastereoisomeric TSs in unequal amounts. The diastereoisomeric organoboranes are then transformed by replacement of the boron atom into a mixture of two enantiomers in unequal amounts; this forms the basis of asymmetric hydroboration.⁴⁻⁶ The first asymmetric hydroboration performed by Brown and Zweifel in 1961,^{7,8} used (-)-diisopinocampheylborane for the hydroboration of *cis*-alkenes and, led after oxidation with alkaline peroxide, to optically active secondary alcohols. This provided the first non-enzymatic asymmetric synthesis. For example, hydroboration of *cis*-2-butene in diglyme with Ipc_2BH (93% e.e.) provided butan-2-ol in 87% e.e. [eqn. (7.1.3)].



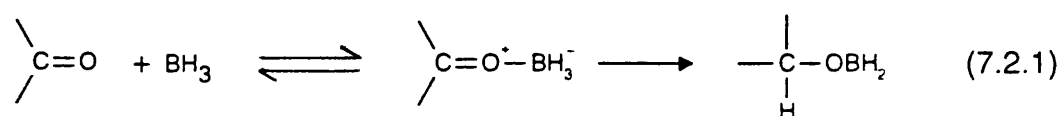
The efficiency of asymmetric hydroboration depends on two factors, the difference between the steric interactions of the two diastereoisomeric TSs and the reactivity of the chiral hydroborating agent with alkenes. Diisopinocampheylborane was for a long time the only chiral hydroborating agent available.⁴⁻⁶ It has large steric requirements and has been very useful for the hydroboration of *cis*-disubstituted-alkenes with relatively low steric requirements (80-90% e.e.), in contrast hydroboration of *trans*-disubstituted and trisubstituted alkenes proceeds more slowly and the degree of chiral induction is dramatically lowered (14-22% e.e.).⁹⁻¹⁰ Monoisopinocampheylborane (IpcBH₂), is the least hindered and most reactive of all chiral organoboranes, and is the most effective chiral hydroborating agent for *trans*-alkenes and trisubstituted alkenes (50-99% e.e.).^{9,11-12} Large differences in steric interactions may increase the efficiency of chiral hydroboration; however, major steric interactions may also result in major decrease in reactivity. Optimum results in the asymmetric system are achieved when the steric requirements of the hydroborating agent and the alkene are carefully matched.⁴⁻⁶

The mechanism for hydroboration suggests that the steric requirements of the methyl group at the 2-position of the apopinene moiety must be critical for achieving high stereocontrol in asymmetric hydroborations.¹³ Introduction of groups such as ethyl, phenyl, and isopropyl at the 2-position of the apopinene moiety to give EapBH₂, PapBH₂ and PraBH₂ respectively, provided Brown and coworkers with new pinene based chiral auxiliaries.¹⁶⁻¹⁷ The

hydroboration results revealed that the effective steric influence of the groups at the 2-position increased in the order, Me < Et < Ph < ⁱPr.¹⁶ A study of asymmetric hydroboration of representative alkenes using these pinene derivatives undertaken by Brown *et al.*, showed that the sterically bulkier chiral borane reagent ⁱPraBH₂, hydroborates prochiral alkenes to achieve significantly better optical induction than obtained using IpcBH₂, EapBH₂, and PapBH₂.¹⁵⁻¹⁷ For example, hydroboration of 1-methylcyclohexene with ⁱPraBH₂ proceeds to give (1*R*,2*R*)-*trans*-2-methylcyclohexanol in 62% yield and 88% e.e., compared with 72% e.e. with IpcBH₂.⁸

7.2. Reduction of Ketones

Reduction of carbonyl groups by borane takes place by addition of the electron-deficient borane to the oxygen atom, followed by irreversible transfer of hydride ion from boron to carbon [eqn. (7.2.1)].¹⁸

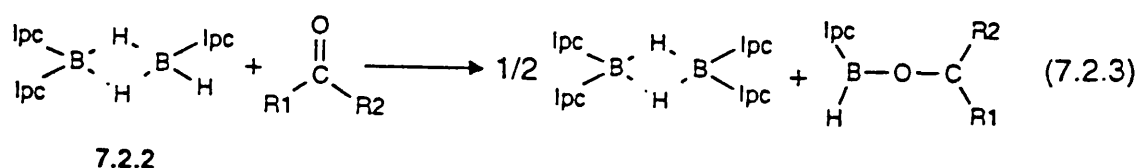
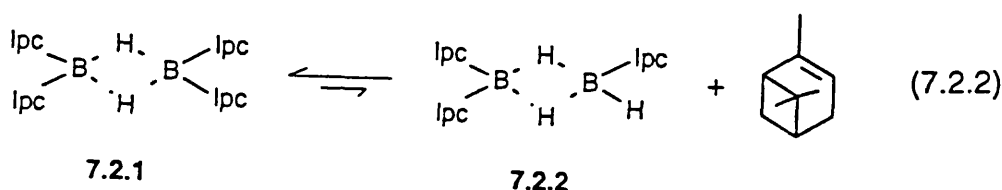


Various reagents have been developed in the past for the asymmetric reduction of prochiral ketones and these provide the product alcohols in good to excellent e.e., but there is no single reagent which is equally effective for all classes of ketones (see Table 7.1).^{5,19-21}

Table 7.1: The 9 different classes of ketones.^{5,19-21}

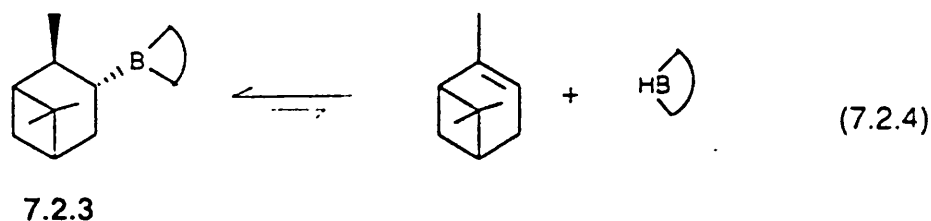
Entry	Class of Ketone
1	acyclic
2	cyclic
3	aralkyl
4	heterocyclic
5	α -haloketones
6	β -keto-esters
7	acyclic conjugated enones
8	cyclic conjugated enones
9	conjugated ynones

Although, Ipc_2BH and IpcBH_2 are good chiral hydroborating agents, they are not so effective for the asymmetric reduction of prochiral ketones.⁹⁻¹⁰ For example, reduction of acetophenone with IpcBH_2 gave the corresponding alcohol in 15% e.e. and with Ipc_2BH in 9% e.e.²²⁻²³ This low optical induction is attributed to a small equilibrium dissociation of the reagent to give α -pinene [eqn. (7.2.2)]. Thus, in cases where reaction of the ketone with the dimer **7.2.1** is slow, a significant amount of the reaction can proceed through **7.2.2** [eqn. (7.2.3)].



The reagent Alpine-borane **7.2.3** also proved to be unsatisfactory for the reduction of aliphatic and aryl ketones. The poor optical induction achieved in the reduction of less reactive ketones (e.g. acetophenone gave the alcohol in 7% e.e.)²⁴ is attributed to an achiral reduction of the substrate by 9-BBN (9-borabicyclo[3.3.1]nonane) which is formed *via* a slow unimolecular dissociation of Alpine-borane [eqn. (7.2.4)].²⁵ However, Brown and Pai showed that both the rate of reaction and chiral induction could be increased by carrying out the

reaction under concentrated conditions;²⁶ when acetophenone is reduced in this way 1-phenylethanol is isolated in 85% e.e. Alternatively, by carrying out the reaction at 6 kbar,²⁷ acetophenone is reduced to the alcohol in *ca.* 100% e.e. The Alpine-borane reagent has been transformed by incorporating ethyl and n-propyl analogues of α -pinene to give Eapine-borane and Prapine-borane, respectively, based on the theory that the steric requirement of the group at the two position of the pinene moiety influences the extent of asymmetric reduction.²⁸ These reagents have provided significant enhancements in optical purity of the product alcohols produced by asymmetric reduction of prochiral α,β -acetylenic ketones. Although acetophenone is quantitatively reduced by Eapine-borane, albeit more slowly than with Alpine-borane, the 1-phenylethanol product is obtained in 78% e.e., compared with 85% with Alpine-borane. This lower induction observed is attributed to the slower rate of reduction of acetophenone with this reagent, thus favouring the dehydroboration mechanism [cf. eqn. (7.2.4)], which is facilitated by the relief of steric strain at the 2-position of the pinene.²⁸

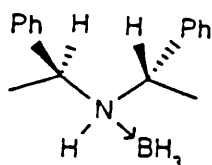


A different approach to the reduction of ketones is the use of reagents such as Ipc_2BCl , where the replacement of a hydrogen atom by a chlorine atom

changes the electronic environment of the boron atom. This reagent is very useful for the reduction of a wide range of prochiral ketones, giving large optical inductions.²⁹ For instance, Ipc_2BCl reduces acetophenone to 1-phenylethanol in 98% e.e.²⁹

Organoborane reagents have also been modified by reaction with a metal hydride, such as lithium hydride, to form a chiral complex metal hydride reducing agent.²¹ These reagents achieve a high degree of stereoselectivity only for the reduction of aromatic ketones.³⁰

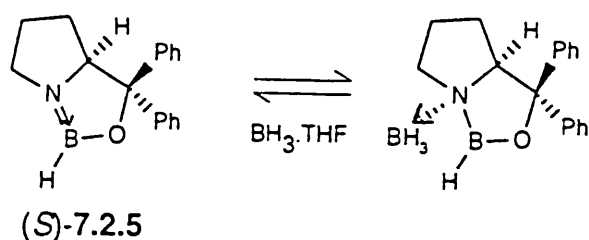
Chiral amine-borane complexes are known to reduce ketones rather slowly. However, the reaction is strongly accelerated either by aqueous acids or by Lewis-acids.^{21,31-34} The chiral reagent di- α -methylbenzylamine. BH_3 complex **7.2.4** reduces acetophenone to 1-phenylethanol in 42% e.e. in the presence of $\text{Et}_2\text{O}.\text{BF}_3$.³²



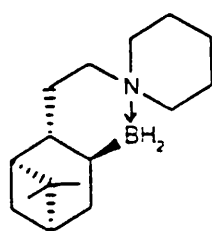
7.2.4

Chiral oxazaborolidines have also been used extensively as catalysts for the borane reduction of a wide range of prochiral ketones.³⁵ These reactions are very fast and proceed in very high yields (80-90%) and good e.e. For

example, the borane reduction of acetophenone using (*S*)-7.2.5 as a catalyst provided the (*R*)-alcohol in 97% e.e.³⁶



In this section of the thesis, we report the use of the polycyclic amine-borane **5.1.8**, formed by cyclisation of *N*-1*R*-nopylpiperidine-borane, for the asymmetric hydroboration of 1-methylcyclohexene in the presence of $\text{BF}_3 \cdot \text{OEt}_2$, followed by alkaline peroxide oxidation to give optically active 2-methylcyclohexanol and, the asymmetric reduction of acetophenone in the presence of $\text{BF}_3 \cdot \text{OEt}_2$ to give optically active 1-phenylethanol. This amine-borane was used in preference to others because it is easily prepared, it is air and moisture stable and it is also soluble in ethers.



5.1.8

7.3. References to Chapter 7

- 1 H.C. Brown, *Boranes in Organic Chemistry*, Cornell University Press, New York, 1972.
- 2 H.C. Brown, G.W. Kramer, A.B. Levy and M.M. Midland, *Organic Synthesis via Boranes*, Wiley-Interscience, New York, 1975.
- 3 H.C. Brown, *Hydroboration*, W.A. Benjamin, New York, 1963.
- 4 H.C. Brown and P.K. Jadhav, *Asymmetric Synthesis*, 1983, **2**, 1.
- 5 M. Srebnik and P.V. Ramachandran, *Aldrichimica Acta*, 1987, **20**, 9.
- 6 H.C. Brown and B. Singaram, *Acc. Chem. Res.*, 1988, **21**, 287.
- 7 H.C. Brown and G. Zweifel, *J. Am. Chem. Soc.*, 1961, **83**, 486.
- 8 H.C. Brown and G. Zweifel, *J. Am. Chem. Soc.*, 1964, **86**, 393.
- 9 H.C. Brown and B. Singaram, *J. Am. Chem. Soc.*, 1984, **106**, 1797.
- 10 H.C. Brown, J.V.N. Vara Prasad, A.K. Gupta and R.K. Bakshi, *J. Org. Chem.*, 1987, **52**, 310.
- 11 A.K. Mandal, P.K. Jadhav and H.C. Brown, *J. Org. Chem.*, 1980, **45**, 3543.
- 12 H.C. Brown, J.R. Schwier and B. Singaram, *J. Org. Chem.*, 1978, **43**, 4395.
- 13 K.N. Houk, N.G. Rondan, Y.-D. Wu, J.T. Metz and M.N. Paddon-Row, *Tetrahedron*, 1984, **40**, 2257.
- 14 H.C. Brown, R.S. Randad, K.S. Bhat, M. Zaidlewicz, S.A. Weissman, P.K. Jadhav and P.T. Perumal, *J. Org. Chem.*, 1988, **53**, 5513.

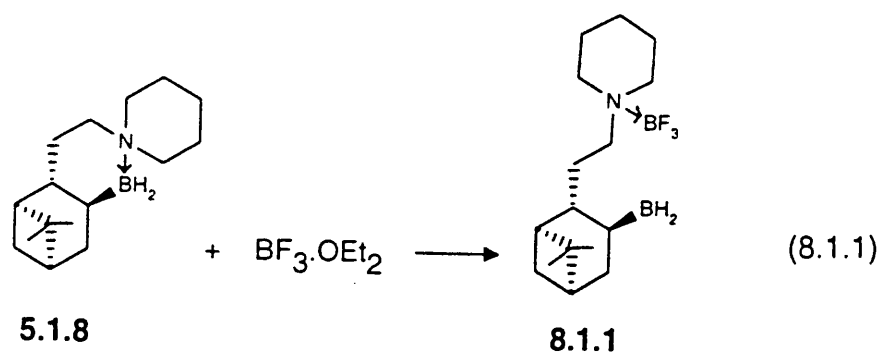
- 15 H.C. Brown and U.P. Dhokte, *J. Org. Chem.*, 1994, **59**, 2365.
- 16 H.C. Brown and U.P. Dhokte, *J. Org. Chem.*, 1994, **59**, 2025.
- 17 U.P. Dhokte and H.C. Brown, *Tetrahedron Lett.*, 1994, **35**, 4715.
- 18 W. Carruthers, *Modern Methods of Organic Synthesis*, 3rd ed., Cambridge Press, 1986.
- 19 H.C. Brown, W.S. Park, B.T. Cho and P.V. Ramachandran, *J. Org. Chem.*, 1987, **52**, 5406.
- 20 H.C. Brown and P.V. Ramachandran, *Acc. Chem. Res.*, 1992, **25**, 16.
- 21 M.M. Midland, *Tetrahedron Asymmetry*, 1983, **2**, 45.
- 22 H.C. Brown and A.K. Mandal, *J. Org. Chem.*, 1977, **42**, 2996.
- 23 H.C. Brown and A.K. Mandal, *J. Org. Chem.*, 1984, **49**, 2558.
- 24 M.M. Midland, S. Greer, A. Tramontano and S.A. Zderic, *J. Am. Chem. Soc.*, 1979, **101**, 2352.
- 25 M.M. Midland, A. Tramontano and S.A. Zderic, *J. Organomet. Chem.*, 1978, **156**, 203.
- 26 H.C. Brown, G.G. Pai, *J. Org. Chem.*, 1985, **50**, 1384.
- 27 M.M. Midland, J.I. McLoughlin and J. Gabriel, *J. Org. Chem.*, 1989, **54**, 159.
- 28 H.C. Brown, P.V. Ramachandran, S.A. Weissman and S. Swaminathan, *J. Org. Chem.*, 1990, **55**, 6328.
- 29 H.C. Brown, J. Chandrasekharan and P.V. Ramachandran, *J. Am. Chem. Soc.*, 1988, **110**, 1539.
- 30 H.C. Brown, S. Krishnamurthy and J.L. Hubbard, *J. Organomet. Chem.*,

- 1979, **166**, 271.
- 31 M.F. Grundon, D.G. McCleery and J.W. Wilson, *J. Chem. Soc., Perkin Trans. 1*, 1981, 231.
- 32 H. Hogeveen and M.B. Eleveld, *Tetrahedron Lett.*, 1986, **27**, 635.
- 33 C. Narayana and M. Periasamy, *J. Organomet. Chem.*, 1987, **323**, 145.
- 34 J.V.B. Kanth and M. Periasamy, *J. Chem. Soc., Chem. Commun.*, 1990, 1145.
- 35 B.T. Cho and Y.S. Chun, *Tetrahedron Asymmetry*, 1992, **3**, 1539.
- 36 E.J. Corey, R.K. Bakshi and S. Shibata, *J. Am. Chem. Soc.*, 1987, **109**, 5551.

Chapter 8: RESULTS AND DISCUSSION

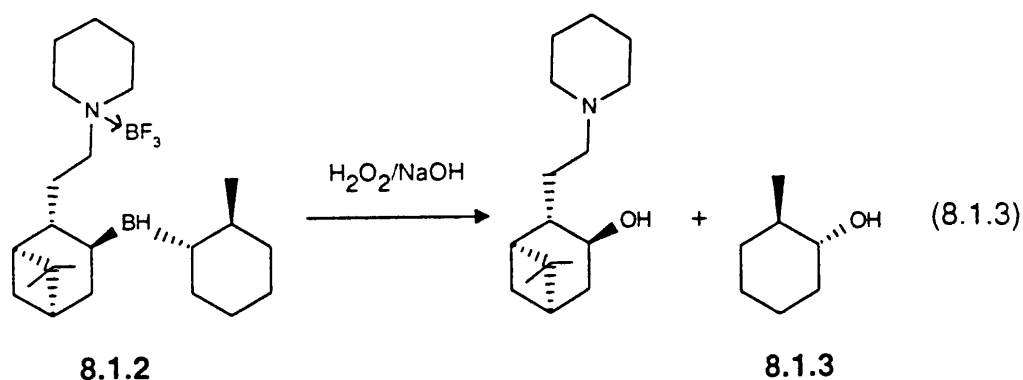
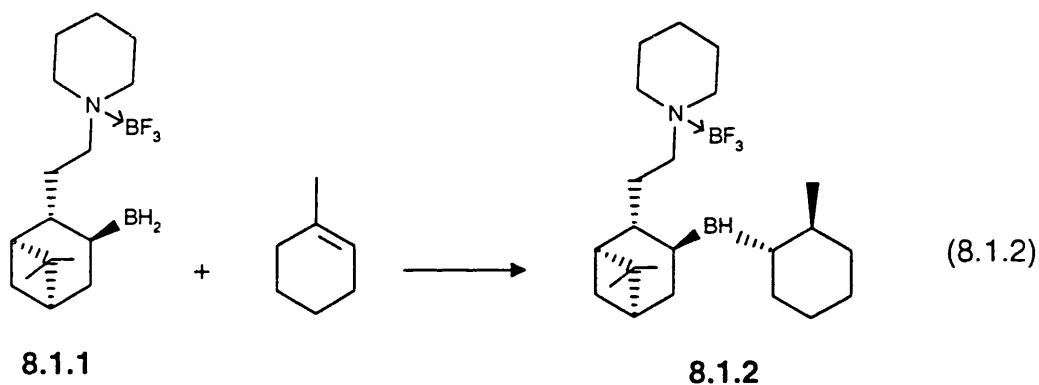
8.1. Hydroboration of 1-Methylcyclohexene

The amine-borane complex **5.1.8** is relatively stable, a result of incorporating the N→B linkage in a 6-membered ring. It is not possible to use this compound directly to hydroborate alkenes, as the reaction of **5.1.8** with an alkene would proceed only at relatively high temperatures, where chiral induction is expected to be greatly reduced.¹ It is thus necessary to cleave the N→B linkage of the complex **5.1.8** in order to increase its reactivity towards alkenes. The reaction of R₃N→BH₃ with BF₃·OEt₂ is known to give R₃N→BF₃ and borane.² Therefore, we considered it likely that BF₃·OEt₂ would cleave the N→B bond of **5.1.8** to give the complex **8.1.1** [see eqn. (8.1.1)]. The species **8.1.1** is expected to be more reactive towards alkenes than **5.1.8**, it should also exhibit significant steric hindrance at the 2-position of the pinene moiety, as required for better chiral discrimination.^{1,3}



Treatment of a diethyl ether solution of **5.1.8** (dichloromethane and THF

have also been used as solvents) with $\text{BF}_3 \cdot \text{OEt}_2$ gave the complex **8.1.1**. This species is unstable to the atmosphere and is readily hydrolysed by traces of water; therefore, it was not isolated. In diethyl ether, the complex **8.1.1** slowly precipitated out of solution as the reaction mixture was stirred at room temperature for 24 h, whilst when the reaction was carried out in CH_2Cl_2 or THF no solid was apparent. Therefore, it appears that the complex **8.1.1** is only slightly soluble in Et_2O , but relatively soluble in THF or CH_2Cl_2 .



A typical procedure for the hydroboration of 1-methylcyclohexene involved cleavage of the $\text{N} \rightarrow \text{B}$ bond by $\text{BF}_3 \cdot \text{OEt}_2$ to form **8.1.1** at room

temperature, followed by the reaction of this species with the alkene to form the organoborane **8.1.2** [eqn. (8.1.2)]. The compound **8.1.2** was then oxidised using alkaline hydrogen peroxide to yield optically active *trans*-2-methylcyclohexanol **8.1.3** [eqn. (8.1.3)]. The purified alcohol was converted to its Mosher ester, by reaction with the Mosher acid chloride derived from (*R*)-(-)- α -methoxy- α -(trifluoromethyl)phenylacetic acid (Mosher acid). The e.e.s were then determined by analysis of the ^{19}F NMR spectrum of the Mosher ester in the region of the CF_3 group ($\delta_{\text{F}}/\text{CDCl}_3$ 1477.70 (*R*) and 1513.85 (*S*) Hz;* Figure 8.1.1).^{4,5}

The hydroboration step was carried out in either Et_2O , THF or CH_2Cl_2 solvents, both at 25 °C and -25 °C. These results are reported in Table 8.1.1. The reaction was found to be usually complete after 24 h of stirring in Et_2O at room temperature, after which time no solid remained. Therefore, the organoborane **8.1.2** which was formed was soluble in Et_2O at 25 °C. It was also soluble in both THF and CH_2Cl_2 as no solid was observed at any stage when the reaction was carried ^{out} in these solvents. However, at -25 °C in Et_2O , a large amount of a crystalline white solid was still present even after 72 h of stirring and oxidation of the reaction mixture at this stage gave essentially no *trans*-2-methylcyclohexanol. When the reaction was repeated in THF, even though no solid was observed during the reaction, oxidation of organoboranes

* (*R*) and (*S*) refer to the chirality of the alcohol.

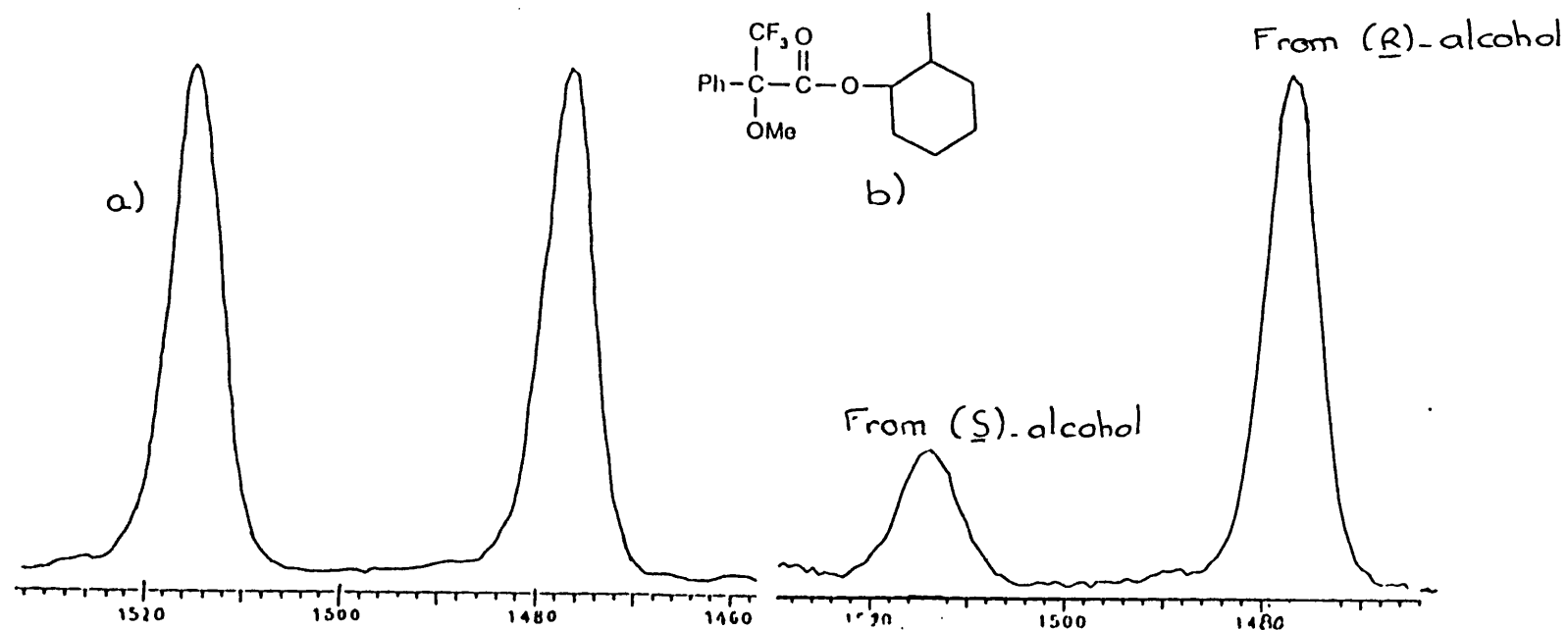


Figure 8.1.1: ^{19}F NMR spectrum, in the region of the CF_3 group for a) the Mosher ester derived from racemic 2-methylcyclohexanol (Aldrich), b) the Mosher ester derived from 2-methylcyclohexanol formed by the hydroboration of 1-methylcyclohexene in diethyl ether at 25 °C (e.e. = 52%).

Table 8.1.1: Asymmetric hydroboration of 1-methylcyclohexene by **5.1.8** in the presence of $\text{BF}_3 \cdot \text{OEt}_2$, in various solvents and temperatures.

Entry	Temp./°C	Solvent	Yield/%	E.e./%	Major enantiomer formed ^a
1	25	Et_2O	70	52	<i>1R,2R</i>
2	25	THF	30	53	<i>1R,2R</i>
3	25	CH_2Cl_2	25	47	<i>1R,2R</i>
4	-25	Et_2O	0	---	<i>1R,2R</i>
5	-25	THF	0	---	<i>1R,2R</i>
6	-25	$\text{Et}_2\text{O}/\text{THF}$	8	55	<i>1R,2R</i>

^a This was determined by correlation of the ^{19}F NMR spectra of the Mosher ester of the alcohol with the optical rotation of the material obtained in Entry **1**, $[\alpha]_{\text{D}}^{20} -9.2^\circ$ (neat) {Lit.⁵ $[\alpha]_{\text{D}}^{20} -17.9^\circ$ (neat), for the (*1R,2R*)-2-methylcyclohexanol.

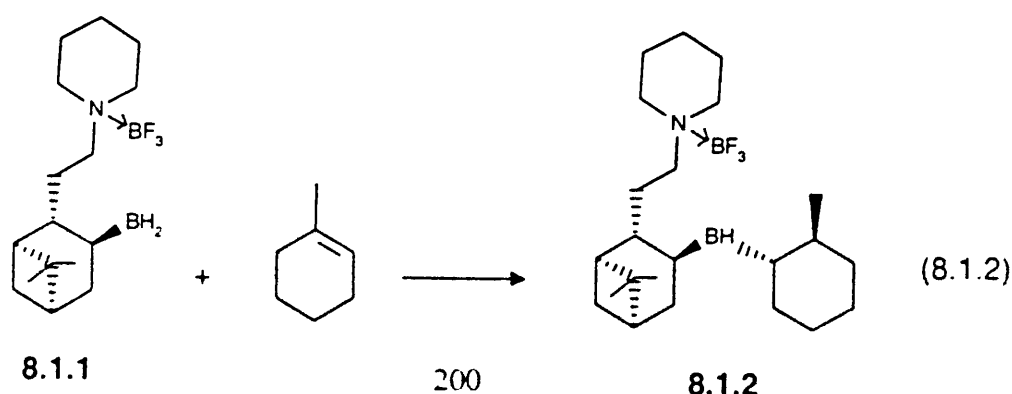
after 72 h of stirring at $-25\text{ }^{\circ}\text{C}$ did not yield any of the cyclohexanol.

When the reaction was carried out by mixing the amine-borane, $\text{BF}_3\cdot\text{OEt}_2$ and the alkene together in Et_2O followed by stirring at room temperature for 24 h, the yield of 2-methylcyclohexanol isolated after oxidation was only 14%, compared with the 70% yield obtained with pre-formed BF_3 complex (see Entry 1 in Table 8.1.1). Therefore, it is necessary to perform the cleavage of the $\text{N}\rightarrow\text{B}$ bond prior to the addition of the alkene.

Larger yields (70% at $25\text{ }^{\circ}\text{C}$) of *trans*-2-methylcyclohexanol were obtained when Et_2O was used as a solvent than with THF or CH_2Cl_2 (30 and 25%, respectively, at $25\text{ }^{\circ}\text{C}$). In an attempt to monitor the progress of the cleavage reaction by $\text{BF}_3\cdot\text{OEt}_2$ with time [eqn. (8.1.1)], in both THF and Et_2O solvent, equimolar amounts of **5.1.8** and $\text{BF}_3\cdot\text{OEt}_2$ were mixed together in an NMR tube in the appropriate solvent (a deuterium oxide capillary was placed in the tube to provide the heteronuclear lock). The ^{11}B NMR spectra of these two mixtures were recorded at regular time intervals. As the reaction progressed a decrease in the intensity of the boron resonances of the BH_2 group of **5.1.8** ($\delta = 1.2\text{ ppm}$) and of the BF_3 group of $\text{BF}_3\cdot\text{OEt}_2$ ($\delta = 0\text{ ppm}$) was expected, whilst the intensity of a third boron resonance arising from the BF_3 group of **8.1.1** was expected to increase. However, no third boron resonance was observed and it is possible that this resonance was obscured by that of $\text{BF}_3\cdot\text{OEt}_2$. For example, $\text{Me}_3\text{N}\rightarrow\text{BF}_3$ and $\text{Et}_3\text{N}\rightarrow\text{BF}_3$ show $\delta_{\text{B}} +0.8$ and -0.6 ppm

in CH₃CN, respectively.⁶ After 9 h, the peak at $\delta = 0$ ppm showed a slight increase in intensity relative to the peak at $\delta = 1.2$ ppm, for both experiments and it is thought that cleavage of the N→B bond by BF₃·OEt₂ is an equilibrium reaction. Initial reaction presumably proceeds rapidly towards a plateau. Because the complex **8.1.1** is only slightly soluble in Et₂O, precipitation of this species will drive the reaction (8.1.1) towards the formation of the complex **8.1.1**. Therefore, the larger yields which were obtained in diethyl ether may be attributed to the fact that the reaction (8.1.1) proceeded further in Et₂O than in THF or CH₂Cl₂. Moreover, in THF the BF₃·OEt₂ complex may exchange the ether ligand to form BF₃·THF and the O→B bond is expected to be stronger for the latter complex. Therefore, the reaction (8.1.1) is even slower in THF.

The hydroboration step (8.1.2) is also thought to be very slow and attempts to follow the progress of this reaction in the above solvents were unsuccessful. This was done by taking aliquots from the reaction mixture, dissolving them in deuterated chloroform and recording the ¹H NMR spectra at regular time intervals. Benzene was added as an unreactive internal standard. No change in the relative intensities of the resonances from the 6 benzene protons and from the alkenyl proton of 1-methylcyclohexene was detected even after 10 h of stirring at room temperature.



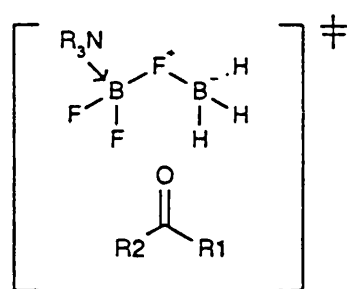
The very low yields obtained when working at $-25\text{ }^{\circ}\text{C}$ were attributed to a further decrease in the rate of hydroboration at lower temperature. In diethyl ether at $-25\text{ }^{\circ}\text{C}$, little of the complex **8.1.1** was in solution and the reaction between this species and 1-methylcyclohexene was very slow. Even when THF (2 cm^3) was added as a co-solvent for the hydroboration step, in order to maintain **8.1.1** in solution, the yield of isolated alcohol following oxidation of organoborane remained very small (8%) and the e.e. did not increase significantly over Entry **1**. We can only conclude, that the hydroboration of 1-methylcyclohexene by **8.1.1** is a very slow process at low temperatures.

The aminoalcohol residue after oxidation of the amine-borane complex **5.1.8** was purified by column chromatography (petroleum spirit b.p. $60\text{--}80\text{ }^{\circ}\text{C}$ -ethyl acetate 9 : 1 v/v eluent) and converted to its Mosher ester. The ^{19}F NMR spectrum of this ester showed only one peak in the region of the CF_3 ($\delta_{\text{F}}/\text{CDCl}_3$ 1948.50 Hz). Therefore, the e.e. of the polycyclic amine-borane **5.1.8** appears to have been enriched to *ca.* 100% after recrystallisation from hexane/ether 7 : 3 % v/v.

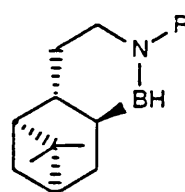
8.2. Asymmetric Reduction of Acetophenone

Amine-boranes ($\text{R}_3\text{N}\rightarrow\text{BH}_3$) are known to reduce aromatic ketones in good yield in the presence of $\text{BF}_3\cdot\text{OEt}_2$, owing to the formation of $\text{R}_3\text{N}\rightarrow\text{BF}_3\text{-BH}_3$ (see the TS structure **8.2.1**).⁷⁻⁸ Polycyclic amine-boranes of the type **8.2.2** are poor

reducing agents towards ketones, but the BF_3 complexes of these species reduce ketones rapidly with good enantioselectivities.⁹ Because the polycyclic amine-borane 5.1.8 has a very similar structure to 8.2.2, it is expected that this complex would also be a poor reducing agent for ketones. Therefore, this amine-borane was used to reduce acetophenone in the presence of 1 or 2 molar equivalents of $\text{BF}_3 \cdot \text{OEt}_2$.



8.2.1



R = Alkyl

8.2.2

A typical reduction procedure involved cleavage of the $\text{N} \rightarrow \text{B}$ bond of 5.1.8, in diethyl ether solvent, using either 1 or 2 molar equivalents of $\text{BF}_3 \cdot \text{OEt}_2$. As described previously for the hydroboration procedure, a white solid precipitated out of solution and was assumed to be the species 8.1.1. After 24 h of stirring at room temperature, acetophenone was added as a solution in Et_2O (ca. $3\text{-}4 \text{ mol dm}^{-3}$) to the reaction mixture at 25, -25 or -78 °C [eqn. (8.2.1)]. The complex 8.2.3 which was formed was then oxidised using alkaline hydrogen peroxide to yield optically active (*R*)-1-phenylethanol 8.2.4 [(eqn. (8.2.2)]. The e.e.s were determined by converting the purified alcohol into its Mosher ester and analysis of the ^{19}F NMR spectrum of this ester (δ_{F} 1522.06 (*S*) and 1598.08 (*R*) Hz, in the region of the CF_3 group, in CDCl_3 ; see Figure 8.2.1).^{4,5} These results are presented in Table 8.2.1. At 25 °C using either 1

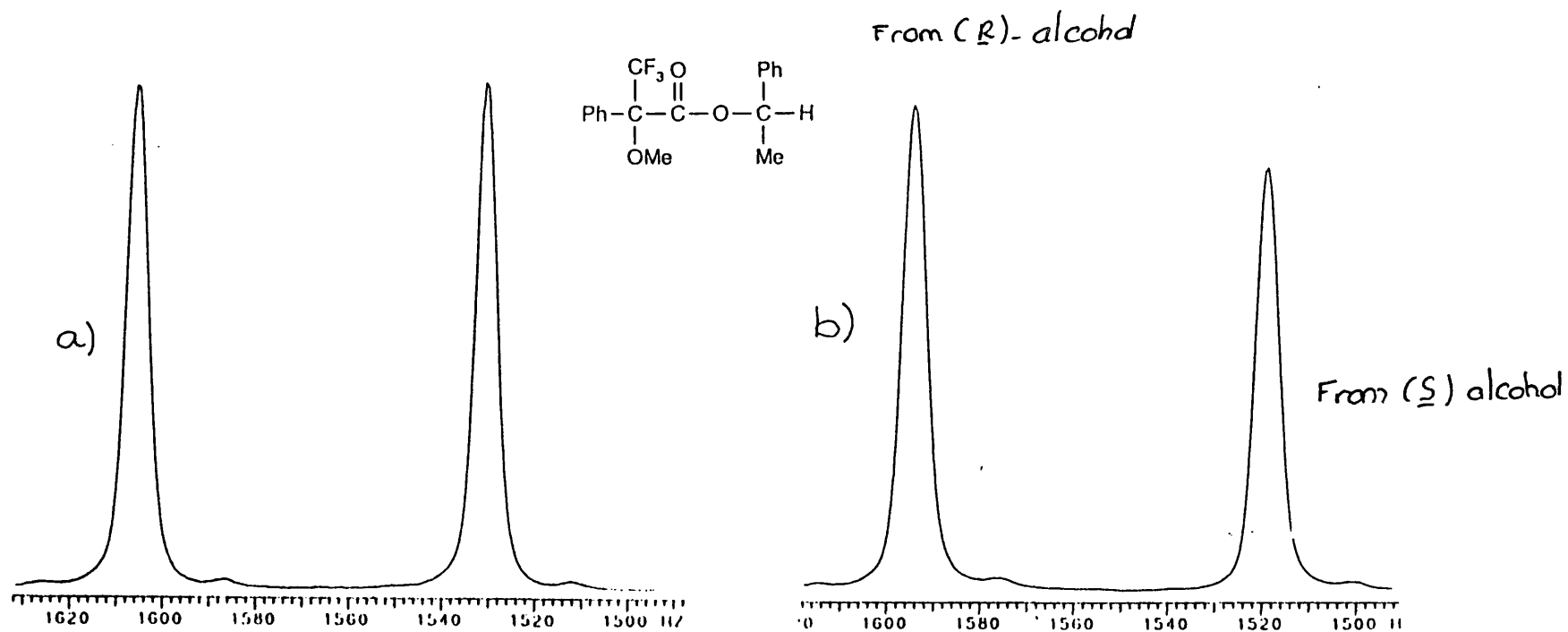


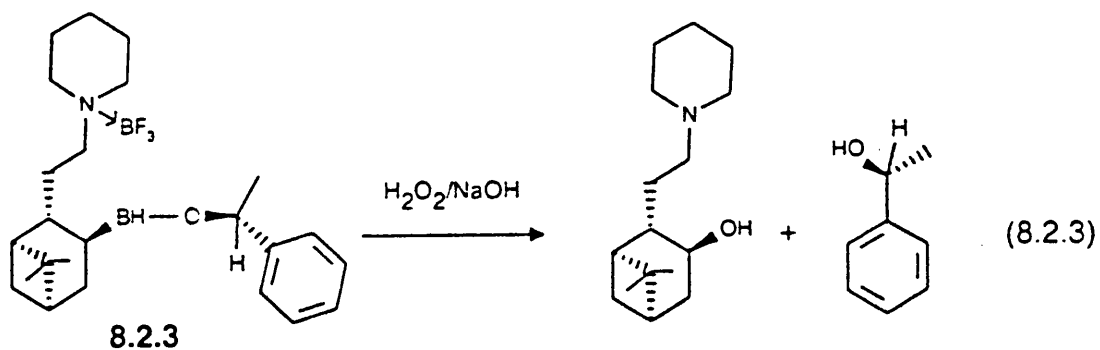
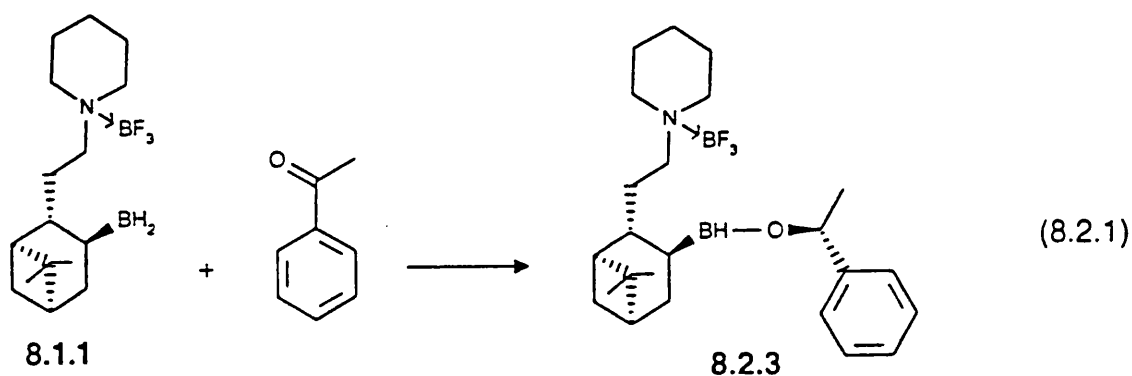
Figure 8.2.1: ^{19}F NMR spectrum, in the region of the CF_3 group for a) the Mosher ester derived from racemic 1-phenylethanol (Aldrich), b) the Mosher ester derived from 1-phenylethanol formed by reduction of acetophenone in diethyl ether/THF at $-78\text{ }^\circ\text{C}$, in the presence of 1 mol eq. of $\text{BF}_3\cdot\text{OEt}_2$ (e.e. 15%)

Table 8.2.1: Asymmetric Reduction of acetophenone by **5.1.8**, in the presence of $\text{BF}_3 \cdot \text{OEt}_2$, in Et_2O at various temperatures.

Entry	Temp./°C	Mol eq. of $\text{BF}_3 \cdot \text{OEt}_2$	Yield/%	E.e./%	Enantiomer formed ^a
1	25	1	80	0.8	<i>R</i>
2	25	2	80	0.5	<i>S</i>
3	-25	1	75	1.4	<i>R</i>
4	-25	2	75	1.6	<i>R</i>
5	-78	2	70	0.6	<i>R</i>
6^b	-78	1	65	15	<i>R</i>

^a This was determined by correlation of the ^{19}F NMR spectra of the Mosher ester of the alcohol with the optical rotation value of the material obtained in Entry **6**; $[\alpha]_{\text{D}}^{20} +9.9^\circ$ ($c = 7.1$ MeOH) {Lit⁵ $[\alpha]_{\text{D}}^{20} +45^\circ$ ($c = 3$, MeOH), for the *R*-1-phenylethanol. ^b THF (2 cm^3) was added as a co-solvent for the hydroboration step.

or 2 molar equivalents of $\text{BF}_3 \cdot \text{OEt}_2$, the insoluble complex **8.1.1** which formed in the first step disappeared instantly upon addition of acetophenone and at $-25\text{ }^\circ\text{C}$ all solid was gone within one hour of stirring. At $-78\text{ }^\circ\text{C}$, when 2 molar equivalents of $\text{BF}_3 \cdot \text{OEt}_2$ were used and acetophenone was added as a solution in diethyl ether, an insoluble white solid was still visible after 24 h of stirring. However, oxidation of the reaction mixture gave 1-phenylethanol in 65% yield but with *ca.* 0% e.e. Presumably, the organoborane **8.2.3** is totally insoluble in ether at $-78\text{ }^\circ\text{C}$. This reaction was repeated using only one molar equivalent of $\text{BF}_3 \cdot \text{OEt}_2$, and adding acetophenone as a solution in THF. No solid was observed and, after 12 h of stirring at $-78\text{ }^\circ\text{C}$, alkaline peroxide oxidation gave the (*R*)-alcohol in 70% yield and 15% e.e.



The e.e.s obtained during these reactions were usually small. The most encouraging result was that obtained at $-78\text{ }^{\circ}\text{C}$ using 1 molar equivalent of $\text{BF}_3\cdot\text{OEt}_2$. These small e.e.s are attributed to the very fast reaction between the ketone and **8.1.1** to form **8.2.3**, which resulted in poor chiral induction. The use of 2 molar equivalents of $\text{BF}_3\cdot\text{OEt}_2$ had the effect of further increasing the rate of reduction; presumably the additional BF_3 resulted in complexation of the $\text{C}=\text{O}$ group making this group more electrophilic.

8.3. Conclusion

The complex **5.1.8** hydroborates 1-methylcyclohexene in diethyl ether, in the presence of $\text{BF}_3\cdot\text{OEt}_2$ at room temperature, in good yield and with good asymmetric induction. This result is comparable to those achieved by Brown and co-workers.³ They isolated (1*S*,2*S*)-*trans*-2-methylcyclohexanol in 62% yield and 88% e.e. after hydroboration-oxidation of 1-methylcyclohexene with (*R*)-isopropylapoisopinocampheylborane at $-25\text{ }^{\circ}\text{C}$. The hydroboration reaction of 1-methylcyclohexene with **5.1.8** is a relatively slow process and it was not possible to improve e.e.s by lowering the temperature, since at $-25\text{ }^{\circ}\text{C}$ the yields of *trans*-2-methylcyclohexanol were very low. The large decrease in the rate of hydroboration at low temperature is attributed to the insolubility of the species **8.1.1**.

The reduction of acetophenone by **5.1.8** in the presence of $\text{BF}_3\cdot\text{OEt}_2$ (1

or 2 mol eq.) is a very fast process, in contrast to the hydroboration^{r of} 1-methylcyclohexene with the same species. 1-Phenylethanol was isolated in good yield even at -78 °C, but e.e.s remained relatively small. It may^{be} possible to improve chiral discrimination by using an amine-borane complex having a sterically more demanding group at the 2-position of the pinene moiety,^{3,9} such as the polycyclic amine-boranes **5.1.9** and **5.1.12**, which have been described in Section 5.1.

8.4. References to Chapter 8

- 1 M. Srebnik and P.V. Ramachandran, *Aldrichimica Acta*, 1987, **20**, 9.
- 2 H.C. Brown, Y.M. Choi and S. Narasimhan, *J. Org. Chem.*, 1982, **47**, 3153.
- 3 U.P. Dhokte and H.C. Brown, *Tetrahedron Lett.*, 1994, **35**, 4715.
- 4 J.A. Dale and H.S. Mosher, *J. Am. Chem. Soc.*, 1973, **95**, 512.
- 5 D.E. Ward and C.K. Rhee, *Tetrahedron Lett.*, 1991, **32**, 7165.
- 6 B. Wrackmeyer, *Ann. Rep. on NMR Spec.*, 1988, **20**, 61.
- 7 M.M. Midland, *Tetrahedron Asymmetry*, 1983, **2**, 45.
- 8 J.V.B. Kanth and M. Periasamy, *J. Chem. Soc., Chem. Commun.*, 1990, 1145.
- 9 M.M. Midland and A. Kazubski, *J. Org. Chem.*, 1992, **57**, 2953.

Chapter 9: EXPERIMENTAL

9.1. NMR Spectroscopy

NMR spectra were recorded using a Varian VXR-400 instrument (400 MHz for ^1H). The solvent was CDCl_3 , unless stated otherwise, and chemical shifts are reported relative to Me_4Si (^1H and ^{13}C), to external $\text{BF}_3\cdot\text{OEt}_2$ (^{11}B) and to external $\text{CF}_3\text{CO}_2\text{H}$ (^{19}F); J values are quoted in Hz.

9.2. Column and Thin Layer Chromatography

See Section 6.5.

9.3. Optical Rotation

See Section 6.6.

9.4. Materials

All preparations and handling of boron-containing compounds were carried out under an atmosphere of dry argon. All solvents were dried by conventional methods and were stored under argon. 1-Methylcyclohexene, acetophenone, Mosher acid and oxalyl chloride (all Aldrich) were used as

received. The polycyclic amine-borane **5.1.8** was prepared according to the procedure described in Section 6.7. Enantiomeric excesses were determined by converting the alcohols to the corresponding Mosher esters and integration of the fluorine resonance from the CF₃ group. δ_F /Hz 1477.7 (*R*), 1513.8 (*S*) for the Mosher ester of *trans*-2-methylcyclohexanol; 1518.06 (*S*) and 1588.88 (*R*) for the Mosher ester from 1-phenylethanol; 1948.50 for the Mosher ester from the alcohol residue of **5.1.8**.^{*} The Mosher esters were prepared according to the procedures described in the literature.^{1,2}

Hydroboration Procedure. - In a 50 cm³ flask equipped with a septum inlet, magnetic stirring bar, and a condenser leading to an argon by-pass was placed the amine-borane **5.1.8** (1.0 g, 0.004 mol) in diethyl ether (8 cm³) and BF₃·OEt₂ (0.49 cm³, 0.004 mol) was added dropwise *via* a microsyringe. The resulting mixture was stirred at room temperature for 24 h. 1-Methylcyclohexene (0.47 cm³, 0.004 mol) was added slowly to the stirred reaction mixture *via* a microsyringe. The reaction mixture was stirred at 25 °C for 24 h, followed by addition of methanol (0.17 cm³, 0.004 mol). The organoboranes were then oxidized by successive addition of 8 cm³ of sodium hydroxide (3 mol dm⁻³) and 1.4 cm³ of alkaline hydrogen peroxide (30% v/v). The mixture was then heated under reflux for 30 min to ensure complete oxidation.³ The workup gave the crude (1*R*,2*R*)-(-)-*trans*-2-methylcyclohexanol.

* (*R*) and (*S*) refer to the chirality of the alcohols.

The alcohol b.p. 68 °C at 10 Torr (Lit³ b.p. 98-100 °C at 65 Torr) was isolated by trap to trap distillation. Further purification by column chromatography (petroleum spirit b.p. 60-80 °C-ethyl acetate, 7 : 3 v/v eluent) gave the (1*R*,2*R*)-alcohol (0.34 g, 75%) and 52% e.e.; $[\alpha]_D^{20}$ -9.2° (neat), {Lit.³ $[\alpha]_D^{20}$ -17.9° (neat)}.

The same procedure was repeated using THF (8 cm³) or dichloromethane (8 cm³) as solvent for the reaction, and (1*R*,2*R*)-(-)-*trans*-2-methylcyclohexanol was isolated in 30% yield, 53% e.e. and 25% yield, 45% e.e., respectively. The procedure for hydroboration at -25 °C in diethyl ether was essentially the same as the room temperature procedure. The reaction was cooled to -25 °C using a RP-100-CT refrigerated immersion probe (Lae Plant Ltd), THF (2 cm³) was added as a co-solvent prior to the addition of 1-methylcyclohexene. This solution was then stirred for 72 h. Alkaline peroxide oxidation gave the alcohol in 8% yield and 55% e.e.

Reduction Procedure. - The procedure was similar to that described for the hydroboration of 1-methylcyclohexene; 1 or 2 molar equivalents of BF₃·OEt₂ were used. The reaction mixture was stirred at room temperature for 24 h, followed by dropwise addition of 1 molar equivalent of acetophenone in solution in diethyl ether (3-4 mol dm⁻³); this was then stirred for a further 1 h at room temperature. Alkaline hydrogen peroxide oxidation of the organoboranes³ yielded (*R*)-(+)-1-phenylethanol, which was purified by distillation under reduced

pressure, b.p. 60 °C at 1.5 torr (Lit.⁴ b.p. 94-100 °C at 18 Torr), in 80% yield and ca. 0% e.e.

For the low temperature reductions, the reaction mixture was cooled to either -25 or -78 °C prior addition of the acetophenone solution (THF may be used in place of diethyl ether as solvent for the acetophenone) and stirring was maintained for a further 2 or 20 h, respectively. Oxidation of organoboranes gave the alcohol in 75% yield at -25 °C using either 1 or 2 equivalents of $\text{BF}_3 \cdot \text{OEt}_2$ and 60% yield at -78 °C using 2 equivalents, all with ca. 0% e.e., when only 1 equivalent of $\text{BF}_3 \cdot \text{OEt}_2$ was used at -78 °C, the (*R*)-2-phenylethanol was isolated in 70% yield and 18% e.e.; $[\alpha]_D^{20} = +9.9^\circ$ ($c = 7.1$, MeOH), {Lit⁵ $[\alpha]_D^{20} +45^\circ$, ($c = 3$, MeOH)}.

9.5. References to Chapter 9

- 1 J.A. Dale and H.S. Mosher, *J. Am. Chem. Soc.*, 1973, **95**, 512.
- 2 D.E. Ward and C.K. Rhee, *Tetrahedron Lett.*, 1991, **32**, 7165.
- 3 H.C. Brown, R.S. Randad, K.S. Bhat, M. Zaidlewicz, S.A. Weissman, P.K. Jadhav and P.T. Perumal, *J. Org. Chem.*, 1988, **53**, 5513.
- 4 J.V.B. Kanth and M. Periasamy, *J. Chem. Soc., Chem. Commun.*, 1990, 1145.
- 5 B.T. Cho and Y.S. Chun, *Tetrahedron Asymmetry*, 1992, **3**, 1539.

Chapter 10: ESR SPECTROSCOPY

ESR spectroscopy is by far the most useful method for the detection of organic free radical species. Analysis of an ESR spectrum can not only help determine the gross chemical structure of a radical, but also its detailed conformation. The sensitivity of the method allows radical concentration as low as 10^{-8} mol dm⁻³ to be observed.

10.1. Principles of ESR Spectroscopy

An unpaired electron possesses spin angular momentum and, since the spin quantum number is $s = 1/2$, it can thus exist in two spin states ($m_s = +1/2$ or $-1/2$) which, in the absence of a magnetic field, are degenerate. Associated with this spin angular momentum, the electron possesses a magnetic moment and in the presence of an externally applied magnetic field the degeneracy of these two spin states is lifted and the magnetic moment of the electron can align itself either with or against the applied field. The difference in energy between the two states is given by equation (10.1.1), where g is a dimensionless proportionality constant (equal to 2.0023 for an isolated electron), μ_B is the Bohr magneton, and B is the strength of the applied field.

$$\Delta E = g\mu_B B \quad (10.1.1)$$

In the presence of electromagnetic radiation of fixed frequency ν_0 , transitions between the two spin states are induced when the resonance condition [eqn. (10.1.2), h is Planck's constant] is satisfied at an applied field B_0 (the resonance field). Although the probability of a transition up is the same as the probability of a transition down, because the population of the lower ($m_s = -1/2$) state is larger, net absorption of electromagnetic radiation will take place when the resonance condition is fulfilled. This gives rise to the ESR spectrum.

$$\Delta E = h\nu_0 = g\mu_B B_0 \quad (10.1.2)$$

In general, for the study of organic free radicals g is close to 2 and B_0 is usually *ca.* 330 mT (3300 G). Irradiation with electromagnetic radiation of frequency *ca.* 9.1 GHz, which corresponds to X-band microwave radiation, results in transitions from the lower ($m_s = -1/2$) to the higher ($m_s = +1/2$) energy levels.

Unlike NMR spectrometers, ESR spectrometers are arranged to record the first-derivative of the absorption spectrum, rather than the absorption curve itself. This gives greater sensitivity and also better resolution. Since the area under the absorption curve is proportional to the number of radicals in the sample, double integration of the first-derivative curve enables the concentration of radicals to be determined.

10.2. Characteristics of ESR Spectra¹

g-Factors. - In a magnetic field, the unpaired electron in a non-linear polyatomic free radical possesses a small amount of unquenched orbital angular momentum, as a consequence of spin-orbit coupling, in addition to its spin angular momentum. This results in the electron having a slightly different effective magnetic moment from that which a free electron would possess. Hence, for a given microwave frequency, radicals with different *g*-factors will resonate at different field strengths. The *g*-factors for most organic free radicals are close to that for a free electron, but the differences are nevertheless significant and can give valuable information about the structure of a radical.

Hyperfine Splittings. - These arise from interaction between the unpaired electron and neighbouring magnetic nuclei (¹H, ¹³C, ¹⁴N, ¹¹B etc). The electron experiences not only the externally applied field, but also the field arising from neighbouring nuclei. In general, interaction with *n* equivalent protons gives rise to (*n* + 1) lines, the intensities of which are given by Pascal's triangle. Interaction with *n* equivalent nuclei of spin *I* results in (*2nI* + 1) lines.

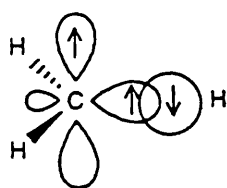
Origin of Hyperfine Splitting. - Isotropic hyperfine splitting results from interaction of the unpaired electron with the nucleus and, for coupling to be observed, the unpaired electron must have non-zero probability of being at the

nucleus in question. This is usually called the Fermi contact interaction. Thus, we would expect to observe coupling only when the electron is in an orbital with some s-character, since only then will there be finite electron density at the nucleus. For π -radicals, no splitting would be expected, since the unpaired electron is in a molecular orbital composed of p-orbitals which have nodes at the nucleus. However, isotropic coupling is observed with in-plane magnetic nuclei in π -radicals and the origin of this coupling is explained below.

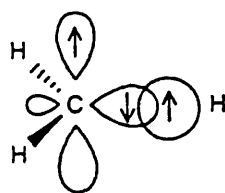
α -Proton Splittings - Spin-Polarisation. - Hyperfine interaction of this type can be best illustrated by reference to the methyl radical CH_3^\bullet (see **10.2.1a/b**). These structures show the spin polarisation mechanism responsible for the α -proton splitting for CH_3^\bullet and of the two possible arrangements of the electron spins **10.2.1a** will be more probable. The electrons in the σ -bond are not perfectly paired due to an exchange interaction which causes the electron with the same spin as the unpaired electron in the π - $2p_z$ to come closer to this electron than will the σ -electron of opposite spin. Hence, a small positive spin population is induced in the C-2s atomic orbital, giving rise to a positive coupling constant with $^{13}\text{C}_\alpha$ in a labelled radical. The spin population induced by the H_α -1s atomic orbital is negative hence $a(\text{H}_\alpha)$ is also negative [for CH_3^\bullet , $a(3\text{H}_\alpha) = 23.0$ G and $a(^{13}\text{C}_\alpha) = 38.6$ G at 178 K.]. McConnell² has shown that for π -radicals $a(\text{H}_\alpha)$ is approximately proportional to the unpaired spin population ($\rho_{\text{C}_\alpha}^\pi$) on the adjacent carbon atom [eqn. (10.2.1)]. The proportionality constant Q is ca. (-)23 G.

$$a(H_\alpha) = Q\rho_{C\alpha}^\pi \quad (10.2.1)$$

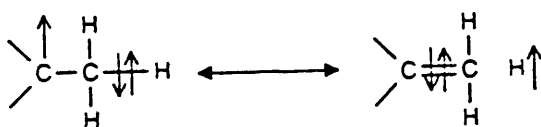
β -Proton Splittings. - These arise through the mechanism of hyperconjugation, which allows some of the unpaired α -spin density to appear at the β -protons, which are no longer constrained to the nodal plane of the C_α - $2p\pi$ orbital. In valence bond terms this may be represented by inclusion of structure 10.2.2.



10.2.1a



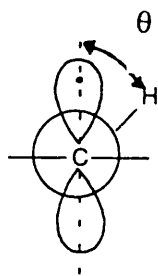
10.2.1b



10.2.2

In terms of simple molecular orbital theory, this means that there must be some overlap between one or more σ C_β -H bonds and the p -orbital containing the unpaired electron. The Heller-McConnell³⁻⁴ equation (10.2.2) relates $a(H_\beta)$ to the dihedral angle θ (see 10.2.3) and to $\rho_{C\alpha}^\pi$.

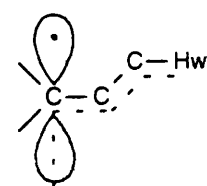
$$a(H_\beta) = (A + B\cos^2\theta)\rho_{C\alpha}^\pi \quad (10.2.2)$$



10.2.3

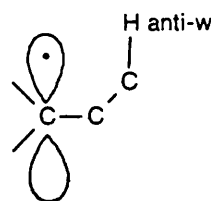
In equation (10.2.2), A is a spin-polarisation constant which has a small value (*ca.* <1 G) and is often neglected; B is a hyperconjugation parameter (*ca.* 58.5 G for alkyl radicals). The coupling constant with a β -proton is thus at a maximum when θ is zero and a minimum when θ is 90° (see 10.2.3).

Long-Range Proton Splittings. - Long-range hyperfine splitting with γ - and δ -protons are usually small, as the positive and negative contributions to these interactions often cancel one another. Long-range hyperfine interactions tend to be very dependent on radical stereochemistry and an extensive review on the subject has been given by King.⁵ Theoretical analyses of long-range hyperfine interactions in both aliphatic and bicyclic free radicals have been given by Ellinger *et al.*^{6,7} Structures 10.2.4a/b illustrate the "W" and "anti-W" rules. The "W"-type interactions give larger values of $a(H_\gamma)$ than do the "anti-W"-type interactions. In the former, contributions from spin-delocalisation and spin-polarisation are both positive and add to give a positive coupling, whereas for the latter, both contributions have opposite sign and often nearly cancel each other.



10.2.4a

219



10.2.4b

10.3. Second-Order Effects

The previous analyses of hyperfine coupling is only valid in cases where the coupling energy is much smaller than the electronic Zeeman energy. When coupling constants are relatively large or the applied magnetic field is very small, additional splittings can occur which cannot be explained using only first-order theory. These additional lines are due to the removal of the degeneracy of certain Zeeman energy levels and furthermore, these lines can also be shifted from their positions predicted according to first-order theory. These effects are called second-order effects. The lines are shifted from the first-order position in units of $(a^2/4B_0)$, where a is the true hyperfine coupling constant and B_0 is the applied magnetic field at the centre of the spectrum.⁸

For example, coupling of an unpaired electron with 3 equivalent protons usually gives rise to a 1:3:3:1 quartet, but if second-order effects are important then the observed splitting pattern is that shown in Figure 10.3.1, along with the intensities of the lines and their shifts from first-order positions, given in units of $(a^2/4B_0)$.

10.4. Methods for Radical Generation

Radicals are generally transient species and hence special experimental techniques have to be used for their observation within the cavity of an ESR

spectrometer. There are three principal methods: a) radicals may be generated and immobilised in a matrix at low temperature, b) they can be produced by U.V. or electron irradiation of a solution of a suitable radical precursor in the cavity of the spectrometer, c) they may be formed and continuously introduced into the cavity by use of a flow system.

For most of the work presented here, radicals were generated by U.V. irradiation of a solution containing di-t-butyl peroxide in the cavity of the spectrometer. The spectrometer was equipped for *in situ* U.V. irradiation of samples and a full description of the equipment has been given in Section 3.1.

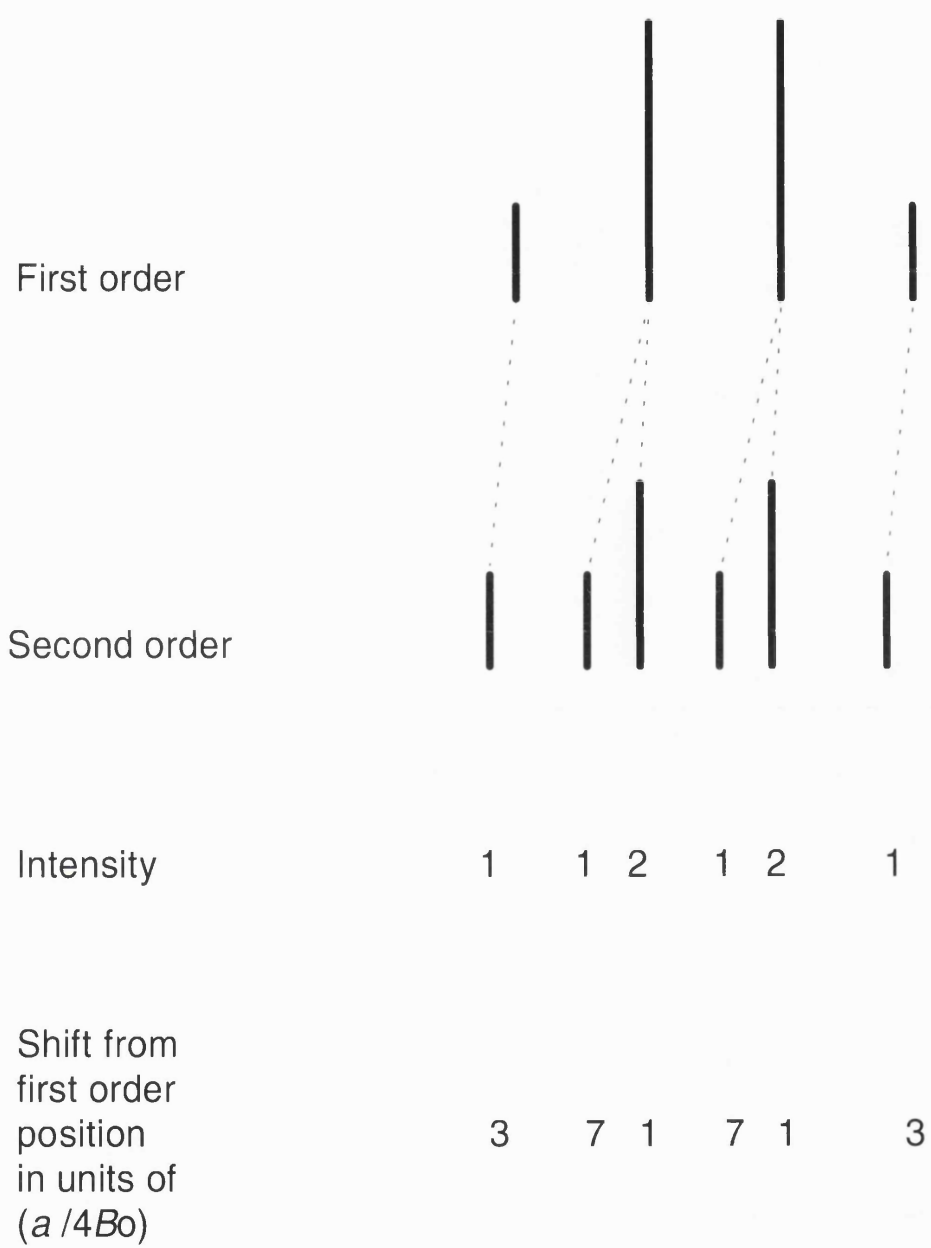


Figure 10.3.1: Second-order shifts observed for coupling of the unpaired electron with three equivalent hydrogens.

10.5. References to Chapter 10

- 1 J.E. Wertz and J.R. Bolton, *Electron Spin Resonance; Elementary Theory and Practical Applications*, McGraw-Hill, New York, 1972.
- 2 H.M. McConnell, *J. Chem. Phys.*, 1956, **24**, 632.
- 3 C. Heller and H.M. McConnell, *J. Chem. Phys.*, 1960, **32**, 1535.
- 4 J.K. Kochi, *Adv. Free Radical Chem.*, 1975, **5**, 189.
- 5 F.W. King, *Chem. Rev.*, 1976, **76**, 157.
- 6 Y. Ellinger, A. Rassat, R. Suba and G. Berthier, *J. Am. Chem. Soc.*, 1973, **95**, 2372.
- 7 Y. Ellinger, R. Suba and G. Berther, *J. Am. Chem. Soc.*, 1978, **100**, 4691.
- 9 R.W. Fessenden, *J. Chem. Phys.*, 1962, **37**, 747.

LIST OF ABBREVIATIONS

TS	Transition State
SOMO	Singly Occupied Molecular Orbital
LUMO	Lowest Occupied Molecular Orbital
HOMO	Highest Occupied Molecular Orbital
CIDEP	Chemically Induced Electron Polarisation
e.e.	Enantiomeric Excess
DTBP	Di-t-Butyl Peroxide
BMS	Boron Methyl Sulfide
THF	Tetrahydrofuran
TMBB	Trimethylamine-butylborane
TMMB	Trimethylamine-methylborane
TMEDA	Tetramethylethylenediamine
DABCO	Diazo-bicyclo[2.2.2]-octane
QN	Quinuclidine
Thx	Thexyl
lpc	Isopinocampheyl
lpcT	Isopinocampheyl-tetramethylethylenediamine-borane
lpcD	Isopinocampheyl-diazo-bicyclo[2.2.2]-octane-borane
lpcQ	Isopinocampheylquinuclidine-borane
Ad	Adamantane